

Riemann surfaces for KPZ with periodic boundaries

Sylvain Prolhac

Laboratoire de Physique Théorique, IRSAMC, UPS, Université de Toulouse, France
sylvain.prolhac@irsamc.ups-tlse.fr

November 15, 2019

1 Abstract

2 The Riemann surface for polylogarithms of half-integer index, which has the
3 topology of an infinite dimensional hypercube, is studied in relation to one-
4 dimensional KPZ universality in finite volume. Known exact results for fluc-
5 tuations of the KPZ height with periodic boundaries are expressed in terms of
6 meromorphic functions on this Riemann surface, summed over all the sheets
7 of a covering map to an infinite cylinder. Connections to stationary large
8 deviations, particle-hole excitations and KdV solitons are discussed.

9

10 Contents

11	1 Introduction	3
12	2 KPZ fluctuations and Riemann surfaces	4
13	2.1 Riemann surfaces $\tilde{\mathcal{R}}$ and \mathcal{R}^Δ	4
14	2.2 Flat initial condition	5
15	2.3 Sharp wedge initial condition	7
16	2.4 Stationary initial condition	8
17	2.5 Multiple-time statistics with sharp wedge initial condition	8
18	2.6 Discussion	9
19	2.6.1 Full dynamics from large deviations	9
20	2.6.2 Particle-hole excitations	10
21	2.6.3 KdV solitons	12
22	2.7 Conclusions	14
23	3 Riemann surfaces and ramified coverings	15
24	3.1 Analytic continuation and Riemann surfaces	15
25	3.2 The Riemann surfaces \mathcal{H}_N and \mathcal{R}_N	17
26	3.3 Genus	20
27	3.4 Ramified coverings	21
28	3.5 Quotient under group action	24
29	3.6 Homotopy and homology	24
30	3.7 Differential 1-forms	25
31	3.8 Infinite genus limit	26
32	3.8.1 Riemann surface \mathcal{R}	26
33	3.8.2 Riemann surface $\tilde{\mathcal{R}}$	28
34	3.8.3 Riemann surface \mathcal{R}^Δ	30
35	3.8.4 Collection $\overline{\mathcal{R}}$ of Riemann surface \mathcal{R}^Δ	31

36	4 Functions on the Riemann surfaces $\mathcal{R}, \check{\mathcal{R}}, \mathcal{R}^\Delta$	33
37	4.1 $2i\pi(\mathbb{Z} + 1/2)$ -continuable functions, translation and analytic continuations	33
38	4.2 Polylogarithms	33
39	4.3 Square roots $\kappa_a(v)$	34
40	4.4 Half-integer polylogarithms and function χ on \mathcal{R}	36
41	4.5 Symmetries of χ	38
42	4.6 Function I_0	38
43	4.7 Functions J_P	39
44	4.8 Functions e^{2I}, e^{I+J} and e^{2J} defined on $\check{\mathcal{R}}$	41
45	4.9 Functions on the Riemann surfaces \mathcal{R}^Δ	43
46	4.9.1 Function χ^Δ	43
47	4.9.2 Functions J_P^Δ	44
48	4.10 Functions $K_{P,Q}, K_{P,Q}^{\Delta,\Gamma}$ and $e^{2K^{\Delta,\Gamma}}$	46
49	4.10.1 Functions $K_{P,Q}$	46
50	4.10.2 Functions $K_{P,Q}^{\Delta,\Gamma}$	51
51	5 Relation with known formulas for KPZ	52
52	5.1 Flat initial condition	52
53	5.1.1 Relation with the generating function of the height	52
54	5.1.2 Relation with Fredholm determinants	53
55	5.2 Sharp wedge initial condition	54
56	5.2.1 Relation with the generating function of the height from [39]	55
57	5.2.2 Relation with the expression from Baik and Liu [40]	56
58	5.3 Multiple-time statistics with sharp wedge initial condition	59
59	5.3.1 Derivation of (13) from Baik-Liu [42]	59
60	5.3.2 Pole structure of (16)	62
61	A Derivation of the identity (76)	62
62	A.1 Case $n = 1$	62
63	A.2 Extension to $n > 1$	63
64	A.3 Extension to $n < 0$	64
65	B Derivation of the identities (106) and (107)	64
66	B.1 Case $n = 1$ for (106)	64
67	B.2 Extension to $n > 1$ and $n < 0$	65
68	B.3 Proof of (107)	65
69	C Calculations of some integrals between $-\infty$ and $\nu \in \mathbb{D}$	66
70	C.1 The functions $\log \kappa_a$ and $\log(\kappa_a + \kappa_b)$ are analytic in \mathbb{D}	66
71	C.2 Integral of $\kappa_a(v)^{-1}\kappa_b(v)^{-1}$	66
72	C.3 Integral of $\chi_\emptyset''(v)/\kappa_a(v)$ between $-\infty$ and a branch point	67
73	C.4 Integral of $\chi_\emptyset''(v)/\kappa_a(v)$ as an infinite sum	67
74	D Calculations of some integrals depending on $(\nu, \mu) \in \mathbb{D}_2$	67
75	D.1 Domain of analyticity of functions $\log(e^{i\theta}(\kappa_a(\nu) + \kappa_b(\mu)))$	67
76	D.2 Integral of $\kappa_a(u + \nu)^{-1}\kappa_b(u + \mu)^{-1}$	68
77	D.3 Integral of $\kappa_b(u + \mu)/\kappa_a(u + \nu)$	68
78	D.4 Integral of $\chi_\emptyset''(u + \mu)/\kappa_a(u + \nu)$	69
79	E Identities for the coefficients W_P, W_P^Δ	69
80	E.1 Differences of W_P	70

81	E.2 Ratios of e^{W_P}	70
82	E.3 Ratios of $e^{2W_P^\Delta}$	71

83	References	71
----	-------------------	-----------

84

85

86 1 Introduction

87 KPZ universality in 1+1 dimension [1–9] describes large scale fluctuations appearing in
 88 a variety of systems such as growing interfaces [10], disordered conductors [11], one-
 89 dimensional classical [12–14] and quantum [15–17] fluids, or traffic flow [18]. The height
 90 field $h_\lambda(x, t)$ characterizing KPZ universality depends on position $x \in \mathbb{R}$, time $t \geq 0$,
 91 and on a parameter $\lambda > 0$ quantifying the strength of non-linear effects and the non-
 92 equilibrium character of the dynamics. The fluctuations of $h_\lambda(x, t)$ are believed to be
 93 universal in the sense that for a given geometry (infinite system, presence of various kinds
 94 of boundaries) and a given initial condition, the probability distribution of the appropriate
 95 height field $h_\lambda(x, t)$ is independent of the specific setting in KPZ universality and of the
 96 precise microscopic model studied at large scales. A prominent model, which has given its
 97 name to the universality class, is the KPZ equation [19], defined as the properly renormal-
 98 ized [20–22] non-linear stochastic partial differential equation $\partial_t h_\lambda = \frac{1}{2} \partial_x^2 h_\lambda - \lambda (\partial_x h_\lambda)^2 + \eta$
 99 with η a unit space-time Gaussian white noise, and which is related by the Cole-Hopf
 100 transform $Z_\lambda(x, t) = e^{-2\lambda h_\lambda(x, t)}$ to the stochastic heat equation with multiplicative noise
 101 $\partial_t Z_\lambda = \frac{1}{2} \partial_x^2 Z_\lambda - 2\lambda Z_\lambda \eta$ and Ito prescription in the time variable.

102 Of particular interest is the limiting object $h(x, t) = \lim_{\lambda \rightarrow \infty} (h_\lambda(x, t/\lambda) - \lambda^2 t/3)$ into
 103 the regime where non-linear effects dominate, and for which a number of exact results have
 104 been obtained in the past 20 years [23–34] for the infinite system geometry $x \in \mathbb{R}$. Most
 105 notably, connections to random matrix theory have been identified: for given time $t \rightarrow \infty$
 106 and position $x \in \mathbb{R}$, the probability distribution of $h(x, t)$ for specific initial conditions are
 107 equal to Tracy-Widom distributions [35], known for describing fluctuations of extremal
 108 eigenvalues in random matrix theory.

109 We are interested in this paper in KPZ universality in finite volume, specifically with
 110 periodic boundary conditions $x \equiv x + 1$, in the strongly non-linear regime $\lambda \rightarrow \infty$. There,
 111 the standard deviation of $h(x, t)$ grows as $t^{1/3}$ at short times like in the infinite system
 112 $x \in \mathbb{R}$, before eventually saturating after the statistics of fluctuations has relaxed to a
 113 stationary distribution where $x \mapsto h(x, t)$ is Brownian. Large deviations in the stationary
 114 state away from typical Gaussian fluctuations are known explicitly [36, 37], and long time
 115 corrections to large deviations have been obtained explicitly [38] for a few specific initial
 116 conditions. Interestingly, the exact expressions in [36–38] involve polylogarithms with
 117 half-integer index. The analytical and topological structure of these special functions is
 118 at the heart of the present paper.

119 The complete evolution in time of KPZ fluctuations with periodic boundaries, crossing
 120 over between the short time limit, where the correlation length is much smaller than the
 121 system size and the fluctuations of the infinite system are recovered, and the long time limit
 122 where stationary large deviations appear, has been studied recently. Exact expressions
 123 have been obtained for the one-point [39–41] distribution $P(h(x, t) < u)$ of the height
 124 field for specific (sharp wedge, stationary and flat) initial conditions, as well as for the
 125 general, multiple-time joint distribution $P(h(x_1, t_1) < u_1, \dots, h(x_n, t_n) < u_n)$ for sharp
 126 wedge initial condition [42]. All these exact expressions have a somewhat complicated

127 structure involving combinations of square roots and half-integer polylogarithms.

128 A goal of the present paper is to show that the full crossover regime for KPZ fluctua-
 129 tions in finite volume have rather simple expressions using objects from algebraic geometry
 130 directly connected to stationary large deviations. More precisely, considering the (infinite
 131 genus) Riemann surface $\tilde{\mathcal{R}}$ on which polylogarithms with half-integer index are defined
 132 globally, the exact expression for the probability $\mathbb{P}(h(x, t) < u)$ with flat initial condition
 133 is rewritten as the integral around an infinitely long cylinder \mathcal{C} of a holomorphic differen-
 134 tial on $\tilde{\mathcal{R}}$ summed over all the sheets of a ramified covering from $\tilde{\mathcal{R}}$ to \mathcal{C} , see equation (1).
 135 Similar expressions are obtained for sharp wedge and stationary initial conditions, with
 136 an additional summation over finite subsets Δ of $\mathbb{Z} + 1/2$, and $\tilde{\mathcal{R}}$ replaced by related Rie-
 137 mann surfaces \mathcal{R}^Δ , see equations (6), (11). Multiple integrals around the cylinder as well
 138 as meromorphic functions on pairs of Riemann surfaces $\mathcal{R}^\Delta \times \mathcal{R}^\Gamma$ are additionally needed
 139 for the multiple-time joint distribution with sharp wedge initial condition, see equation
 140 (16).

141 The paper is organized as follows. In section 2, our main results expressing KPZ fluc-
 142 tuations with periodic boundaries in terms of infinite genus Riemann surfaces $\tilde{\mathcal{R}}$, \mathcal{R}^Δ and
 143 ramified coverings from them to the infinite cylinder \mathcal{C} are given. Interpretations in terms
 144 of particle-hole excitations and KdV solitons are pointed out at the end of the section. In
 145 section 3, we recall some classical aspects of the theory of Riemann surfaces and ramified
 146 coverings used in the rest of the paper, and define the Riemann surfaces $\tilde{\mathcal{R}}$ and \mathcal{R}^Δ . In
 147 section 4, we study several meromorphic functions defined on these Riemann surfaces and
 148 needed for KPZ fluctuations. Finally, we explain in section 5 how our main results from
 149 section 2 are related to earlier exact formulas [39–42]. Some technical calculations are
 150 presented in appendix.

151 2 KPZ fluctuations and Riemann surfaces

152 In this section, we give exact expressions for KPZ fluctuations with periodic boundary
 153 conditions equivalent to those obtained in [39–42], but written in a more unified way by
 154 interpreting various terms as natural objects living on Riemann surfaces evaluated on
 155 distinct sheets. Connections to stationary large deviations and interpretations in terms of
 156 particle-hole excitations and KdV solitons are discussed in some detail toward the end of
 157 the section.

158 2.1 Riemann surfaces $\tilde{\mathcal{R}}$ and \mathcal{R}^Δ

159 The exact formulas for KPZ fluctuations given below involve Riemann surfaces $\tilde{\mathcal{R}}$ and
 160 \mathcal{R}^Δ , quotient under groups of holomorphic automorphisms of a Riemann surface \mathcal{R} which
 161 has the topology of an infinite dimensional hypercube and which is a natural domain of
 162 definition for some infinite sums of square roots with branch points $2i\pi a$, $a \in \mathbb{Z} + 1/2$. An
 163 introduction to several topics related to Riemann surfaces used in this paper is given in
 164 section 3, starting with a finite genus analogue \mathcal{R}_N of \mathcal{R} before giving precise definitions
 165 of $\tilde{\mathcal{R}}$ and \mathcal{R}^Δ .

166 The Riemann surface \mathcal{R} has a kind of translation invariance inherited from that of the
 167 branch points $2i\pi a$, and which is eliminated by definition in $\tilde{\mathcal{R}}$. The Riemann surfaces
 168 \mathcal{R}^Δ are indexed by finite sets Δ of half-integers, which we write as $\Delta \sqsubset \mathbb{Z} + 1/2$. The
 169 elements $a \in \Delta$ index branch points $2i\pi a$ that have been removed from the infinite sum
 170 of square roots defined on \mathcal{R} . The translation invariance of \mathcal{R} implies that $\mathcal{R}^\Delta \sim \mathcal{R}^{\Delta+1}$
 171 are isomorphic Riemann surfaces.

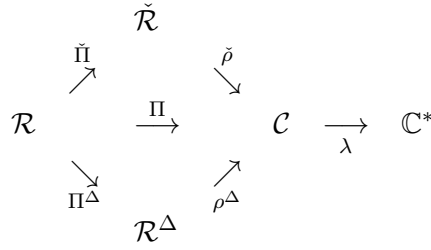


Figure 1: Summary of several useful covering maps between the Riemann surfaces considered in this paper.

172 The Riemann surface \mathcal{R} can be partitioned into sheets \mathbb{C}_P , $P \in \mathbb{Z} + 1/2$, copies of the
 173 complex plane glued together along branch cuts of the square roots, and we write $[v, P]$,
 174 $v \in \mathbb{C}$, $P \in \mathbb{Z} + 1/2$ for a point of \mathcal{R} with branch cuts chosen as in figure 18 right. The
 175 Riemann surfaces $\tilde{\mathcal{R}}$ and \mathcal{R}^Δ are identified as fundamental domains for corresponding
 176 group actions on \mathcal{R} , see respectively sections 3.8.2 and 3.8.3, and may be partitioned
 177 by portions of the sheets \mathbb{C}_P . For $\tilde{\mathcal{R}}$, one can choose the union of infinite strips $\mathcal{S}_P^0 =$
 178 $\{[v, P], -\pi < \text{Im } v \leq \pi\}$, $P \in \mathbb{Z} + 1/2$, see figure 13 left. For \mathcal{R}^Δ , a possible fundamental
 179 domain is the union of all \mathbb{C}_P , $P \cap \Delta = \emptyset$, see figure 16. Additionally, the collection of
 180 non-isomorphic \mathcal{R}^Δ , $\Delta \equiv \Delta + 1$, may also be partitioned into the infinite strips \mathcal{S}_P^0 from
 181 all \mathcal{R}^Δ without the restriction $\Delta \equiv \Delta + 1$, see figure 17.

182 The definitions of $\tilde{\mathcal{R}}$ and \mathcal{R}^Δ from \mathcal{R} provide covering maps $\tilde{\Pi}$ and Π^Δ from \mathcal{R} to $\tilde{\mathcal{R}}$
 183 and \mathcal{R}^Δ , see figure 1. Additionally, there exists natural covering maps $\check{\rho}$ and ρ^Δ from $\tilde{\mathcal{R}}$
 184 and \mathcal{R}^Δ to the infinite cylinder $\mathcal{C} = \{v \in \mathbb{C}, v \equiv v + 2i\pi\}$, with ramification points $[2i\pi a, P]$,
 185 $a \in \mathbb{Z} + 1/2$ (and additionally $a \notin \Delta$ for ρ^Δ). One-point statistics of the KPZ height field
 186 with periodic boundaries are expressed below for various initial conditions as an integral
 187 over a loop around the cylinder. The integrand involves holomorphic differentials traced
 188 over the covering maps $\check{\rho}$ or ρ^Δ , i.e. summed over all the sheets of the Riemann surfaces
 189 covering the cylinder. The functions and meromorphic differentials needed are studied in
 190 detail in section 4.

191 2.2 Flat initial condition

192 We consider in this section the one-point distribution $\mathbb{P}_{\text{flat}}(h(x, t) > u)$ of KPZ fluctuations
 193 with periodic boundary conditions, $h(x, t) = h(x + 1, t)$, and flat initial condition $h(x, 0) =$
 194 0 . We claim that the properly renormalized random field $h(x, t)$ has the cumulative density
 195 function ¹

$$\mathbb{P}_{\text{flat}}(h(x, t) > u) = \int_{\gamma} (\text{tr}_{\check{\rho}} Z_{t,u}^{\text{flat}})(\nu) \, \nu, \quad (1)$$

196 with γ a loop around the infinite cylinder \mathcal{C} with winding number 1. The holomorphic
 197 differential $Z_{t,u}^{\text{flat}}$ on the Riemann surface $\tilde{\mathcal{R}}$, defined away from ramification points of $\check{\rho}$ as

$$Z_{t,u}^{\text{flat}}([\nu, P]) = \exp \left(\int_{[-\infty, \emptyset]}^{[\nu, P]} S_{t,u}^{\text{flat}} \right) \frac{d\nu}{2i\pi}, \quad (2)$$

¹The definition of $h(x, t)$ used in this paper corresponds to a growth of the height function for TASEP in the positive direction, which after proper rescaling gives a growth of the KPZ height function in the negative direction, $h(x, t) \rightarrow -\infty$ when $t \rightarrow \infty$, corresponding to a negative coefficient $-\lambda \rightarrow -\infty$ in front of the non-linear term in the KPZ equation. The same convention for the sign of u is used in [39]. The opposite convention is used in [40], with the notation $x = -u$ there.

198 is built from an integral of the meromorphic differential $S_{t,u}^{\text{flat}}$ on $\tilde{\mathcal{R}}$ given by

$$S_{t,u}^{\text{flat}}(p) = \left(t\chi'(p) - u\chi''(p) - \frac{1/4}{1 + e^{-v}} + \frac{\chi''(p)^2}{2} \right) dv \quad (3)$$

199 at $p = [v, P] \in \tilde{\mathcal{R}}$ away from ramification points of $\tilde{\rho}$. Here, χ, χ', χ'' are meromor-
 200 phic functions on $\tilde{\mathcal{R}}$, obtained by analytic continuations of the polylogarithm $\chi_\theta(\nu) =$
 201 $-\text{Li}_{5/2}(-e^\nu)/\sqrt{2\pi}$ and its derivatives, see sections 4.4 and 4.5, and equations (66), (64),
 202 (57), (50) for precise definitions. We also refer to section 4 for explicit formulas for analytic
 203 continuations and proofs that $Z_{t,u}^{\text{flat}}$ is indeed holomorphic on $\tilde{\mathcal{R}}$ and independent from the
 204 path of integration in (2).

205 The trace of a meromorphic differential with respect to a covering map is defined in
 206 (34). For the covering map $\tilde{\rho} : [\nu, P] \mapsto \nu$ from the Riemann surface $\tilde{\mathcal{R}}$ to the infinite
 207 cylinder \mathcal{C} , the trace $\text{tr}_{\tilde{\rho}}$ consists in summing over all the infinite strips $\mathcal{S}_P^0 = \{[\nu, P], -\pi <$
 208 $\text{Im } \nu \leq \pi\}$ partitioning $\tilde{\mathcal{R}}$, see sections 3.8.1 and 3.8.2 for a precise definition of $\tilde{\mathcal{R}}$, and
 209 especially the left side of figure 13 for a graphical representation of how $\tilde{\mathcal{R}}$ is partitioned
 210 into infinite strips. The integral in (1) is independent of the loop γ , since $\text{tr}_{\tilde{\rho}} Z_{t,u}^{\text{flat}}$ is
 211 holomorphic on the cylinder \mathcal{C} by the properties of the trace. With the change of variable
 212 $z = e^\nu$, defining a covering map λ from \mathcal{C} to the punctured plane $\mathbb{C}^* = \mathbb{C} \setminus \{0\}$, the
 213 expression (1) can alternatively be written as the integral over a loop encircling 0 in \mathbb{C}^* ,
 214 and $\mathbb{P}_{\text{flat}}(h(x, t) > u)$ is then the residue at the essential singularity $z = 0$ of $\text{tr}_{\lambda \circ \tilde{\rho}} Z_{t,u}^{\text{flat}}$.

215 The trace in (1) can be evaluated explicitly by considering a partition into infinite
 216 strips $\mathcal{S}_P^0, P \in \mathbb{Z} + 1/2$ of the Riemann surface $\tilde{\mathcal{R}}$, see figure 13 left, so that $(\text{tr}_{\tilde{\rho}} Z_{t,u}^{\text{flat}})(\nu) =$
 217 $\sum_{P \in \mathbb{Z} + 1/2} Z_{t,u}^{\text{flat}}([\nu, P])$. In terms of the functions χ_P and I_0 defined in (64), (68) one has

$$\mathbb{P}_{\text{flat}}(h(x, t) > u) = \sum_{P \in \mathbb{Z} + 1/2} \frac{(-1)^{|P|} V_P^2}{4^{|P|}} \int_{c-i\pi}^{c+i\pi} \frac{d\nu}{2i\pi} e^{t\chi_P(\nu) - u\chi'_P(\nu) + I_0(\nu) + \frac{1}{2} \int_{-\infty}^{\nu} dv \chi''_P(v)^2}, \quad (4)$$

218 with $c \in \mathbb{R}^*$. The summation is over all finite subsets P of $\mathbb{Z} + 1/2$, and V_P is the
 219 Vandermonde determinant

$$V_P = \prod_{\substack{a, b \in P \\ a > b}} \left(\frac{2i\pi a}{4} - \frac{2i\pi b}{4} \right). \quad (5)$$

220 The function χ_P is the restriction of χ to the sheet \mathbb{C}_P , I_0 is given by $e^{I_0(\nu)} = (1 + e^\nu)^{-1/4}$
 221 if $c < 0$ or $e^{I_0(\nu)} = e^{-\nu/4}(1 + e^{-\nu})^{-1/4}$ if $c > 0$, and $\int_{-\infty}^{\nu} dv \chi''_P(v)^2 = \lim_{\Lambda \rightarrow \infty} -|P|^2 \log \Lambda +$
 222 $\int_{-\Lambda}^{\nu} dv \chi''_P(v)^2$. The extra factor $(-1)^{|P|} V_P^2/4^{|P|}$ in (4) compared to (1) comes from the
 223 analytic continuation of $\int_{-\infty}^{\nu} dv \chi''_\theta(v)^2$ from \mathbb{C}_θ to \mathbb{C}_P , see sections 4.7 and 4.8.

224 The expression (1) is justified in section 5.1 by showing that (4) is equivalent to ex-
 225 act results obtained previously in [39, 40] from large scale asymptotics for the totally
 226 asymmetric simple exclusion process (TASEP), a discrete interface growth model in KPZ
 227 universality. This shows in particular that the corresponding expressions from [39] and [40]
 228 agree, which had not been properly derived before, and simply represent distinct choices
 229 for a fundamental domain $\tilde{\mathcal{R}}$ in \mathcal{R} .

230 The probability $\mathbb{P}_{\text{flat}}(h(x, t) > u)$ is interpreted in section 2.6.3 as a N -soliton τ function
 231 for the KdV equation, $N \rightarrow \infty$, averaged over the common velocity ν of the solitons,
 232 which is also identified as a moduli parameter for specific singular hyperelliptic Riemann
 233 surfaces.

234 **2.3 Sharp wedge initial condition**

235 We consider in this section one-point statistics of KPZ fluctuations with sharp wedge ² ini-
 236 tial condition $h(x, 0) = -\frac{|x-1/2|}{0^+}$, where $h(x, t)$ is defined after appropriate regularization.
 237 More generally, it is expected from large deviation results [38] that any initial condition
 238 of the form $h(x, 0) = h_0(x)/\epsilon$ where h_0 is continuous on the circle $x \equiv x + 1$ with a global
 239 minimum 0 reached at $x = 1/2$ only, is equivalent in the limit $\epsilon \rightarrow 0^+$ to sharp wedge
 240 initial condition.

241 We show in section 5.2 that known exact formulas [39, 40] for the cumulative density
 242 function of the KPZ height are equivalent to

$$\mathbb{P}_{\text{sw}}(h(x, t) > u) = \sum_{\substack{\Delta \subset \mathbb{Z}+1/2 \\ \Delta \equiv \Delta+1}} \Xi_x^\Delta \int_\gamma (\text{tr}_{\tilde{\rho}^\Delta} Z_{t,u}^{\Delta, \text{sw}})(\nu), \quad (6)$$

243 with γ as in (1), $\tilde{\rho}^\Delta = \rho^\Delta$, $\Delta \neq \emptyset$ the covering map defined in section 3.8.3 from \mathcal{R}^Δ to
 244 the infinite cylinder \mathcal{C} and $\tilde{\rho}^\emptyset = \tilde{\rho}$ the covering map defined in section 3.8.1 from $\tilde{\mathcal{R}}$ to \mathcal{C} ,
 245 where $\tilde{\mathcal{R}} = \mathcal{R}/\tilde{\mathfrak{g}}$ is the quotient of $\mathcal{R}^\emptyset = \mathcal{R}$ by a group $\tilde{\mathfrak{g}}$ of translation automorphisms
 246 that exist only for $\Delta = \emptyset$. The trace with respect to $\tilde{\rho}^\Delta$ gives a holomorphic differential
 247 on the cylinder \mathcal{C} , periodic in ν with period $2i\pi$. The sum over non-isomorphic Riemann
 248 surfaces \mathcal{R}^Δ is weighted by

$$\Xi_x^\Delta = (i/4)^{|\Delta|} \sum_{\substack{A \subset \Delta \\ |A| = |\Delta \setminus A|}} e^{2i\pi x \left(\sum_{a \in A} a - \sum_{a \in \Delta \setminus A} a \right)} V_A^2 V_{\Delta \setminus A}^2. \quad (7)$$

249 with V_A the Vandermonde determinant (5) and $2\pi \left(\sum_{a \in A} a - \sum_{a \in \Delta \setminus A} a \right)$ the momentum
 250 coupled to the coordinate x along the interface, which appears only through Ξ_x^Δ in (6).
 251 Only sets Δ with cardinal $|\Delta|$ even contribute. The holomorphic differential

$$Z_{t,u}^{\Delta, \text{sw}}([\nu, P]) = \exp \left(\int_{[-\infty, \emptyset]}^{[\nu, P]} S_{t,u}^{\Delta, \text{sw}} \right) \frac{d\nu}{2i\pi} \quad (8)$$

252 is built from an integral with appropriate regularization at $[-\infty, \emptyset]$ of the meromorphic
 253 differential $S_{t,u}^{\Delta, \text{sw}}$ on \mathcal{R}^Δ given by

$$S_{t,u}^{\Delta, \text{sw}}(p) = (t\chi'^\Delta(p) - u\chi''^\Delta(p) + \chi''^\Delta(p)^2)dv \quad (9)$$

254 at $p = [\nu, P] \in \mathcal{R}^\Delta$ away from ramification points of ρ^Δ . The functions χ^Δ , χ'^Δ , χ''^Δ ,
 255 analogues of χ , χ' , χ'' from the previous section with ramification points $[2i\pi a, P]$, $a \in \Delta$
 256 removed, are defined in (86), (91).

257 The trace in (6) can be evaluated more explicitly by considering appropriate parti-
 258 tions into sheets of the Riemann surfaces $\tilde{\mathcal{R}}$ and \mathcal{R}^Δ . For the term $\Delta = \emptyset$, one has
 259 $(\text{tr}_{\tilde{\rho}} Z_{t,u}^{\emptyset, \text{sw}})(\nu) = \sum_{P \subset \mathbb{Z}+1/2} Z_{t,u}^{\emptyset, \text{sw}}([\nu, P])$ like for flat initial condition, see figure 13 left.
 260 For $\Delta \neq \emptyset$, one has to sum instead over all strips \mathcal{S}_P^m , $P \cap \Delta = \emptyset$, $m \in \mathbb{Z}$, see figure 16,
 261 leading to an integral between $c - i\infty$ and $c + i\infty$ of $Z_{t,u}^{\emptyset, \text{sw}}([\nu, P])$, summed over all P ,
 262 $P \cap \Delta = \emptyset$. The symmetry of the extension to $\tilde{\mathcal{R}}$ of $Z_{t,u}^{\emptyset, \text{sw}}$ under the holomorphic automor-
 263 phism $\bar{\mathcal{T}}$ defined in (44), see section 3.8.4, allows to sum instead over all Δ and not just
 264 equivalence classes $\Delta \equiv \Delta + 1$, and integrate only over the strip \mathcal{S}_P^0 from each \mathcal{R}^Δ . Using

²Also called step or domain wall initial condition in the context of TASEP as a microscopic model.

265 explicit analytic continuations from section 4.9.2, we finally obtain that (6) is equivalent
 266 to the more explicit expression

$$\mathbb{P}_{\text{sw}}(h(x, t) > u) = \sum_{\Delta \in \mathbb{Z} + 1/2} \Xi_x^\Delta \sum_{\substack{P \in \mathbb{Z} + 1/2 \\ P \cap \Delta = \emptyset}} (i/4)^{2|P|} \left(\prod_{a \in P} \prod_{\substack{b \in P \cup \Delta \\ b \neq a}} \left(\frac{2i\pi a}{4} - \frac{2i\pi b}{4} \right)^2 \right) \\ \times \int_{c-i\pi}^{c+i\pi} \frac{d\nu}{2i\pi} e^{t\chi_P^\Delta(\nu) - u\chi'_P(\nu) + f_{-\infty}^\nu \int d\nu \chi''_P^\Delta(\nu)^2}, \quad (10)$$

267 with $|P|$ the number of elements in P , χ_P^Δ the restriction of χ^Δ to the sheet \mathbb{C}_P of \mathcal{R}^Δ
 268 given in (87), and f the regularized integral subtracting the divergent logarithmic term
 269 at $-\infty$ like in (92). The expression (10) is derived in section 5.2 from earlier works [39]
 270 and [40] using the structure of the Riemann surfaces \mathcal{R}^Δ detailed in section 3.8.3 and
 271 explicit analytic continuations obtained in section 4.9.2. This shows in particular that
 272 the expressions from [39] and [40] about sharp wedge initial condition agree, which was
 273 missing so far.

274 2.4 Stationary initial condition

275 Exact results have also been obtained for one-point statistics of the KPZ height with
 276 stationary initial condition [39, 41], where $x \mapsto h(x, 0)$ is a standard Brownian bridge. The
 277 formulas in that case are essentially the same as for sharp wedge initial condition, with
 278 only an additional harmless factor. Starting either with equation (7) of [39] (for $x = 0$) or
 279 with equation (2.1) of [41] for general x , we obtain by comparison to (6)

$$\mathbb{P}_{\text{stat}}(h(x, t) > u) = \sum_{\substack{\Delta \in \mathbb{Z} + 1/2 \\ \Delta \equiv \Delta + 1}} \Xi_x^\Delta \int_\gamma (\text{tr}_{\rho^\Delta} Z_{t,u}^{\Delta, \text{stat}})(\nu), \quad (11)$$

280 with

$$Z_{t,u}^{\Delta, \text{stat}}([\nu, P]) = -\sqrt{2\pi} e^{-\nu} \partial_u Z_{t,u}^{\Delta, \text{sw}}([\nu, P]) \quad (12)$$

281 and the same notations as in (6). A more explicit formula can be written by inserting the
 282 extra factor $-\sqrt{2\pi} e^{-\nu} \partial_u$ into (10).

283 2.5 Multiple-time statistics with sharp wedge initial condition

284 The joint distribution of the height at multiple times $0 < t_1 < \dots < t_n$ and corresponding
 285 positions x_j was obtained by Baik and Liu for sharp wedge initial condition in [42]. After
 286 some rewriting in section 5.3.1 based on explicit analytic continuations from section 4.9
 287 and 4.10, we obtain

$$\mathbb{P}(h(x_1, t_1) > u_1, \dots, h(x_n, t_n) > u_n) \quad (13) \\ = \left(\prod_{\ell=1}^n \sum_{\Delta_\ell \in \mathbb{Z} + 1/2} \sum_{\substack{P_\ell \in \mathbb{Z} + 1/2 \\ P_\ell \cap \Delta_\ell = \emptyset}} \right) \int_{c_1 - i\pi}^{c_1 + i\pi} \frac{d\nu_1}{2i\pi} \dots \int_{c_n - i\pi}^{c_n + i\pi} \frac{d\nu_n}{2i\pi} \Xi_{x_1, \dots, x_n}^{\Delta_1, \dots, \Delta_n}(\nu_1, \dots, \nu_n) \\ \times \left(\prod_{\ell=1}^n e^{(t_\ell - t_{\ell-1})\chi^{\Delta_\ell} - (u_\ell - u_{\ell-1})\chi'^{\Delta_\ell} + 2J^{\Delta_\ell}(p_\ell)} \right) \left(\prod_{\ell=1}^{n-1} e^{-2K^{\Delta_\ell, \Delta_{\ell+1}}(p_\ell, p_{\ell+1})} \right),$$

288 with $t_0 = u_0 = 0$, $c_n < \dots < c_1 < 0$, $p_\ell = [\nu_\ell, P_\ell]$ a point on the Riemann surface $\mathcal{R}^{\Delta_\ell}$, χ^{Δ_ℓ}
 289 and χ'^{Δ_ℓ} holomorphic functions on $\mathcal{R}^{\Delta_\ell}$ given in (86), (91), $e^{2J^{\Delta_\ell}}$ the meromorphic function

290 on \mathcal{R}^Δ from (96) and $e^{2K^{\Delta,\Gamma}}$ a meromorphic function on $\mathcal{R}^\Delta \times \mathcal{R}^\Gamma$ defined by (118). The
 291 collection of Riemann surfaces $\mathcal{R}^{\Delta_\ell}$ in (13) is weighted by the meromorphic function on
 292 \mathbb{C}^n

$$\begin{aligned} & \Xi_{x_1, \dots, x_n}^{\Delta_1, \dots, \Delta_n}(\nu_1, \dots, \nu_n) \\ &= \left(\prod_{\ell=1}^n \sum_{\substack{A_\ell \sqsubset \Delta_\ell \\ |A_\ell| = |\Delta_\ell \setminus A_\ell|}} \right) \prod_{\ell=1}^n \left((i/4)^{|\Delta_\ell|} V_{A_\ell}^2 V_{\Delta_\ell \setminus A_\ell}^2 e^{2i\pi(x_\ell - x_{\ell-1}) \left(\sum_{a \in A_\ell} a - \sum_{a \in \Delta_\ell \setminus A_\ell} a \right)} \right) \\ & \quad \times \prod_{\ell=1}^{n-1} \frac{(1 - e^{\nu_{\ell+1} - \nu_\ell})^{|\Delta_\ell|/2} (1 - e^{\nu_\ell - \nu_{\ell+1}})^{|\Delta_{\ell+1}|/2}}{(1 - e^{\nu_{\ell+1} - \nu_\ell}) V_{A_\ell, A_{\ell+1}}(\nu_\ell, \nu_{\ell+1}) V_{\Delta_\ell \setminus A_\ell, \Delta_{\ell+1} \setminus A_{\ell+1}}(\nu_\ell, \nu_{\ell+1})}, \end{aligned} \quad (14)$$

293 with $x_0 = 0$, V_A the Vandermonde determinant (5) and

$$V_{A,B}(\nu, \mu) = \prod_{a \in A} \prod_{b \in B} \left(\frac{2i\pi a - \nu}{4} - \frac{2i\pi b - \mu}{4} \right). \quad (15)$$

294 Since $\Xi_{x_1, \dots, x_n}^{\Delta_1, \dots, \Delta_n}(\nu_1, \dots, \nu_n) = 0$ when any of the $|\Delta_\ell|$ is odd because of the constraints
 295 $|A_\ell| = |\Delta_\ell \setminus A_\ell|$, only sets Δ_ℓ containing an even number of elements contribute to (13).

296 The same reasoning as the one between (10) and (6) allows to express (13) in terms of
 297 non-isomorphic Riemann surfaces and a trace over covering maps. One has

$$\begin{aligned} & \mathbb{P}(h(x_1, t_1) > u_1, \dots, h(x_n, t_n) > u_n) \\ &= \left(\prod_{\ell=1}^n \sum_{\substack{\Delta_\ell \sqsubset \mathbb{Z} + 1/2 \\ \Delta_\ell = \Delta_{\ell+1}}} \right) \int_{\gamma_1} \dots \int_{\gamma_n} \Xi_{x_1, \dots, x_n}^{\Delta_1, \dots, \Delta_n}(\nu_1, \dots, \nu_n) \\ & \quad \times \text{tr}_{\tilde{\rho}^{\Delta_1}} \dots \text{tr}_{\tilde{\rho}^{\Delta_n}} \frac{\prod_{\ell=1}^n Z_{t_\ell - t_{\ell-1}, u_\ell - u_{\ell-1}}^{\Delta_\ell, \text{sw}}(\nu_\ell)}{\prod_{\ell=1}^{n-1} e^{2K^{\Delta_\ell, \Delta_{\ell+1}}}(\nu_\ell, \nu_{\ell+1})}, \end{aligned} \quad (16)$$

298 with $\text{tr}_{\tilde{\rho}^{\Delta_\ell}}$ acting on ν_ℓ , $Z_{\delta t, \delta u}^{\Delta, \text{sw}}$ the holomorphic differential from (8), and a loop γ_ℓ with
 299 winding number 1 around the infinite cylinder \mathcal{C} for the variable ν_ℓ . Because of the
 300 trace, the integrand in (16) is meromorphic in \mathbb{C}^n . The loops γ_ℓ do not cross each other,
 301 as the order $\text{Re } \nu_n < \dots < \text{Re } \nu_1$ must be preserved because of the presence of simple
 302 poles at $\nu_{\ell+1} = \nu_\ell + 2i\pi m$, $m \in \mathbb{Z}$. Interestingly, it can be shown that such poles exist
 303 only when $\Delta_{\ell+1} = \Delta_\ell + m$ and $P_{\ell+1} = P_\ell + m$ (and only the sector $A_{\ell+1} = A_\ell + m$ of
 304 $\Xi_{x_1, \dots, x_n}^{\Delta_1, \dots, \Delta_n}$ contributes to them), corresponding to points $p_\ell = [\nu_\ell, P_\ell]$ and $p_{\ell+1} = [\nu_{\ell+1}, P_{\ell+1}]$
 305 coinciding on the Riemann surface $\mathcal{R}^{\Delta_\ell} \sim \mathcal{R}^{\Delta_{\ell+1}}$, see section 5.3.2.

306 2.6 Discussion

307 In this section, we discuss various interpretations of the exact formulas given above for
 308 KPZ fluctuations with periodic boundaries.

309 2.6.1 Full dynamics from large deviations

310
 311 In the long time limit, KPZ fluctuations in finite volume converge to a stationary state
 312 where the interface has the same statistics as a Brownian motion with appropriate bound-
 313 ary conditions. Large deviations corresponding to fluctuations of the height with an ampli-
 314 tude of order t when $t \rightarrow \infty$ are on the other hand non-Gaussian and can be characterized
 315 by a generating function of the form [36, 43]

$$\langle e^{sh(x,t)} \rangle \simeq \theta(s) e^{te(s)}, \quad (17)$$

316 where $e(s)$ involves an infinite sum of square roots. At finite time, the generating function
 317 of the height is given exactly by a sum of infinitely many terms of the same form,

$$\langle e^{sh(x,t)} \rangle = \sum_n \theta_n(s) e^{t e_n(s)} \quad (18)$$

318 with n an index labelling sheets of Riemann surfaces, see equations (122), (131). Known
 319 results for the spectrum of TASEP [44, 45] indicate that the stationary contribution cor-
 320 responds to the sheet \mathbb{C}_\emptyset of \mathcal{R} when $\text{Re } s > 0$.

321 These observations suggest the possibility to guess the full finite time dynamics of
 322 KPZ fluctuations in finite volume from the solution of the static problem of stationary
 323 large deviations alone. For flat initial condition in particular, the functions $\theta_P(s)$, $e_P(s)$
 324 (or, more properly, their analogues for the probability (4) after Fourier transform, see
 325 section 5.1.1) are simply analytic continuations of $\theta_\emptyset(s)$, $e_\emptyset(s)$ to all the sheets of the
 326 Riemann surface $\check{\mathcal{R}}$. The situation is less straightforward for sharp wedge and stationary
 327 initial conditions, where a natural interpretation is still missing for the coefficients Ξ_x^Δ
 328 weighting the Riemann surfaces \mathcal{R}^Δ covered by \mathcal{R} in (6) and (11).

329 The stationary large deviations problem can be studied independently from the dynam-
 330 ics, using e.g. matrix product representations for discrete models [46, 47]. This approach
 331 was recently exploited in [38] to express the factor $\theta(s)$ in (17) for general initial condition
 332 as the probability that a gas of infinitely many non-intersecting Brownian bridges with
 333 density $1/s$ stays under the graph of the initial condition $h(x, 0) = h_0(x)$. More precisely,
 334 it was shown that

$$\theta(s) = \frac{\mathbb{P}(b_{-1} < h_0 | \dots < b_{-2} < b_{-1})}{\mathbb{P}(b_{-1} < b_0 | \dots < b_{-2} < b_{-1}, b_1 < b_2 < \dots)}, \quad (19)$$

335 where $b_j(x) - b_j(0)$, $j \in \mathbb{Z}$ are independent standard Brownian bridges with $b_j(0) = b_j(1)$,
 336 distances between consecutive endpoints $b_{j+1}(0) - b_j(0)$ are independent exponentially
 337 distributed random variables with parameter s , and $b_0(0) = h_0(0)$. Deriving exact formulas
 338 from the Brownian bridge representation is still an open problem, though, even for the
 339 simple initial conditions (flat, Brownian, sharp wedge) for which the result is known from
 340 Bethe ansatz, see however [48] for related work.

341 The idea that the contributions of the excited states of a theory should follow from
 342 that of the ground state by analytic continuation with respect to some parameter is not
 343 new, see for instance [49] for the quantum quartic oscillator, [50] for the Ising field theory
 344 on a circle (where the ground state energy is interestingly also given by an infinite sum
 345 of square roots, but with conjugate branch points paired), or [51] for models described
 346 by the thermodynamic Bethe ansatz. In the context of the Schrödinger equation for a
 347 particle in a potential, a unifying scheme appears to be exact WKB analysis [52], which
 348 uses tools from the theory of resurgent functions in order to reconstruct a single valued
 349 eigenfunction from the multivalued classical action. Such an approach might be useful for
 350 KPZ in order to derive known exact formulas without having to consider discrete models,
 351 by starting directly from the associated backward Fokker-Planck equation, a rather formal
 352 infinite dimensional linear partial differential equation acting on the functional space of
 353 allowed initial heights.

354 2.6.2 Particle-hole excitations

355
 356 The finite sets of half-integers labelling the sheets of the Riemann surfaces $\check{\mathcal{R}}$, \mathcal{R}^Δ con-
 357 sidered in this paper have a natural interpretation in terms of particle-hole excitations

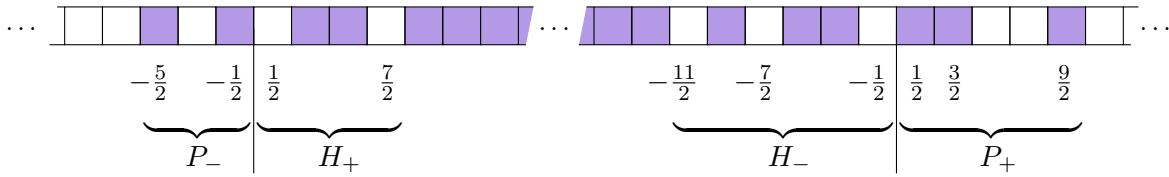


Figure 2: Picture of particle-hole excitations at both edges of the Fermi sea corresponding to sets P , H of half-integers. The notations P_{\pm} , H_{\pm} indicate the positive and negative elements of the sets.

358 at both edges of a Fermi sea, see figure 2. This is most clearly seen on the expressions
 359 from [39] for the generating function $\langle e^{sh(x,t)} \rangle$ of the KPZ height discussed in sections 5.1.1
 360 and 5.2.1.

361 From the exact Bethe ansatz solution of TASEP, eigenstates of the time evolution
 362 operator in the KPZ scaling regime are labelled by sets P and H corresponding to particle-
 363 hole excitations, interpreted respectively as momenta of quasiparticle and hole excitations
 364 relative to the Fermi momentum on both sides of the Fermi sea, see figure 2. Excitations
 365 only occur in particle-hole pairs, with “neutral charge”: no particle or hole excitation
 366 alone occurs. The stationary state $P = H = \emptyset$ corresponds in particular to the completely
 367 filled Fermi sea.

368 For sharp wedge initial condition, the sets P and H must satisfy the constraint $|P|_{\pm} =$
 369 $|H|_{\mp}$ that the number of positive elements of P is equal to the number of negative elements
 370 of H and vice versa, see equations (131), (133). This corresponds to the fact that particle-
 371 hole excitations occur independently on both sides of the Fermi sea, i.e. quasiparticles
 372 at a finite distance from either side of the Fermi sea may be excited above the Fermi
 373 momentum but will stay at a finite distance of the same edge of the Fermi sea: excitation
 374 from one edge to the other (known as Umklapp processes in condensed matter physics) are
 375 suppressed for KPZ. It is remarkable that the constraints $|P|_{\pm} = |H|_{\mp}$ are automatically
 376 verified in (6), (11) from the way the collection of non-isomorphic Riemann surfaces \mathcal{R}^{Δ}
 377 are partitioned into sheets \mathbb{C}_P , with $H = P \ominus \Delta$ the symmetric difference of P and Δ
 378 (union minus intersection), see section 5.2.1.

379 Flat initial condition (122), (123) corresponds to the special case $P = H$, where mo-
 380 menta of quasiparticles excitations on one side of the Fermi sea are identical to momenta
 381 of hole excitations on the other side of the Fermi sea. It is again quite remarkable that the
 382 resulting constraint $|P|_{+} = |P|_{-}$ naturally appears for the sets P labelling (half)-sheets
 383 of the Riemann surface $\tilde{\mathcal{R}}$, see figure 13 on the right. The extra constraint $P = H$ for flat
 384 initial condition is understood from TASEP as the fact that a specific microscopic state
 385 representing a flat interface has nonzero overlap only with Bethe eigenstates correspond-
 386 ing to particle-hole excitations satisfying the constraint [53]. This has the consequence to
 387 increase the spectral gap (i.e. to reduce the relaxation time) compared to a generic initial
 388 state, as was already recognized in [54].

389 Compared to the states contributing for flat initial condition, which have zero momen-
 390 tum, a non-empty symmetric difference $\Delta = P \ominus H$ corresponds to an imbalance between
 391 both sides of the Fermi sea, and is related through the coefficients Ξ_x^{Δ} in (7) to motion
 392 along the KPZ interface, with momentum $2\pi(\sum_{a \in P} a - \sum_{a \in H} a)$.

393 The interpretation of KPZ fluctuations in terms of particle-hole excitations close to the
 394 Fermi level is reminiscent of Luttinger liquid universality describing large scale dynamics
 395 of one-dimensional quantum fluids, with however several important distinctions. In addi-
 396 tion to the absence mentioned above of Umklapp terms for KPZ, unlike in the Luttinger
 397 liquid setting, the dispersion relation, linear for the Luttinger liquid by construction after

398 expanding around the Fermi level, is given for KPZ by $\kappa_a(\nu)^3 \sim |a|^{3/2}$ at large wave num-
 399 ber $2\pi a$, indicating the existence of a singularity at the Fermi level. From a mathematical
 400 point of view, the difference amounts to the presence of polylogarithms with integer index
 401 (especially the dilogarithm Li_2) for various quantities in the Luttinger liquid case, while
 402 half-integer polylogarithms appear for KPZ.

403 2.6.3 KdV solitons

404
 405 The exact formula for the probability $\mathbb{P}_{\text{flat}}(h(y, 3t) > x)$ ³ with flat initial condition has
 406 a nice interpretation in terms of a solution to the Korteweg-de Vries (KdV) equation
 407 representing infinitely many solitons in interaction, see e.g. [55–57] for an introduction to
 408 classical non-linear integrable equations. As explained below, the relation to KdV suggests
 409 that the parameter ν appearing in various expressions in sections 2.2 to 2.5 should be
 410 interpreted as a moduli parameter for a class of degenerate hyperelliptic Riemann surfaces.
 411 The relation to KdV is most visible on the Fredholm determinant expression (22), (23)
 412 for $\mathbb{P}_{\text{flat}}(h(y, 3t) > x)$, which has the same kind of Cauchy kernel (24) as KdV N -soliton
 413 τ functions with $N \rightarrow \infty$.

414 We recall that any determinant of the form $\tau(x, t) = \det(1 - M_N^{\text{KdV}}(x, t))$ where
 415 $M_N^{\text{KdV}}(x, t)$ is a $N \times N$ square matrix with matrix elements $M_N^{\text{KdV}}(x, t)_{a,b} = e^{2x\kappa_a + 2t\kappa_a^3 + \lambda_a}$
 416 $/(\kappa_a + \kappa_b)$ depending on $2N$ arbitrary coefficients κ_a, λ_a is called a τ function for KdV,
 417 such that $u(x, t) = 2\partial_x^2 \log \tau(x, t)$ is a solution of the KdV equation

$$4\partial_t u = 6u\partial_x u + \partial_x^3 u. \quad (20)$$

418 Such a solution corresponds to N solitons in interaction, the constants κ_a determining the
 419 asymptotic velocities $-\kappa_a^2$ of the solitons when they are far away from each other, and
 420 the whole Cauchy determinant $\det(1 - M_N^{\text{KdV}}(x, t))$ describing how the solitons interact
 421 otherwise.

422 The KdV equation (20) belongs to a family of non-linear partial differential equations
 423 known as the KdV hierarchy. The n -th equation of the hierarchy, n odd, involves deriva-
 424 tives with respect to the space variable x and to a time variable t_n . The case $n = 3$
 425 corresponds to (20), with $t_3 = t$. Soliton solutions to higher equations in the hierarchy are
 426 obtained by replacing $2t\kappa_a^3$ in $M_N^{\text{KdV}}(x, t)_{a,b}$ above by $2t_n\kappa_a^n$.

427 We observe that the probability $\mathbb{P}_{\text{flat}}(h(y, 3t) > x)$ of the KPZ height with flat initial
 428 condition, independent of y , can be written as an integral over ν of a determinant (of
 429 Fredholm type, i.e. corresponding to an infinite dimensional operator) with a kernel of
 430 the same form as $M_\infty^{\text{KdV}}(x, t)$ above. Indeed, using (4), (64), (51), (184) and the Cauchy
 431 determinant identity

$$\det\left(\frac{1}{\kappa_a + \kappa_b}\right)_{a,b \in P} = \frac{\prod_{a>b \in P} (\kappa_a - \kappa_b)^2}{\prod_{a,b \in P} (\kappa_a + \kappa_b)}, \quad (21)$$

432 see section 5.1.2 for more details, one has

$$\mathbb{P}_{\text{flat}}(h(y, 3t) > x) = \int_{c-i\pi}^{c+i\pi} \frac{d\nu}{2i\pi} \tau_{\text{flat}}(x, t; \nu), \quad (22)$$

433 with the τ function defined by⁴

$$\tau_{\text{flat}}(x, t; \nu) = e^{3t\chi_\emptyset(\nu) - x\chi'_\emptyset(\nu) + I_0(\nu) + J_\emptyset(\nu)} \det(1 - M_{\text{flat}}(x, t; \nu)), \quad (23)$$

³The change $(t, u, x) \rightarrow (3t, x, y)$ in this section is needed to conform to standard notations for KdV.

⁴The exponential of a linear function of x in front of the Fredholm determinant does not contribute to $u_{\text{flat}} = 2\partial_x^2 \log \tau_{\text{flat}}$, which is thus still solution of the KdV equation.

434 where χ_\emptyset is defined in (57), I_0 in (68) and J_\emptyset in (74). The operator $M_{\text{flat}}(x, t; \nu)$, acting
 435 on sequences indexed by $\mathbb{Z} + 1/2$, has the kernel

$$M_{\text{flat}}(x, t; \nu)_{a,b} = \frac{e^{2x\kappa_a(\nu) + 2t\kappa_a^3(\nu) + 2 \int_{-\infty}^{\nu} dv \frac{\chi_\emptyset''(v)}{\kappa_a(v)}}}{\kappa_a(\nu) (\kappa_a(\nu) + \kappa_b(\nu))} \quad (24)$$

436 with $\kappa_a(v)$ a specific branch of $\sqrt{4i\pi a - 2v}$ defined in (50). When $c < 0$, this is directly
 437 the result from [40], see equations (124), (125). When $c > 0$, a little more work is needed
 438 in order to rewrite into (22) the integral for ν between $c - i\infty$ and $c + i\infty$ of the Fredholm
 439 determinant in [39], which corresponds to a representation of $\check{\mathcal{R}}$ distinct from the one in
 440 (4), see section 5.1.1.

441 KPZ with flat initial condition thus involves a τ function for KdV, i.e. $u_{\text{flat}}(x, t; \nu) =$
 442 $2\partial_x^2 \log \tau_{\text{flat}}(x, t; \nu)$ is a solution of the KdV equation (20) for any ν . This solution corre-
 443 sponds to a gas of infinitely many solitons with (complex) velocities $-\kappa_a^2(v) = 2\nu - 4i\pi a$,
 444 $a \in \mathbb{Z} + 1/2$. The probability $\mathbb{P}_{\text{flat}}(h(y, 3t) > x)$ is obtained by averaging $\tau_{\text{flat}}(x, t; \nu)$ over
 445 the common velocity modulo $2i\pi$ of the solitons. Time variables for higher equations in
 446 the KdV hierarchy naturally appear in (24) as $t_{2m+1} = \chi_\emptyset^{(m+2)}(\nu)/(2m+1)!!$, see equation
 447 (187).

448 The possibility to interpret KPZ as a gas of solitons was put forward by Fogedby [58]
 449 starting with the WKB solution of the Fokker-Planck equation in the weak noise limit, with
 450 in particular the prediction of the dispersion relation $|k|^{3/2}$ as a function of momentum k ,
 451 corresponding in our notations to $\kappa_a^3(\nu) \sim |a|^{3/2}$ for large a , see also [59] for recent related
 452 work.

453 Since flat initial condition corresponds to $h(y, 0) = 0$, the probability $\mathbb{P}_{\text{flat}}(h(y, 3t) > x)$
 454 is expected to converge to $1_{\{x < 0\}}$ when $t \rightarrow 0$. Furthermore, since the KPZ height in finite
 455 volume at short time must have the same statistics as the KPZ fixed point on \mathbb{R} [60], one
 456 should have $\mathbb{P}_{\text{flat}}(h(y, 4t) > -t^{1/3}x) \rightarrow F_1(x)$ when $t \rightarrow 0$, where F_1 is the GOE Tracy-
 457 Widom distribution from random matrix theory. This was checked numerically with good
 458 agreement in [39]. In terms of the KdV interpretation, we conjecture that the short time
 459 limit corresponds to the known scaling solution $(t/4)^{2/3}u(-(t/4)^{1/3}x, t/3) = V'(x) - V^2(x)$
 460 of (20), where V is a solution of the Painlevé II equation $V''(z) = 2V^3(z) + zV(z) + \alpha$ and
 461 α a constant which may depend on ν , see e.g. [61].

462 The relation to KdV allows to interpret the integration variable ν in (1) as a mod-
 463 uli parameter for a class of singular hyperelliptic Riemann surfaces with infinitely many
 464 branch points. A soliton solutions of KdV can indeed be seen as the limit $\delta \rightarrow 0$ of a
 465 solution of KdV built in terms of the theta function of the hyperelliptic Riemann surface
 466 with branch points $0, \infty, \kappa_a^2 + \delta, \kappa_a^2 - \delta$ when branch points $\kappa_a^2 \pm \delta$ merge together on the
 467 Riemann surface, see [55, 56]. The ∞ -soliton solution u_{flat} corresponds in particular to
 468 the hyperelliptic Riemann surface with branch points $0, \infty$ and singular points $4i\pi a - 2\nu$,
 469 $a \in \mathbb{Z} + 1/2$, or equivalently to branch points ν, ∞ and singular points $2i\pi a$, $a \in \mathbb{Z} + 1/2$.
 470 The Riemann surface \mathcal{R} on which the parameter ν lives before taking the trace in (1)
 471 thus describes the monodromy of the branch point ν of the hyperelliptic Riemann surface
 472 above around the singular points $2i\pi a$.

473 For sharp wedge initial condition, the Fredholm determinant expressions for $\mathbb{P}_{\text{sw}}(h(2y,$
 474 $3t) > x)$ from [39, 40] are instead reminiscent of soliton solutions for the Kadomtsev-
 475 Petviashvili (KP) equation $3\partial_y^2 u = \partial_x(4\partial_t u - (6u\partial_x u + \partial_x^3 u))$, a generalization of the
 476 KdV equation for a function $u(x, y, t)$ with two spatial dimensions, see e.g. [55–57]. The
 477 τ functions related to u by $u(x, y, t) = 2\partial_x^2 \log \tau(x, y, t)$ and corresponding to N -soliton
 478 solutions of the KP equation are of the form $\tau(x, y, t) = \det(1 - M_N^{\text{KP}}(x, y, t))$, where the
 479 $N \times N$ matrix $M_N^{\text{KP}}(x, y, t)_{a,b} = e^{x(\kappa_a - \eta_b) + y(\kappa_a^2 - \eta_b^2) + t(\kappa_a^3 - \eta_b^3) + \lambda_a} / (\kappa_a - \eta_b)$ depends on $3N$

480 arbitrary constants $\kappa_a, \eta_b, \lambda_a$. For KPZ with sharp wedge initial condition, calculations
 481 similar to the ones leading to (22), see section 5.2.2 for more details, allow to rewrite (10)
 482 in terms of a Fredholm determinant as

$$\mathbb{P}_{\text{sw}}(h(2y, 3t) > x) = \int_{c-i\pi}^{c+i\pi} \frac{d\nu}{2i\pi} e^{t\chi_0(\nu) - u\chi'_0(\nu) + 2J_0(\nu)} \det(1 - M_{\text{sw}}(x, y, t; \nu)), \quad (25)$$

483 with $M_{\text{sw}}(x, y, t; \nu) = L_{\text{sw}}(x, y, t; \nu)L_{\text{sw}}(x, -y, t; \nu)$ and

$$L_{\text{sw}}(x, y, t; \nu)_{a,b} = \frac{e^{x\kappa_a(\nu) + y\kappa_a^2(\nu) + t\kappa_a^3(\nu) + 2 \int_{-\infty}^{\nu} dv \frac{\chi''_0(v)}{\kappa_a(v)}}{\kappa_a(\nu)(\kappa_a(\nu) + \kappa_b(\nu))}. \quad (26)$$

484 When $c < 0$, this is essentially the result from [40], see section 5.2.2. A similar Fredholm
 485 determinant was also given in [39] for $c > 0$, corresponding to a distinct representation of
 486 the Riemann surfaces in (10).

487 The dependency on x, y and t in (25) is essentially the same as for KP solitons,
 488 with $N \rightarrow \infty$, $\kappa_a = \kappa_a(\nu)$ and $\eta_b = -\kappa_b(\nu)$. The rest of the expression is similar to but
 489 different from the Cauchy determinant M_N^{KP} required for KP solitons. Interestingly, proper
 490 ∞ -soliton solutions of the KP hierarchy are known to appear for Laplacian growth [62],
 491 which belongs to a universality class of growing interfaces distinct from KPZ.

492 A paper by Quastel and Remenik [63] about KPZ fluctuations on \mathbb{R} appeared shortly
 493 after our paper. There, the one-point cumulative distribution function with general initial
 494 condition is shown to be a τ function for the KP equation, without an extra integration
 495 like in (22), while multiple-point distributions at a given time correspond to a matrix
 496 generalization of KP. This suggest that there might still be a way to properly understand
 497 (25) in terms of KP solitons, maybe a matrix generalization such as the one in [63].
 498 Additionally, the distinction between the solutions of Quastel-Remenik and ours for KPZ
 499 fluctuations is highly reminiscent of the one for the KdV / KP equations between solutions
 500 on the infinite line, where an extension to more singular initial conditions is required for
 501 KPZ [63], and quasi-periodic solutions involving compact Riemann surfaces, which appear
 502 to become non-compact for KPZ.

503 2.7 Conclusions

504 Several exact results for KPZ fluctuations with periodic boundaries have been reformulated
 505 in this paper in a compact way in terms of meromorphic differentials on Riemann surfaces
 506 related to polylogarithms with half-integer index. We believe that KPZ universality would
 507 benefit from a more systematic use of tools from algebraic geometry, especially more recent
 508 developments about non-compact Riemann surfaces of infinite genus [64]. Conversely, the
 509 very singular and universal nature of KPZ fluctuations suggests that objects appearing
 510 naturally for KPZ might also be of some interest in themselves for the field of algebraic
 511 geometry, especially when studying limits where the genus of Riemann surfaces goes to
 512 infinity.

513 A possible extension concerns the renormalization group flow $h_\lambda(x, t)$ from the equilib-
 514 rium fixed point $\lambda \rightarrow 0$ to the KPZ fixed point $\lambda \rightarrow \infty$ considered in this paper. Whether
 515 the dynamics for finite λ may also be expressed in a natural way in terms of Riemann
 516 surfaces is unclear at the moment. Hints of a duality [65] between the equilibrium fixed
 517 point in an infinite system and the KPZ fixed point for periodic boundaries, with half-
 518 integer polylogarithms describing large deviations on both sides [66], suggest however the
 519 existence of a tight structure holding everything together. Partial exact results relevant
 520 to finite λ with periodic boundaries have been obtained using the replica solution [37] of
 521 the KPZ equation and a weakly asymmetric exclusion process [67, 68] (see also [69, 70] for

522 recent exact results with arbitrary asymmetry). The appearance of half-integer polylog-
 523 arithms and ζ functions in related contexts of non-intersecting lattice paths [71], largest
 524 eigenvalues in the real Ginibre ensemble [72,73] and return probabilities for the symmetric
 525 exclusion process [74] and quantum spin chains [75] on \mathbb{Z} with domain wall initial condition
 526 might also have some connections to the equilibrium side of the duality.

527 Finally, the results of this paper are based on complicated asymptotics of Bethe ansatz
 528 formulas for TASEP in the limit where the number of lattice sites L and the number of
 529 particles N go to infinity with fixed density N/L [39–42]. A natural question is whether
 530 TASEP with finite L, N can already be described in terms of (finite genus) Riemann
 531 surfaces, so that the infinite genus Riemann surface \mathcal{R} would emerge in a more transparent
 532 fashion in the large L, N limit. Tools from algebraic geometry have already been used in
 533 the study of the more complicated Bethe equations for the asymmetric exclusion process
 534 with hopping in both directions [76] and the related XXZ spin chains with finite anisotropy
 535 [77,78]. The limit where the anisotropy of the spin chain goes to infinity, corresponding
 536 for the exclusion process to the TASEP limit, seems however a better starting point since
 537 the Bethe equations have a much simpler structure in that case, see e.g. [79,80] for related
 538 works.

539 3 Riemann surfaces and ramified coverings

540 In this section, we recall a few classical results about (compact) Riemann surfaces and
 541 ramified coverings. The various properties are illustrated using two examples: hyperelliptic
 542 Riemann surfaces \mathcal{H}_N , which are the proper domain of definition for square roots of
 543 polynomials, and Riemann surfaces \mathcal{R}_N defined from sums of square roots, which have
 544 the topology of $N - 1$ -dimensional hypercubes. The Riemann surfaces \mathcal{R}_N are finite genus
 545 analogues of the non-compact Riemann surfaces \mathcal{R} introduced in section 3.8 and used for
 546 KPZ fluctuations in section 2. We refer to [81–83] for good self-contained introductions
 547 to compact Riemann surfaces and ramified coverings.

548 3.1 Analytic continuation and Riemann surfaces

549 Let us consider a function g_0 analytic in the complex plane \mathbb{C} except for the existence of
 550 branch cuts, i.e. paths in \mathbb{C} across which g_0 is discontinuous. Extremities of branch cuts,
 551 called branch points, correspond to genuine singularities of the function g_0 . The branch
 552 cuts themselves, on the other hand, are somewhat arbitrary. The domain of definition
 553 of g_0 can be extended by analytic continuation along paths crossing the branch cuts. In
 554 the favourable case considered in this paper, successive iterations of this procedure lead
 555 to functions $g_i, i \in I$ analytic in \mathbb{C} except for the same branch cuts as g_0 , such that
 556 the function g_i on one side of a branch cut continues analytically to another function g_j
 557 on the other side of the same branch cut. The collection of all branches g_i represents a
 558 multivalued function. Multivalued basic special functions usually come with a standard
 559 choice for the principal value g_0 .

560 Considering the domains of definition of the functions g_i as distinct copies \mathbb{C}_i of the
 561 complex plane ⁵, the Riemann surface \mathcal{M} for the function g_0 is built by gluing together
 562 the *sheets* \mathbb{C}_i along branch cuts, and we use the notation $[z, i], z \in \mathbb{C}$ for the points on the

⁵For the sake of simplicity, we consider in this paper *concrete Riemann surfaces*, defined in terms of analytic continuation of functions and close to Riemann’s original presentation, and not the more abstract modern formalism in terms of an atlas of charts and transition functions. All the Riemann surfaces considered in this paper can be understood as the natural domain of definition of some explicit multivalued function, and thus come with a natural ramified covering from the Riemann surface to \mathbb{C} .

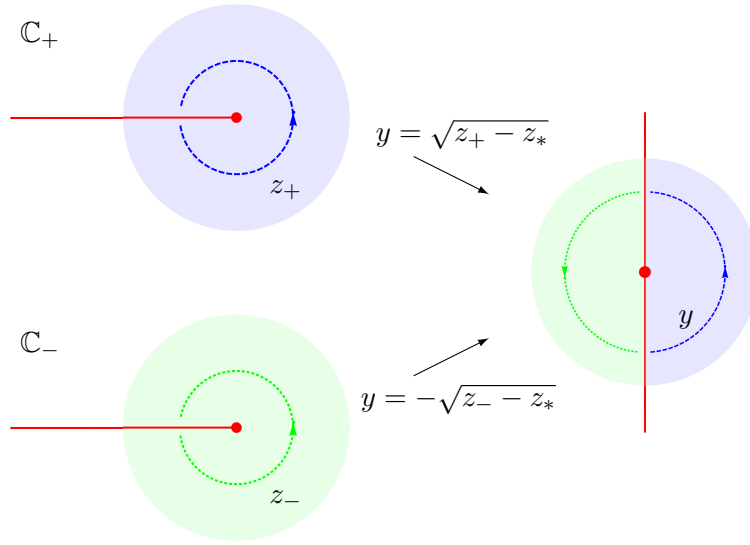


Figure 3: Neighbourhood of a point $q = [z_*, \mathbb{C}_+] = [z_*, \mathbb{C}_-]$ in a Riemann surface (right) such that z_* is a branch point of the function g_0 from which the Riemann surface is built. The neighbourhood is formed by gluing together along the branch cut originating from q two half-disks obtained from taking the square root of full disks from the sheets \mathbb{C}_\pm (left). The complex numbers z_\pm parametrize half a neighbourhood of q in \mathbb{C}_\pm . The local parameter y at q is a complex number that fully parametrizes the neighbourhood of q .

563 sheet \mathbb{C}_i of \mathcal{M} . More precisely, let z_* be a branch point of g_i and γ a branch cut issued
 564 from z_* . Calling by “left” and “right” the two sides of γ , we glue the left side of the cut
 565 in the sheet \mathbb{C}_i to the right side of the cut in the sheet \mathbb{C}_j if g_i is analytically continued
 566 from the left to g_j across the cut, and we glue the right side of the cut in the sheet \mathbb{C}_i to
 567 the left side of the cut in the sheet \mathbb{C}_k if g_i is analytically continued from the right to g_k
 568 across the cut. Additionally, the branch points $[z_*, i]$, $[z_*, j]$, $[z_*, k]$ of the sheets \mathbb{C}_i , \mathbb{C}_j ,
 569 \mathbb{C}_k represent a single point on \mathcal{M} , $[z_*, i] = [z_*, j] = [z_*, k]$. The Riemann surface \mathcal{M} is
 570 independent of the precise choice of branch cuts for g_0 : the branch cuts only determine
 571 a partition of \mathcal{M} into sheets \mathbb{C}_i , and the notation $[z, i]$ for the points of \mathcal{M} thus depends
 572 implicitly on the choice of branch cuts.

573 A function g can then be defined on the Riemann surface \mathcal{M} by $g([z, i]) = g_i(z)$.
 574 Locally, the neighbourhood of any point of \mathcal{M} looks like an open disk of \mathbb{C} , and the function
 575 g is analytic there. This is obvious by construction, except around branch points where
 576 one needs to introduce a non-trivial local coordinate y to parametrize the neighbourhood.
 577 We mainly consider in the following branch points z_* of square root type, such that
 578 $g_i(z) \simeq \tilde{g}_i(z)\sqrt{z - z_*}$ when $z \rightarrow z_*$, where the \tilde{g}_i are analytic and with a branch cut for the
 579 square root determined by the branch cuts of the g_i . A possible local parameter is then
 580 $y = \sqrt{z - z_*}$, and $g_i(z) \simeq y \tilde{g}_i(z_* + y^2)$ is indeed analytic around $y = 0$. A neighbourhood
 581 of z_* in \mathcal{M} may be built using the local parameter y by gluing together two half-disks as
 582 in figure 3.

583 All the construction goes through in the presence of isolated poles, with analytic func-
 584 tions replaced by meromorphic functions. Additionally, it is often convenient to make
 585 Riemann surfaces compact by adding the points at infinity of the sheets, with appropriate
 586 local parameters ensuring that the neighbourhoods of these points are regular. In the
 587 simplest case where g_0 is a rational function without branch points and \mathcal{M} is thus made of

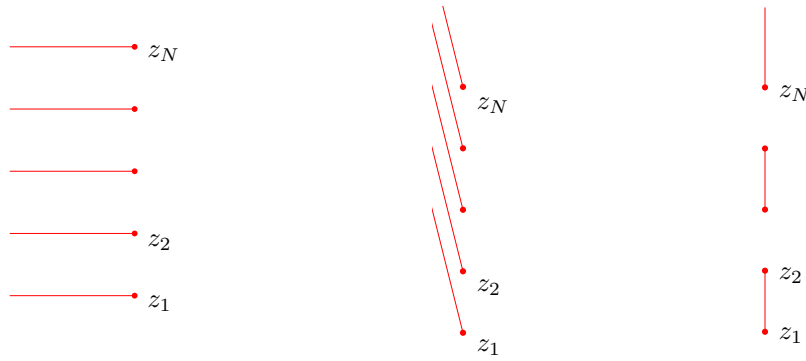


Figure 4: Three different choices of branch cuts (solid lines) for the function h_+ defined in (27) with $N = 5$. The branch points z_j are represented by dots. The function h_+ is multiplied by -1 after crossing any branch cut.

588 a single sheet \mathbb{C} , the associated compact Riemann surface is called ⁶ the Riemann sphere
 589 $\widehat{\mathbb{C}} = \mathbb{C} \cup \{\infty\}$.

590 3.2 The Riemann surfaces \mathcal{H}_N and \mathcal{R}_N

591 We consider in this section two concrete examples of the construction above. Let $z_1, \dots,$
 592 z_N be distinct complex numbers, that are fixed in the following. We choose for simplicity
 593 of the pictures (and also because it will be the case of interest for KPZ) the z_j 's to be
 594 purely imaginary and equally spaced, $\text{Im } z_1 < \dots < \text{Im } z_N$, but this choice is not essential
 595 here. We define the functions

$$h_+(z) = \sqrt{z - z_1} \times \dots \times \sqrt{z - z_N} \tag{27}$$

596 and

$$f_\emptyset(z) = \sqrt{z - z_1} + \dots + \sqrt{z - z_N} \tag{28}$$

597 of a complex variable z , which inherit branch cuts from the square roots (see respectively
 598 figures 4 and 5 for some possible choices of branch cuts). The functions h_+ and f_\emptyset can be
 599 extended by the procedure described in the previous section to analytic functions h and
 600 f defined on compact Riemann surfaces \mathcal{H}_N and \mathcal{R}_N . The Riemann surface \mathcal{H}_N , called
 601 hyperelliptic and used here mainly for illustrative purpose, has links to the KdV equation
 602 discussed in section 2.6.3. The Riemann surface \mathcal{R}_N , on the other hand, is a simplified,
 603 finite genus version of the Riemann surface \mathcal{R} introduced in section 3.8, and in terms of
 604 which KPZ fluctuations are expressed in section 2.

605 We begin with the function h_+ defined in (27), analytic on a sheet called \mathbb{C}_+ , with
 606 the choice of branch cuts on the left in figure 4. Analytic continuation across branch cuts
 607 gives $h_- = -h_+$, which lives on another sheet \mathbb{C}_- . The Riemann surface \mathcal{H}_N is formed
 608 by the two sheets \mathbb{C}_\pm glued together, and h_+ extends analytically to a function h defined
 609 on \mathcal{H}_N by $h([z, \pm]) = h_\pm(z)$. Locally, the neighbourhood of any point of \mathcal{H}_N looks like
 610 an open disk of \mathbb{C} (see figure 3 for the neighbourhood of $[z_j, \pm]$), and the function h is
 611 analytic there. The points at infinity $[\infty, \pm]$ are poles of the function h . A local parameter
 612 y for these points is $y = z^{-1}$ if N is even and $y = z^{-1/2}$ if N is odd. In the former case,
 613 the poles of h at $[\infty, +]$ and $[\infty, -]$, which are distinct points of \mathcal{H}_N , are of order $N/2$.
 614 In the latter case, ∞ is a branch point of h_\pm and the point $[\infty, +] = [\infty, -]$ is a pole of
 615 order N of h . The function h also has N zeroes, the points $[z_j, +] = [z_j, -]$, $j = 1, \dots, N$.

⁶Other notations for $\widehat{\mathbb{C}}$ include $\overline{\mathbb{C}}$, \mathbb{C}_∞ , or $\mathbb{P}^1(\mathbb{C})$, $\mathbb{C}\mathbb{P}^1$ when interpreted as the complex projective line.



Figure 5: Two different choices of branch cuts (solid lines) for the function f_θ defined in (28) with $N = 5$. The branch points are represented by dots. The sets labelling the sheet reached after crossing branch cuts from either side starting from the sheet labelled by $P \subset \{1, 2, 3, 4, 5\}$ is indicated near the branch cuts.

616 The total number of poles of h , counted with multiplicity, is thus equal to its number of
 617 zeroes. This is in fact a general property valid for any meromorphic function on a compact
 618 Riemann surface.

619 Compared to the hyperelliptic case discussed above, analytic continuations across
 620 branch cuts of f_θ defined in (28) have a richer structure, since all the square roots are inde-
 621 pendent: each one may change sign independently across branch cuts. The corresponding
 622 Riemann surface \mathcal{R}_N is thus made of 2^N sheets labelled by sets of integers between 1
 623 and N , $P \subset \llbracket 1, N \rrbracket$, indicating the square roots coming with a minus sign. It will be
 624 convenient in the following to distinguish two systems of sheets \mathcal{G}_P and \mathcal{F}_P partitioning
 625 \mathcal{R}_N , corresponding respectively to the choice of branch cuts on the left and on the right
 626 in figure 5. The points of \mathcal{R}_N will be written as $[z, \mathcal{G}_P]$ or $[z, \mathcal{F}_P]$ when specifying the
 627 choice of sheets is needed, and simply as $[z, P]$ otherwise. The analytic function f on \mathcal{R}_N
 628 induced by f_θ is defined by $f([z, P]) = f_P(z)$, with $f_P(z) = \sum_{j=1}^N \sigma_j(P) \sqrt{z - z_j}$ and

$$\sigma_a(P) = \begin{cases} 1 & a \notin P \\ -1 & a \in P \end{cases} . \quad (29)$$

629 The number of square roots that have changed sign in f_P compared to f_θ is equal to the
 630 number $|P|$ of elements in P .

631 The connectivity of the sheets \mathcal{G}_P and \mathcal{F}_P in \mathcal{R}_N following from analytic continuation
 632 can be expressed in terms of the symmetric difference operator \ominus , defined as union minus
 633 intersection:

$$P \ominus Q = (P \cup Q) \setminus (P \cap Q) . \quad (30)$$

634 The symmetric difference operator \ominus is associative, commutative and verifies $P \ominus P = \emptyset$
 635 and ${}^7 P \ominus Q + n = (P + n) \ominus (Q + n)$ for $n \in \mathbb{Z}$. A collection of sets closed under union,
 636 intersection and complement forms a group with the operation \ominus . The identity element is
 637 the empty set \emptyset , and the maps σ_a act as group homomorphisms, $\sigma_a(P \ominus Q) = \sigma_a(P) \sigma_a(Q)$.

638 Crossing the branch cut associated to z_j from the sheet \mathcal{G}_P leads to $\mathcal{G}_{P \ominus \{j\}}$ (see fig-
 639 ure 5), and one has the local parameters $y = \pm \sqrt{z - z_j}$ with the same half-disk construc-

⁷We choose symmetric difference to have precedence over addition, so that $P \ominus Q + n$ means $(P \ominus Q) + n$.

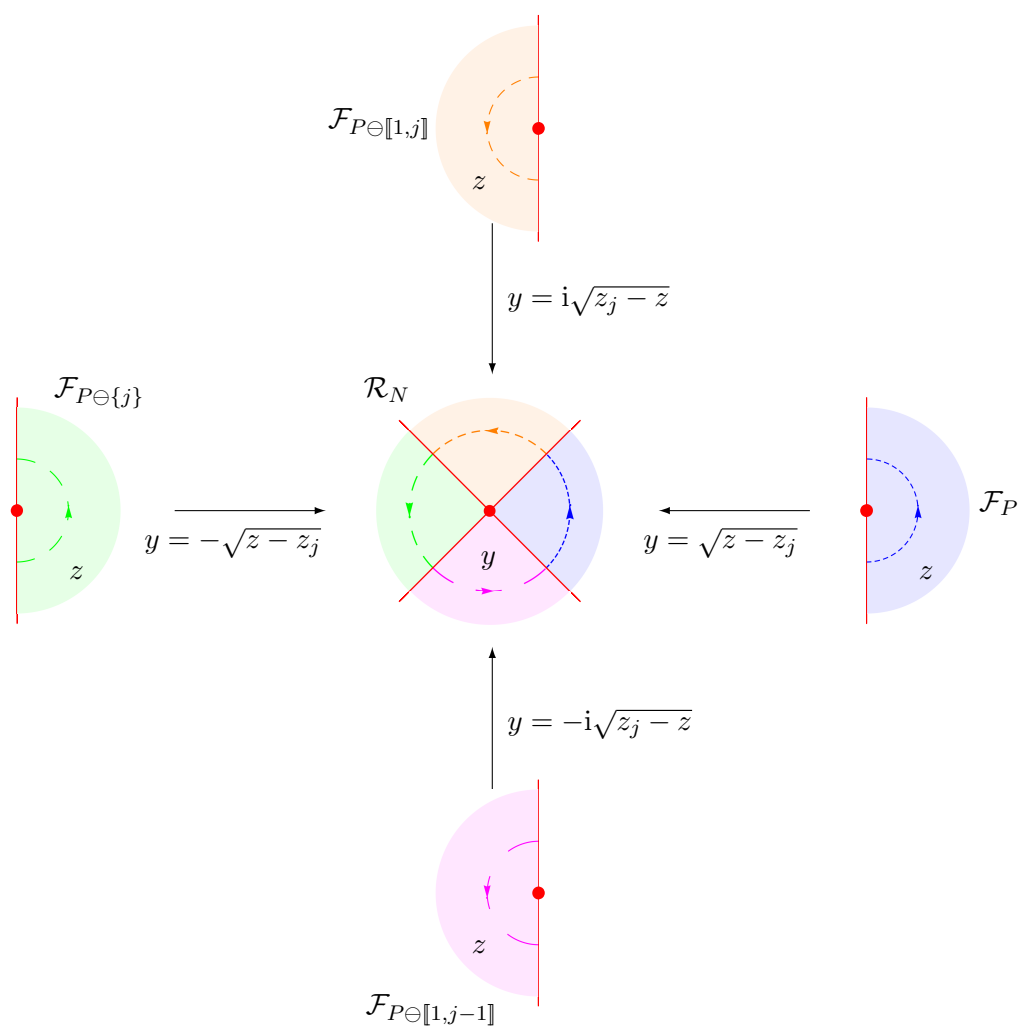


Figure 6: Neighbourhood of $q = [(z_j)_r, \mathcal{F}_P] = [(z_j)_l, \mathcal{F}_{P\ominus[1,j]}] = [(z_j)_r, \mathcal{F}_{P\ominus\{j\}}] = [(z_j)_l, \mathcal{F}_{P\ominus[1,j-1]}]$, $2 \leq j \leq N - 1$ in \mathcal{R}_N , formed by gluing four quarter-disks obtained from taking the square root of half-disks in the sheets \mathcal{F}_P , $\mathcal{F}_{P\ominus[1,j]}$, $\mathcal{F}_{P\ominus\{j\}}$ and $\mathcal{F}_{P\ominus[1,j-1]}$. The complex numbers z parametrize quarters of neighbourhoods of q in the various sheets. The local parameter y fully parametrizes a neighbourhood of q , with $y = 0$ corresponding to q .

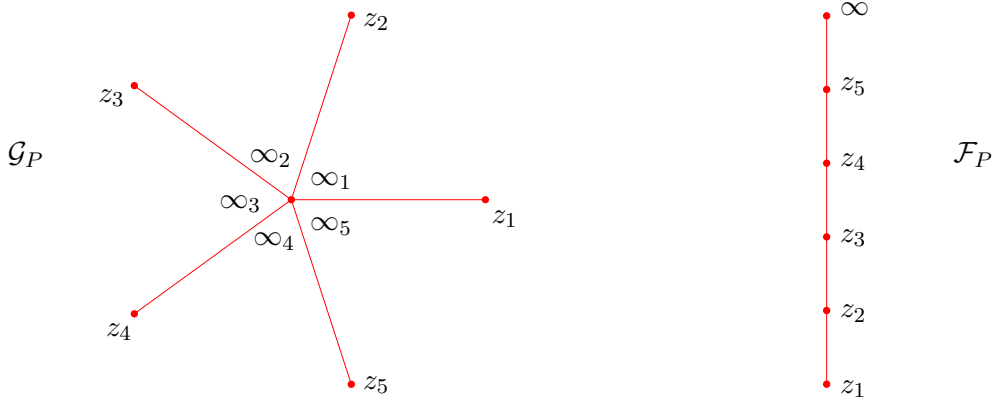


Figure 7: Compact representation of branch cuts for the sheets \mathcal{G}_P (left) and \mathcal{F}_P (right) of \mathcal{R}_5 after adding the points at infinity. The branch cuts are represented as straight lines for clarity, and distances are not meaningful.

tion of figure 3 as for \mathcal{H}_N around the points $[z_j, \mathcal{G}_P] = [z_j, \mathcal{G}_{P \ominus \{j\}}]$. In the sheet \mathcal{F}_P on the other hand, crossing the branch cut between z_j and z_{j+1} (with $z_{N+1} = \infty$) leads to $\mathcal{F}_{P \ominus [1, j]}$ (see figure 5). There, an additional difficulty for constructing local parameters is that the branch points z_j , $j = 2, \dots, N-1$ lie on branch cuts, and must thus be labelled by an additional index l or r depending on whether the point is on the left side (l) or the right side (r) of the cut. A neighbourhood of $[(z_j)_r, \mathcal{F}_P] = [(z_j)_l, \mathcal{F}_{P \ominus [1, j-1]}] = [(z_j)_r, \mathcal{F}_{P \ominus \{j\}}] = [(z_j)_l, \mathcal{F}_{P \ominus [1, j-1]}]$ is constructed in figure 6 by gluing quarter disks together.

The points at infinity are branch points of the functions f_P . Considering the partition of \mathcal{R}_N with sheets \mathcal{F}_P , one has $[\infty, \mathcal{F}_P] = [\infty, \mathcal{F}_{P \ominus [1, N]}]$, see figures 5 and 7 right. For the sheets \mathcal{G}_P , points at infinity can be reached from N directions in figure 5 left, and one has to distinguish points $[\infty_j, \mathcal{G}_P]$, $j = 1, \dots, N$, with the identifications $[\infty_j, \mathcal{G}_P] = [\infty_{j-1}, \mathcal{G}_{P \ominus \{j\}}]$, see figure 7 left.

3.3 Genus

From a purely topological point of view, a Riemann surface is a two-dimensional connected manifold. In the case of a closed (i.e. without boundary), compact Riemann surface such as $\hat{\mathbb{C}}$, \mathcal{H}_N or \mathcal{R}_N above, the manifold is fully characterized up to homeomorphisms (i.e. continuous deformations with continuous inverse) by a single non-negative integer, its genus g , corresponding to the maximal number of simple non-intersecting closed curves along which the manifold can be cut while still being connected. The case $g = 0$ corresponds to a sphere, $g = 1$ to a torus and $g \geq 2$ to a chain of g tori glued together, see figure 8.

The additional complex structure of Riemann surfaces detailing how sheets are glued together gives more freedom, and two Riemann surfaces of the same genus are not necessarily isomorphic (i.e. there may not exist a holomorphic homeomorphism with holomorphic inverse transforming one into the other). The genus 0 case is an exception, for which a single Riemann surface exists up to isomorphism, the Riemann sphere $\hat{\mathbb{C}}$. For genus 1, the equivalence classes up to isomorphism are indexed by a single complex number τ (defined up to modular transformations), such that the parallelogram with vertices $0, 1, 1 + \tau, \tau$ becomes a torus when opposite sides are glued together. For higher genus $g \geq 2$, the moduli space of all Riemann surfaces is parametrized by $3g - 3$ complex parameters.

The Riemann surfaces \mathcal{H}_1 and \mathcal{H}_2 are both isomorphic to the Riemann sphere, while \mathcal{H}_3 and \mathcal{H}_4 are tori. More generally, the genus of the hyperelliptic Riemann surface \mathcal{H}_N

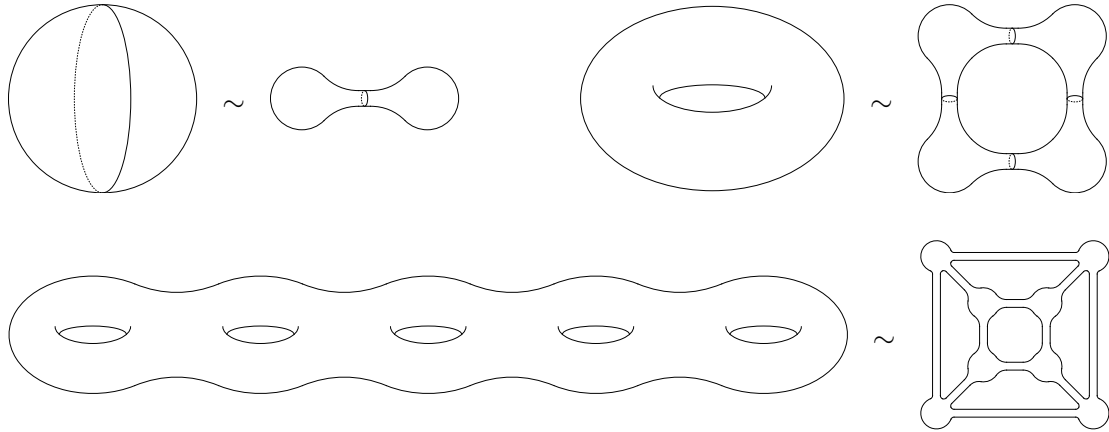


Figure 8: Sphere, torus, and surface with genus $g = 5$, along with hypercubes of dimensions 1, 2, 3 made of spheres connected with cylinders that can be mapped to them by continuous deformations.

672 is known to be equal to either $(N - 1)/2$ or $(N - 2)/2$ depending on the parity of N .
 673 Similarly, \mathcal{R}_1 (which is exactly the same as \mathcal{H}_1 since $f_\emptyset = h_+$ when $N = 1$) and \mathcal{R}_2 (see
 674 figure 9) are also isomorphic to the Riemann sphere, while \mathcal{R}_3 is a torus, see figure 10.
 675 More generally, the genus g_N of \mathcal{R}_N grows exponentially fast with N , as

$$g_N = 1 + (N - 3)2^{N-2}, \tag{31}$$

676 which can be proved by induction on N . Indeed, cutting \mathcal{R}_N along a path joining $[z_N, \mathcal{F}_P]$
 677 and $[\infty, \mathcal{F}_P]$ in every sheet \mathcal{F}_P splits \mathcal{R}_N into two disconnected pieces (corresponding to
 678 sheets \mathcal{F}_P with either $N \in P$ or $N \notin P$), each component having 2^{N-1} boundaries cor-
 679 responding to the cycles $[\infty, \mathcal{F}_P] = [\infty, \mathcal{F}_{P \ominus [1, N]}] \rightarrow [(z_N)_l, \mathcal{F}_{P \ominus [1, N]}] = [(z_N)_r, \mathcal{F}_P] \rightarrow$
 680 $[\infty, \mathcal{F}_P]$. Both pieces are homeomorphic to \mathcal{R}_{N-1} with 2^{N-1} boundaries, which are con-
 681 nected two by two in \mathcal{R}_N . This leads to the recurrence relation $g_{N+1} = 2g_N + 2^{N-1} - 1$,
 682 since gluing together both pieces along a first boundary leads to a surface with twice
 683 the genus of \mathcal{R}_{N-1} , and each additional gluing adds a handle to the surface and hence
 684 increases the genus by 1. We observe that the Riemann surface \mathcal{R}_N is thus homeomor-
 685 phic to a $N - 1$ -dimensional hypercube [84] whose nodes are spheres and edges cylinders
 686 connecting the spheres, see figure 8.

687 3.4 Ramified coverings

688 Maps between Riemann surfaces acting as holomorphic functions on local parameters,
 689 called holomorphic maps, are a powerful tool in the study of Riemann surfaces. They
 690 allow in particular to define a notion of equivalence between Riemann surfaces having
 691 essentially the same complex structure: two Riemann surfaces are called isomorphic when
 692 there exists a bijective holomorphic map with holomorphic inverse between them.

693 Given two Riemann surfaces \mathcal{M} and \mathcal{N} , a ramified covering (or branched covering, or
 694 simply covering map ⁸ here for simplicity) such that \mathcal{M} covers \mathcal{N} (or \mathcal{N} is covered by \mathcal{M})
 695 is a non-constant holomorphic map from \mathcal{M} to \mathcal{N} , which is then surjective by analyticity.
 696 Ramified coverings allow to relate complicated Riemann surfaces to simpler Riemann
 697 surfaces. In particular, for any Riemann surface \mathcal{M} , there exists at least one ramified
 698 covering from \mathcal{M} to the Riemann sphere $\widehat{\mathbb{C}}$, i.e. a non-constant meromorphic function on
 699 \mathcal{M} . Conversely, defining a concrete Riemann surface $\mathcal{M} = \{[z, i], z \in \widehat{\mathbb{C}}, i \in I\}$ by gluing

⁸Not to be confused with the topological notion of a covering, which does not have ramification points.

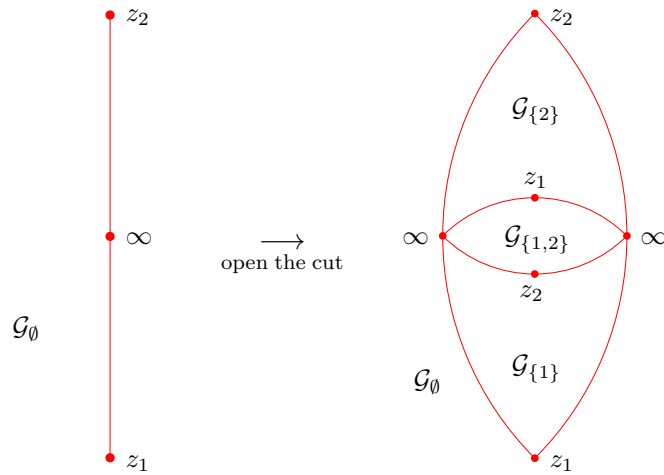


Figure 9: Representation of the surface corresponding to the Riemann surface \mathcal{R}_2 . The sheet \mathcal{G}_\emptyset is represented on the left, with a cut linking the points $[z_1, \mathcal{G}_\emptyset]$, $[z_2, \mathcal{G}_\emptyset]$ and $[\infty, \mathcal{G}_\emptyset]$. Opening the cut, all the other sheets $\mathcal{G}_{\{1\}}$, $\mathcal{G}_{\{2\}}$, $\mathcal{G}_{\{1,2\}}$ fit within the opening. The graph made by the cuts of all sheets is planar, and \mathcal{R}_2 is isomorphic to the Riemann sphere $\widehat{\mathbb{C}}$.

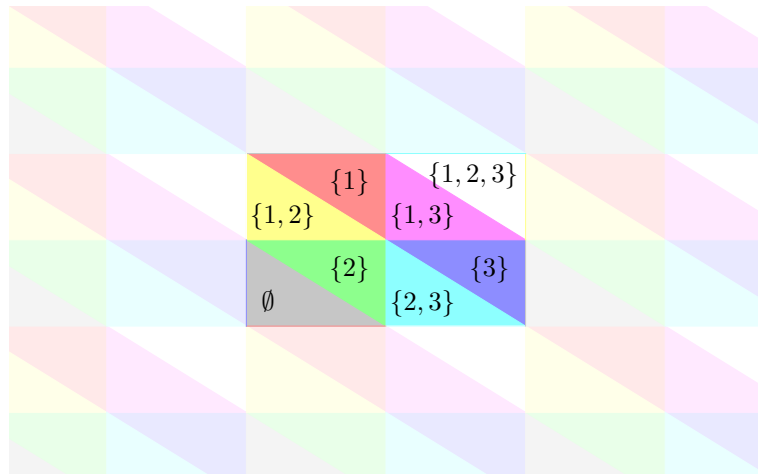


Figure 10: Representation of the torus homeomorphic to the Riemann surface \mathcal{R}_3 . Opposite sides of the fundamental domain represented by the region in the middle are identified. The connectivity of the sheets \mathcal{G}_P partitioning \mathcal{R}_3 is represented by the labels $P \subset \{1, 2, 3\}$ of the sheets.

domains of definition of branches $i \in I$ of a multivalued function gives the natural covering map $[z, i] \mapsto z$.

Let $\rho : \mathcal{M} \rightarrow \mathcal{N}$ be a branched covering and $p \in \mathcal{M}$. Then, there exists a unique positive integer $e_p \in \mathbb{N}^*$ such that one can choose local coordinates y and z for the neighbourhoods around p and $\rho(p)$ in such a way that $z = y^{e_p}$. The integer e_p is called the ramification index of the point p for the covering map ρ . A ramification point of ρ is then a point $p \in \mathcal{M}$ such that $e_p \geq 2$, with $e_p = 2$ corresponding to ramification points of square root type. Around such points, the mapping ρ is not injective, and the inverse function ρ^{-1} is multivalued. The branch points $q \in \mathcal{N}$ of ρ are the images by ρ of the ramification points $p \in \mathcal{M}$.

Ramification points form a discrete subset of \mathcal{M} . Furthermore, if \mathcal{M} is compact, the number of branch points is finite, and so is the number of preimages of any $q \in \mathcal{N}$ by ρ . In that case, there exists a unique positive integer $d \in \mathbb{N}^*$, the degree of the branched covering, such that for any $q \in \mathcal{N}$, $d = \sum_{p \in \rho^{-1}(q)} e_p$. For generic points $q \in \mathcal{N}$ not branch points of ρ , the set of preimages $\rho^{-1}(q) \subset \mathcal{M}$ has exactly d distinct elements.

The construction of a concrete Riemann surface \mathcal{M} by gluing together a discrete number of copies $\widehat{\mathbb{C}}_i$, $i \in I$ of the Riemann sphere along branch cuts of some function, which we used above to define \mathcal{H}_N and \mathcal{R}_N , naturally gives the ramified covering $[z, i] \mapsto z$ from \mathcal{M} to $\widehat{\mathbb{C}}$.

New meromorphic function can be built from known ones using ramified coverings. Let $\rho : \mathcal{M} \rightarrow \mathcal{N}$ be a branched covering and $\varphi_{\mathcal{M}}$, $\varphi_{\mathcal{N}}$ meromorphic functions defined respectively on \mathcal{M} and \mathcal{N} . Then, the composition $\varphi_{\mathcal{N}} \circ \rho$ is a meromorphic function on \mathcal{M} . For instance, the ramified covering $\rho : [z, P] \mapsto [z, (-1)^{|P|}]$ from \mathcal{R}_N to \mathcal{H}_N generates from the function h on \mathcal{H}_N defined from (27) the function $h \circ \rho$ meromorphic on \mathcal{R}_N , which is essentially the same function as h but defined on a bigger space: \mathcal{H}_N is only the “minimal” closed, compact Riemann surface on which h_{\pm} can be extended to a meromorphic function.

Conversely, tracing over preimages of ρ defines a function $\text{tr}_{\rho} \varphi_{\mathcal{M}}$ as

$$(\text{tr}_{\rho} \varphi_{\mathcal{M}})(q) = \sum_{\substack{p \in \mathcal{M} \\ \rho(p)=q}} \varphi_{\mathcal{M}}(p), \quad (32)$$

which can be shown [85] to be meromorphic on \mathcal{N} . This can be illustrated by considering the covering map $\rho : [z, P] \mapsto z$ from \mathcal{R}_N to $\widehat{\mathbb{C}}$. Starting with the function f meromorphic on \mathcal{R}_N defined from (28), all the square roots cancel in the trace and one has $\text{tr}_{\rho} f = 0$ which is indeed defined on $\widehat{\mathbb{C}}$. Less trivially, allowing essential singularities at infinity, the function $(\text{tr}_{\rho} e^{\lambda f})(z) = 2^N \prod_{j=1}^N \cosh(\lambda \sqrt{z - z_j})$ is also analytic in \mathbb{C} .

The Riemann-Hurwitz formula gives a relation between ramification indices e_p for a branched covering $\rho : \mathcal{M} \rightarrow \mathcal{N}$ of degree d and the respective genus $g_{\mathcal{M}}$, $g_{\mathcal{N}}$ of the Riemann surfaces \mathcal{M} and \mathcal{N} :

$$g_{\mathcal{M}} = d(g_{\mathcal{N}} - 1) + 1 + \frac{1}{2} \sum_{p \in \mathcal{M}} (e_p - 1), \quad (33)$$

where only ramification points contribute to the sum. In particular, one has always $g_{\mathcal{M}} \geq g_{\mathcal{N}}$. Considering a triangulation of \mathcal{M} with vertices at ramification points of ρ , the Riemann-Hurwitz formula is a simple consequence of the expression for the Euler characteristics $\chi = 2 - 2g$ in terms of the number of vertices, edges and faces of the triangulation.

The Riemann-Hurwitz formula allows one to recover the expression (31) for the genus of \mathcal{R}_N . We introduce the ramified covering $[z, P] \mapsto z$ from \mathcal{R}_N to $\widehat{\mathbb{C}}$ for some choice of branch cuts. This covering has degree $d = 2^N$, and its ramification points, all with

744 ramification index 2, are the $[z_j, P]$ and $[\infty, P]$. Each one is shared between two sheets (or
 745 four half-sheets, compare figures 3 and 6), so that the total number of ramification points
 746 is equal to $(N + 1)2^{N-1}$. Taking $g_N = 0$ in (33) since the target space is $\widehat{\mathbb{C}}$ gives again
 747 (31).

748 3.5 Quotient under group action

749 Quotients of Riemann surfaces by the action of their holomorphic automorphisms (i.e.
 750 bijective holomorphic maps from the Riemann surface to itself) generate new Riemann
 751 surfaces. Let \mathcal{M} be a Riemann surface and \mathfrak{h} a group of holomorphic automorphisms
 752 of \mathcal{M} acting properly discontinuously on \mathcal{M} , i.e. for any point $p \in \mathcal{M}$, there exists
 753 a neighbourhood U of p in \mathcal{M} such that the set $\{h \in \mathfrak{h}, hU \cap U \neq \emptyset\}$ is finite, with
 754 $hU = \{hq, q \in U\}$. The quotient \mathcal{M}/\mathfrak{h} is then also a Riemann surface, whose points
 755 $q \in \mathcal{M}/\mathfrak{h}$ are identified to orbit of $p \in \mathcal{M}$ under the action of \mathfrak{h} , and the covering map
 756 $p \mapsto q$ from \mathcal{M} to \mathcal{M}/\mathfrak{h} is ramified at the fixed points of \mathfrak{h} .

757 Instead of considering the points of \mathcal{M}/\mathfrak{h} as equivalence classes under the action of \mathfrak{h} ,
 758 it is often convenient to choose a fundamental domain \mathcal{F} in \mathcal{M} such that $\{h\mathcal{F}, h \in \mathfrak{h}\}$ is a
 759 partition of \mathcal{M} . Then, \mathcal{M}/\mathfrak{h} can be identified as \mathcal{F} with additional boundary conditions.
 760 A genus 1 Riemann surface, which has the topology of a torus, can for instance be defined
 761 as the quotient of \mathbb{C} by a group of translations in two directions, and the fundamental
 762 domain may always be chosen as a parallelogram whose opposite sides are glued together,
 763 see figure 10.

764 Given two Riemann surfaces \mathcal{M}, \mathcal{N} and a covering map ρ from \mathcal{M} to \mathcal{N} , a holomorphic
 765 automorphism h of \mathcal{M} is called a deck transformation for ρ if h is compatible with ρ , i.e.
 766 $\rho \circ h = \rho$. A deck transformation is fully determined by the permutation it induces on
 767 $\rho^{-1}(q)$ with $q \in \mathcal{N}$ not a branch point of ρ .

768 3.6 Homotopy and homology

769 Let \mathcal{M} be a Riemann surface and $p \in \mathcal{M}$. Closed loops on \mathcal{M} with base point p are
 770 continuous paths on \mathcal{M} starting and ending at p . The set of equivalence classes of such
 771 loops under homotopy (i.e. continuous deformations) forms a group $\pi_1(\mathcal{M})$ for the con-
 772 catenation of the paths, called the first homotopy group (or fundamental group), which is
 773 independent from the base point up to group isomorphism.

774 Let \mathcal{M} and \mathcal{N} be two Riemann surfaces, $\rho : \mathcal{M} \rightarrow \mathcal{N}$ a covering map, $p \in \mathcal{M}$ not a
 775 ramification point of ρ and γ a continuous path in \mathcal{N} starting at $\rho(p)$ and avoiding the
 776 branch points of ρ . The lift $\gamma \cdot p$ of γ to the point p is the unique path in \mathcal{M} starting at p
 777 whose image by ρ is γ . Considering a partition of \mathcal{M} into sheets \mathbb{C}_i such that any point
 778 $q \in \mathcal{N}$ has a single preimage under ρ in each sheet \mathbb{C}_i , we also write $\gamma \cdot \mathbb{C}_i$ for the lift of
 779 the path $\gamma \subset \mathcal{N}$ to the preimage $p \in \mathbb{C}_i$ of the starting point of γ . Even if γ is a closed
 780 path on \mathcal{N} , the lift $\gamma \cdot \mathbb{C}_i$ is not necessarily a loop on \mathcal{M} , since its endpoint may be in any
 781 sheet \mathbb{C}_j , but loops from any equivalence class in $\pi_1(\mathcal{M})$ may be obtained by the lifting
 782 procedure.

783 Considering the example of the covering map $\rho : [z, \mathcal{G}_P] \mapsto z$ from \mathcal{R}_N to $\widehat{\mathbb{C}}$, we call θ_j
 784 the loop in $\widehat{\mathbb{C}}$ encircling only the branch point z_j , once in the counter-clockwise direction.
 785 Then, the lift $\theta_j^2 \cdot \mathcal{G}_P$ is homotopic to an empty loop on \mathcal{R}_N , see dashed path in figure 3.
 786 Any loop on \mathcal{R}_N may be written up to homotopy as $\theta_{j_k} \dots \theta_{j_1} \cdot \mathcal{G}_P$, where each θ_j appears
 787 an even number of times in the product so that the final sheet \mathcal{G}_Q , $Q = P \ominus \{j_1\} \ominus \dots \ominus \{j_k\}$
 788 is the same as the initial sheet \mathcal{G}_P .

789 Considering several loops based at a point p of a Riemann surface \mathcal{M} , the homotopy
 790 class of their product γ may depend on the order of the loops in γ . On the other hand, the

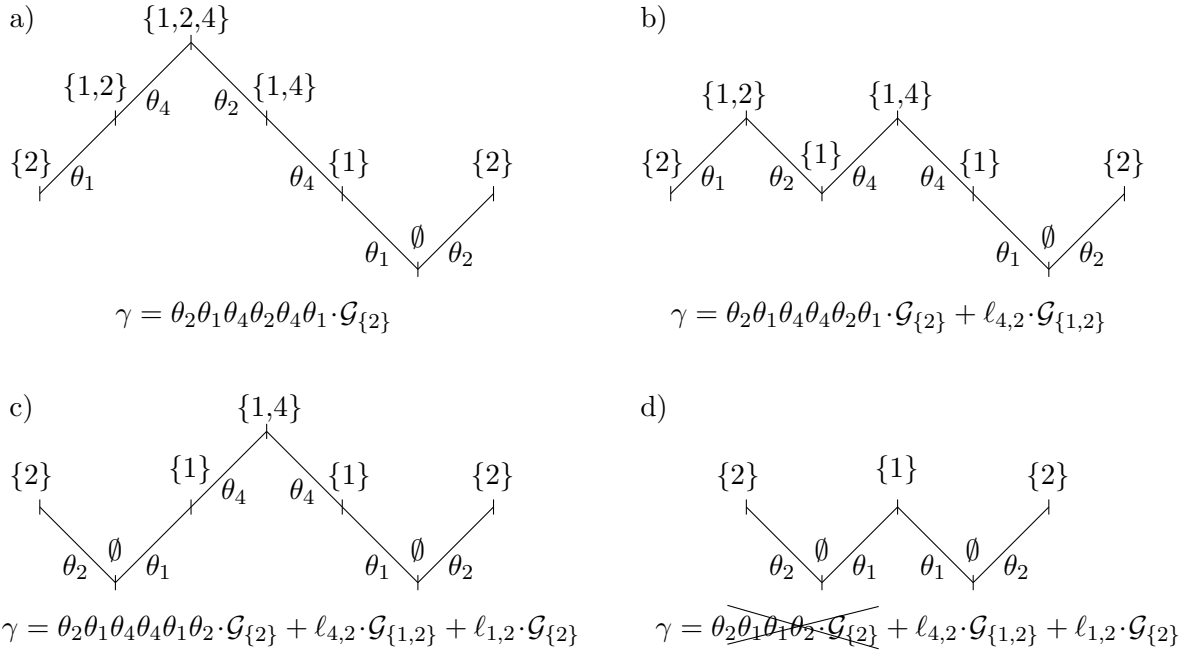


Figure 11: Homology class of a loop $\gamma = \theta_{j_k} \dots \theta_{j_1} \mathcal{G}_P$ on the Riemann surface \mathcal{R}_N rewritten as a combination of loops $\ell_{a,b} \cdot \mathcal{G}_Q$.

791 integral of a holomorphic differential (see next section) over γ is independent of the order
 792 of the loops in γ . This motivates the definition of the first homology group $H_1(\mathcal{M}, \mathbb{Z})$,
 793 a commutative version of the fundamental group $\pi_1(\mathcal{M})$, for which an additive notation
 794 is used for the concatenation of loops. For a compact Riemann surface of genus g , it is
 795 known that a minimal set of generators of $H_1(\mathcal{M}, \mathbb{Z})$ must have $2g$ elements.

796 An overcomplete set of generators for $H_1(\mathcal{R}_N, \mathbb{Z})$ is given by the loops $\ell_{a,b} \cdot \mathcal{G}_P$, $1 \leq$
 797 $a < b \leq N$, $P \subset \llbracket 1, N \rrbracket$, with $\ell_{a,b} = \theta_b \theta_a \theta_b \theta_a$. Indeed, considering a general loop $\gamma =$
 798 $\theta_{j_k} \dots \theta_{j_1} \cdot \mathcal{G}_P$ of $\pi_1(\mathcal{R}_N)$, the sets $P = Q_0, Q_1, \dots, Q_{k-1}, Q_k = P$ indexing the sheets
 799 \mathcal{G}_Q crossed by γ are such that two consecutive sets Q_i, Q_{i+1} may only differ by a single
 800 element, and their cardinals $|Q_i|, |Q_{i+1}|$ differ by ± 1 . Choosing an index i such that $|Q_i|$
 801 is a local maximum in the sequence, two situations can occur: if $Q_{i-1} = Q_{i+1}$, then $j_{i-1} = j_i$
 802 and $\theta_{j_i} \theta_{j_{i-1}}$ is homotopic to the identity and can be erased. Otherwise $Q_{i-1} \neq Q_{i+1}$, and
 803 there exists $a, b \in \llbracket 1, N \rrbracket$, $a \neq b$ such that Q_i contains both a and b , $Q_{i-1} = Q_i \setminus \{b\}$ and
 804 $Q_{i+1} = Q_i \setminus \{a\}$. The loop then contains the factor $\theta_b \theta_a$, which can be replaced by $\theta_a \theta_b$,
 805 reducing the value of $|Q_i|$ by 2 at the price of adding $\ell_{a,b} \cdot Q_{i-1}$ to the loop, which has the
 806 form desired, see figure 11 for an example.

807 3.7 Differential 1-forms

808 Let \mathcal{M} be a concrete Riemann surface equipped with a covering map $\rho : [z, i] \mapsto z$ from
 809 \mathcal{M} to $\widehat{\mathbb{C}}$. A meromorphic differential ω on \mathcal{M} , also called an Abelian differential, is a
 810 differential 1-form such that at any $p = [z, i] \in \mathcal{M}$ away from branch points of ρ one can
 811 write $\omega(p) = h_i(z) dz$ with h_i the branch of a meromorphic function h on the sheet \mathbb{C}_i
 812 of \mathcal{M} . At a ramification point $[z_*, i]$ of ρ with ramification index $e \geq 2$, one has instead
 813 $\omega([z_*, i]) = e y^{e-1} h_i(z_* + y^e) dy$ in terms of the local coordinate y , $y^e = z - z_*$.

814 A meromorphic differential has a pole (respectively a zero) of order n at $p = [z, i]$ away
 815 from ramification points if the function h as above has a pole (resp. a zero) of order n at
 816 p , and the residue of the pole is equal to the corresponding residue of h_i . For ramification

817 points with local coordinate chosen as above, poles and zeroes of ω correspond to poles and
 818 zeroes of $e y^{e-1} h_i(z_* + y^e)$ at $y = 0$, and the residue of a pole, equal to the corresponding
 819 residue at $y = 0$, is independent from the choice of local coordinate. We observe that poles
 820 of h at branch points may be cancelled in ω by the factor y^{e-1} if the order of the pole
 821 is strictly lower than the ramification index. For a compact Riemann surface of genus g ,
 822 the degree of a meromorphic differential, i.e. the total number of zeroes minus the total
 823 number of poles counted with multiplicity, is equal to $2g - 2$.

824 It is convenient to classify meromorphic differentials into three kinds depending on their
 825 poles. Meromorphic differentials of the first kind, also called holomorphic differentials,
 826 correspond to the special case where the differential has no poles. Holomorphic differentials
 827 are closed, i.e. the integral of a holomorphic differential on a path on \mathcal{M} does not change
 828 if the path is deformed continuously while its endpoints are kept fixed. Equivalently, the
 829 integral of a holomorphic differential over a loop depends only on the equivalence class
 830 of the loop under homology. In particular, if the loop is homologous to $0 \in H_1(\mathcal{M}, \mathbb{Z})$,
 831 the integral is equal to $0 \in \mathbb{C}$ even though the loop may not be homotopic to an empty
 832 loop. Holomorphic differentials form a vector space $H^1(\mathcal{M}, \mathbb{C})$ of dimension $2g$, dual to the
 833 first homology group $H_1(\mathcal{M}, \mathbb{Z})$, and are the basic ingredients to build theta functions,
 834 a fundamental object in the theory of compact Riemann surfaces in terms of which τ
 835 functions for the KdV equation can for instance be built. For the Riemann surface \mathcal{R}_N , a
 836 basis of holomorphic differentials is given by the $\omega_{Q,k}$, $Q \subset \llbracket 1, N \rrbracket$, k integer with $0 \leq k \leq$
 837 $(|Q| - 3)/2$, equal at $[z, P]$ not a ramification point to $\omega_{Q,k}([z, P]) = z^k dz / \prod_{\ell \in Q} \sqrt{z - z_\ell}$.
 838 One can check that there are indeed $2g_N$ holomorphic differentials $\omega_{Q,k}$, each one having
 839 degree $2g_N - 2$ with g_N given by (31).

840 Meromorphic differentials of the second and third kind have poles. Meromorphic dif-
 841 ferentials of the second kind only have multiple poles with no residues, and are thus closed
 842 like holomorphic differentials. Meromorphic differentials of the third kind, on the other
 843 hand, also have poles with non-zero residue, and the integral over a small loop with winding
 844 number 1 around a pole is equal to $2i\pi$ times the residue of the pole, like for meromorphic
 845 functions on \mathbb{C} .

846 As with meromorphic functions, the trace of a meromorphic differential ω on \mathcal{M} with
 847 respect to a covering map ρ from \mathcal{M} to \mathcal{N} is defined as a sum over all preimages of ρ ,

$$(\text{tr}_\rho \omega)(q) = \sum_{\substack{p \in \mathcal{M} \\ \rho(p)=q}} \omega(p) . \tag{34}$$

848 If ω is holomorphic on \mathcal{M} , $\text{tr}_\rho \omega$ is then holomorphic on \mathcal{N} [85]. This observation is crucial
 849 for the application to KPZ in section 2 in order to move freely contours of integration
 850 between the left side and the right side of the cylinder \mathcal{C} .

851 3.8 Infinite genus limit

852 We consider in this section an infinite genus version \mathcal{R} of the Riemann surface \mathcal{R}_N . Rie-
 853 mann surfaces $\tilde{\mathcal{R}}$ and \mathcal{R}^Δ in terms of which KPZ fluctuations are described in section 2 are
 854 constructed as quotients of \mathcal{R} under the action of groups of holomorphic automorphisms.

855 3.8.1 Riemann surface \mathcal{R}

856

857 The Riemann surface \mathcal{R} can be understood informally as a limit $N \rightarrow \infty$ of \mathcal{R}_N with the
 858 choice of branch points $2i\pi(\mathbb{Z} + 1/2)$ for the covering map $[v, P] \mapsto v$. Topologically, \mathcal{R} is
 859 thus an infinite dimensional hypercube made of spheres connected by cylinders, see figure 8

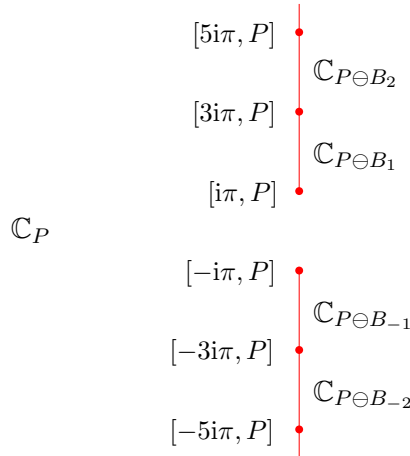


Figure 12: Choice of branch cuts (red, vertical lines) partitioning the Riemann surface \mathcal{R} into the sheets \mathbb{C}_P , $P \subset \mathbb{Z} + 1/2$. The ramification points of the covering map Π from \mathcal{R} to the infinite cylinder \mathcal{C} are represented with red dots. The connectivity of the sheets is indicated near the cuts, with B_n defined in (35) and \ominus the symmetric difference operator from (30).

860 for finite genus analogues \mathcal{R}_N . The Riemann surface \mathcal{R} is understood more concretely in
 861 section 4.4 as a natural domain of definition for polylogarithms with half-integer index,
 862 which generalize the finite sum of square roots (28) on \mathcal{R}_N .

863 Branch cuts are chosen such that \mathcal{R} is partitioned into infinitely many sheets \mathbb{C}_P
 864 indexed by subsets P of $\mathbb{Z} + 1/2$ ⁹, copies of the complex plane slit along the cut $(-i\infty, -i\pi] \cup$
 865 $[i\pi, i\infty)$ with the points on the cut belonging by convention to e.g. the left part of the cut.
 866 Introducing for $n \in \mathbb{Z}$ the sets

$$\begin{aligned} B_0 &= \emptyset & n &= 0 \\ B_n &= \{1/2, 3/2, \dots, n - 1/2\} & n &> 0 \\ B_n &= \{n + 1/2, \dots, -3/2, -1/2\} & n &< 0 \end{aligned} \quad (35)$$

867 the sheets \mathbb{C}_P and $\mathbb{C}_{P \ominus B_n}$ are glued together along both sides of the cut $2i\pi(n - 1/2, n + 1/2)$
 868 ¹⁰, with \ominus the symmetric difference operator defined in (30), see figure 12.

869 Since the branch points $2i\pi a$, $a \in \mathbb{Z} + 1/2$ are equally spaced, there exists a covering
 870 map $\Pi : [v, P] \mapsto v - 2i\pi[\frac{\text{Im } v}{2\pi}]$, with $[\frac{\text{Im } v}{2\pi}]$ the integer closest to $\frac{\text{Im } v}{2\pi}$, from \mathcal{R} to the infinite
 871 cylinder $\mathcal{C} = \{v \in \mathbb{C}, v \equiv v + 2i\pi\}$, see figure 1. Using the covering map $\lambda : v \mapsto e^v$,
 872 the infinite cylinder is completely equivalent to $\mathbb{C}^* = \mathbb{C} \setminus \{0\}$, i.e. the Riemann sphere
 873 punctured twice $\mathbb{C}^* = \widehat{\mathbb{C}} \setminus \{0, \infty\}$.

874 A subtle issue concerns whether sheets indexed by infinite sets P should be considered
 875 when building \mathcal{R} , as such sheets can not be reached from sheets indexed by finite sets
 876 without crossing infinitely many branch cuts. Since only sheets indexed by finite sets
 877 appear in our formulas for KPZ fluctuations in section 2, we avoid this issue completely
 878 and define \mathcal{R} by gluing together only the sheets indexed by finite sets $P \subset \mathbb{Z} + 1/2$ with
 879 cardinal $|P|$. A related issue concerns the status of the points at infinity in \mathcal{R} . Unlike
 880 in \mathcal{R}_N , we may not add these points to \mathcal{R} since they correspond to an accumulation of

⁹The choice of sets of half-integers instead of integers to label the sheets is for symmetry between analytic continuations above and under the real axis for the functions of section 4.

¹⁰The choice of “vertical” branch cuts like for the sheets \mathcal{F}_P of \mathcal{R}_N instead of “horizontal” branch cuts like for the sheets \mathcal{G}_P is for better compatibility with translations by integer multiples of $2i\pi$ later on.

881 ramification points for the covering map $[z, P] \mapsto z$. The two points at infinity on each
 882 sheet (on the left side and on the right side of the cut) are thus considered as punctures
 883 of \mathcal{R} , i.e. infinitesimal boundaries.

884 Homology classes of loops on \mathcal{R} avoiding the punctures are generated by the same loops
 885 $\ell_{a,b} \cdot P$, $a < b \in \mathbb{Z} + 1/2$ as the ones defined for the finite genus analogue \mathcal{R}_N in section 3.6,
 886 with θ_a now encircling $2i\pi a$. Additionally, paths between punctures play an important
 887 role for explicit computation of analytic continuations between the various sheets \mathbb{C}_P for
 888 the functions needed to express KPZ fluctuations.

889 3.8.2 Riemann surface $\tilde{\mathcal{R}}$

890

891 Anticipating the fact that some functions on \mathcal{R} defined in section 4 have special symmetries
 892 when their variable $[v, P] \in \mathcal{R}$ is replaced by $[v + 2i\pi, P]$, we are lead to define also the
 893 quotient $\tilde{\mathcal{R}}$ of \mathcal{R} under the action of a group of translations.

894 Let us consider the bijective operators $T_{|r}$ ¹¹ acting on finite sets $P \subset \mathbb{Z} + 1/2$ by
 895 $T_l P = P + 1$ and $T_r P = (P + 1) \ominus \{1/2\}$. For any $m \in \mathbb{Z}$, the iterated composition of
 896 these operators is given by

$$\begin{aligned} T_l^m P &= P + m \\ T_r^m P &= (P + m) \ominus B_m . \end{aligned} \tag{36}$$

897 The operators $T_{|r}$ generate two groups $G_{|r} = \{T_{|r}^m, m \in \mathbb{Z}\}$ acting on $\mathbb{Z} + 1/2$. The empty
 898 set is invariant under T_l , and $\{\emptyset\}$ thus constitutes an orbit under the action of G_l . The
 899 other orbits under the action of G_l are the infinite collections of sets P obtained from one
 900 another by shifting all the elements by an integer m , and equivalence classes of sets in the
 901 same orbit may be labelled by e.g. sets P whose smallest element is equal to $1/2$. Each
 902 orbit under the action of G_r , on the other hand, contains infinitely many elements. The
 903 identity

$$|(P + m) \ominus B_m|_+ - |(P + m) \ominus B_m|_- = |P|_+ - |P|_- + m , \tag{37}$$

904 with $|P|_+$ (respectively $|P|_-$) denoting the number of positive (resp. negative) elements
 905 of the set P , indicates that each orbit under the action of G_r contains a single element P
 906 with $|P|_+ = |P|_-$, which may be used to label the equivalence class.

907 Let us now consider the map \mathcal{T} defined on the left side of the sheet \mathbb{C}_\emptyset of \mathcal{R} by
 908 $\mathcal{T}[v, \emptyset] = [v + 2i\pi, \emptyset]$, $\text{Re } v < 0$. The map \mathcal{T} can be extended from the left side of \mathbb{C}_\emptyset to \mathcal{R}
 909 by lifting as follows: let $v_0 \in \mathbb{C}$ with $\text{Re } v_0 < 0$ and $\gamma = \{\gamma(t), 0 \leq t \leq 1\}$, a path contained
 910 in $\mathbb{C} \setminus 2i\pi(\mathbb{Z} + 1/2)$ starting at $\gamma(0) = v_0$. The lifts $\gamma \cdot \emptyset$ and $(\gamma + 2i\pi) \cdot \emptyset$ are paths on \mathcal{R}
 911 starting respectively at $[v_0, \emptyset]$ and $[v_0 + 2i\pi, \emptyset]$. Calling $[v, P]$ the endpoint of $\gamma \cdot \emptyset$, induction
 912 on the number of times γ crosses the imaginary axis implies that the endpoint of $(\gamma + 2i\pi) \cdot \emptyset$
 913 is $[v + 2i\pi, P + 1]$ if $\text{Re } v < 0$ and $[v + 2i\pi, (P + 1) \ominus \{1/2\}]$ if $\text{Re } v > 0$, independently of
 914 v_0 and γ . Checking carefully what happens when v is on the imaginary axis, especially in
 915 a neighbourhood of points of the form $[(2i\pi a)_{|r}, P]$, we observe that the map \mathcal{T} defined
 916 by $\mathcal{T}([v, P]) = [v + 2i\pi, P + 1]$ when $\text{Re } v < 0$, $\mathcal{T}([v, P]) = [v + 2i\pi, (P + 1) \ominus \{1/2\}]$
 917 when $\text{Re } v > 0$ and extended by continuity to $\text{Re } v = 0$ is a homeomorphism of \mathcal{R} , and
 918 hence an automorphism since it is locally holomorphic. The map \mathcal{T} is additionally a deck
 919 transformation for the covering map Π from \mathcal{R} to the infinite cylinder \mathcal{C} . The iterated
 920 composition \mathcal{T}^m , $m \in \mathbb{Z}$ is given by

$$\mathcal{T}^m([v, P]) = \begin{cases} [v + 2i\pi m, T_l^m P] & \text{Re } v < 0 \\ [v + 2i\pi m, T_r^m P] & \text{Re } v > 0 \end{cases} \tag{38}$$

¹¹We write $|r$ in the following as a shorthand for either the left side l or the right side r of a cut.

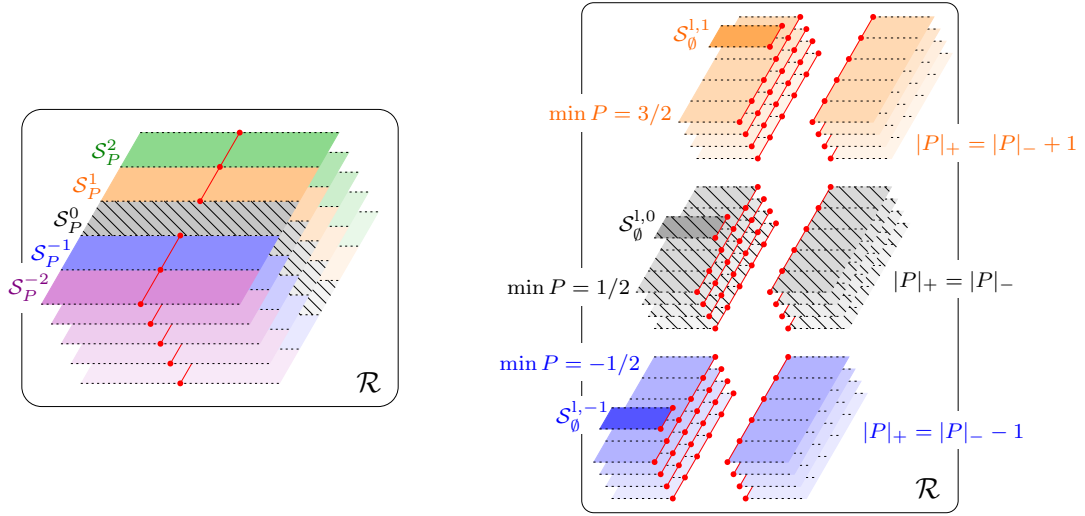


Figure 13: Two choices for a fundamental domain of \mathcal{R} under the action of $\check{\mathfrak{g}}$, from which $\check{\mathcal{R}} = \mathcal{R}/\check{\mathfrak{g}}$ is built. The fundamental domain is the hatched portion. How sheets are glued together along branch cuts (red lines, with dots for the branch points) is not represented for clarity. The picture on the left represents all sheets \mathbb{C}_P , $P \in \mathbb{Z} + 1/2$ above one another, with the fundamental domain made of the infinite strips \mathcal{S}_P^0 corresponding to points $[v, P]$ with $-\pi < \text{Im } v \leq \pi$. The picture on the right represents half-sheets \mathbb{C}_P^1 grouped according to the value of $\min P$ (if $P \neq \emptyset$; the half-sheet \mathbb{C}_\emptyset^1 is cut into half-infinite strips $\mathcal{S}_\emptyset^{1,m}$) and half-sheets \mathbb{C}_P^1 grouped by the value of $|P|_+ - |P|_-$.

921 with $T_{\parallel r}^m$ defined in (36). The group $\check{\mathfrak{g}} = \{\mathcal{T}^m, m \in \mathbb{Z}\}$ acts properly discontinuously on
 922 \mathcal{R} , and we call $\check{\mathcal{R}} = \mathcal{R}/\check{\mathfrak{g}}$ the Riemann surface quotient of \mathcal{R} under the action of $\check{\mathfrak{g}}$.

923 The Riemann surface $\check{\mathcal{R}}$ may be partitioned into half-sheets $\mathbb{C}_P^{\parallel r}$ by taking as a funda-
 924 mental domain for $\check{\mathfrak{g}}$ the left side of the sheets \mathbb{C}_P of \mathcal{R} with some choice of representatives
 925 P for the orbits under the action of G_1 plus the right side of the sheets \mathbb{C}_P with some choice
 926 P of representatives for the orbits under the action of G_r , with the additional identification
 927 $v = v + 2i\pi$ for the sheet \mathbb{C}_\emptyset^1 since $\{\emptyset\}$ is an orbit under the action of G_1 , see figure 13
 928 right. How sheets are glued together along the cuts depends on which representatives are
 929 chosen for the orbits.

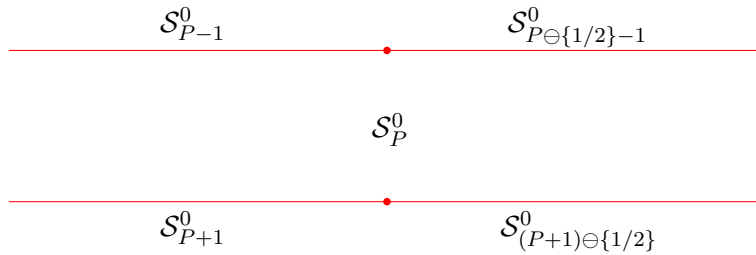


Figure 14: Connectivity of the infinite strips \mathcal{S}_P^0 , $P \in \mathbb{Z} + 1/2$ partitioning the Riemann surface $\check{\mathcal{R}}$. The red dots represent ramification points for the covering map $\check{\rho}$ sending all the strips to the infinite cylinder \mathcal{C} .

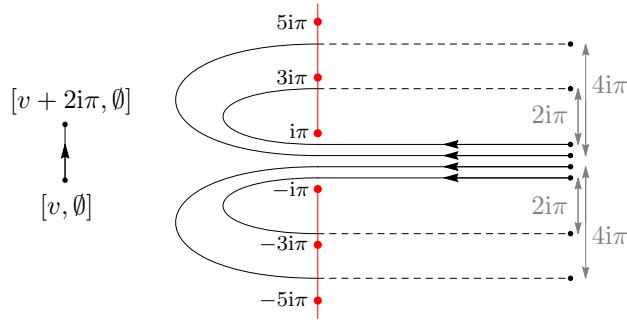


Figure 15: Examples of paths on \mathcal{R} which are also closed loops on $\check{\mathcal{R}}$. The solid curves belong to \mathbb{C}_\emptyset and the dashed lines to \mathbb{C}_{B_m} , $m = 2, 1, -1, -2$ from top to bottom.

930 Alternatively, we consider a partition of \mathcal{R} into half-infinite strips

$$\begin{aligned} \mathcal{S}_P^{l,m} &= \{[v, P], \operatorname{Re} v \leq 0, 2\pi(m - 1/2) < \operatorname{Im} v \leq 2\pi(m + 1/2)\} \\ \mathcal{S}_P^{r,m} &= \{[v, P], \operatorname{Re} v > 0, 2\pi(m - 1/2) < \operatorname{Im} v \leq 2\pi(m + 1/2)\}. \end{aligned} \quad (39)$$

931 The domain $\mathcal{S}_P^m = \mathcal{S}_P^{l,m} \cup \mathcal{S}_P^{r,m}$, contained in the sheet \mathbb{C}_P , is connected only when $m = 0$,
 932 see figure 13 left. A fundamental domain for the action of $\check{\mathfrak{g}}$ in \mathcal{R} may be chosen as the
 933 \mathcal{S}_P^0 indexed by all $P \sqsubset \mathbb{Z} + 1/2$. In the Riemann surface $\check{\mathcal{R}}$, the upper part $\operatorname{Im} v = \pi$ of
 934 \mathcal{S}_P^0 is glued to the lower part $\operatorname{Im} v \rightarrow -\pi$ of \mathcal{S}_{P-1}^0 on the left side, while the upper part of
 935 \mathcal{S}_P^0 is glued to the lower part of $\mathcal{S}_{P \ominus \{1/2\}-1}^0$ on the right side, see figure 14. This choice of
 936 a fundamental domain naturally defines the covering maps $\check{\Pi} : [v, P] \mapsto [v - 2i\pi[\frac{\operatorname{Im} v}{2\pi}], P]$
 937 from \mathcal{R} to $\check{\mathcal{R}}$ and $\check{\rho} : [v, P] \mapsto v$ from $\check{\mathcal{R}}$ to the infinite cylinder \mathcal{C} . KPZ fluctuations
 938 with flat initial condition are expressed in section 2.2 in terms of the trace over $\check{\rho}$ of a
 939 holomorphic differential on $\check{\mathcal{R}}$.

940 The existence of the covering map $\check{\Pi}$ from \mathcal{R} to $\check{\mathcal{R}}$ implies that any loop $\ell_{a,b} \cdot P$ on \mathcal{R}
 941 project to a loop on $\check{\mathcal{R}}$. There exists however loops on $\check{\mathcal{R}}$ that may not be obtained in
 942 such a way, for instance starting from \mathbb{C}_\emptyset , the paths $[v - i\pi, \emptyset] \rightarrow [v + i\pi, \emptyset]$, $\operatorname{Re} v < 0$ and
 943 $[v, \emptyset] \rightarrow [(2i\pi m)_l, \emptyset] = [(2i\pi m)_r, B_m] \rightarrow [v + 2i\pi m, B_m]$, $\operatorname{Re} v > 0$, $m \in \mathbb{Z}$ represented in
 944 figure 15 are closed on $\check{\mathcal{R}}$ but not on \mathcal{R} .

945 3.8.3 Riemann surface \mathcal{R}^Δ

946 We define in this section Riemann surfaces \mathcal{R}^Δ , $\Delta \sqsubset \mathbb{Z} + 1/2$ such that the elements
 947 $a \in \Delta$ correspond to branch points $2i\pi a$ that have been “removed” compared to \mathcal{R} .
 948

949 Let us consider the involutions D_a , $a \in \mathbb{Z} + 1/2$ acting on finite sets $P \sqsubset \mathbb{Z} + 1/2$ by

$$D_a P = P \ominus \{a\}. \quad (40)$$

950 For $\Delta \sqsubset \mathbb{Z} + 1/2$, we call G^Δ the commutative group generated by the D_a , $a \in \Delta$. The
 951 orbit of any $P \sqsubset \mathbb{Z} + 1/2$ under the action of G^Δ is the collection of all sets $Q \sqsubset \mathbb{Z} + 1/2$
 952 such that $Q \setminus \Delta = P \setminus \Delta$, and orbits can thus be labelled by the sets P such that $P \cap \Delta = \emptyset$.

953 The group G^Δ acting on sets can be upgraded to a group acting on the Riemann
 954 surface \mathcal{R} . By the commutativity of symmetric difference, the maps \mathcal{D}_a , $a \in \mathbb{Z} + 1/2$
 955 defined by

$$\mathcal{D}_a[v, P] = [v, D_a P] \quad (41)$$

956 are holomorphic automorphisms of \mathcal{R} , and deck transformations for the covering map Π
 957 from \mathcal{R} to the infinite cylinder \mathcal{C} . The group \mathfrak{g}^Δ generated by the \mathcal{D}_a , $a \in \Delta$ acts properly

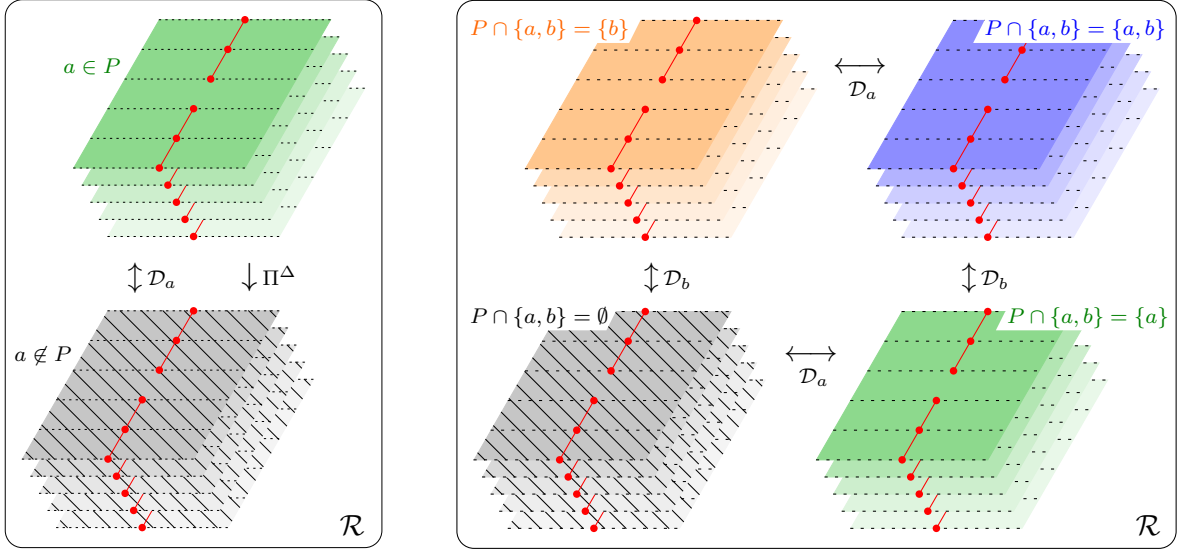


Figure 16: Choice of a fundamental domain of \mathcal{R} under the action of \mathfrak{g}^Δ with $\Delta = \{a\}$ (left) and $\Delta = \{a, b\}$ (right). The sheets \mathbb{C}_P , partitioned along dashed lines into pairs of half-infinite strips $\mathcal{S}_P^m = \mathcal{S}_P^{l,m} \cup \mathcal{S}_P^{r,m}$ from (39), are grouped together according to the value of $P \cap \Delta$. The fundamental domain corresponding to \mathcal{R}^Δ is the hatched portion, made from the sheets \mathbb{C}_P with $P \cap \Delta = \emptyset$. How sheets are glued together along branch cuts (red lines, with dots for the branch points) is not represented for clarity.

958 discontinuously on \mathcal{R} , and the quotient $\mathcal{R}^\Delta = \mathcal{R}/\mathfrak{g}^\Delta$ is a Riemann surface. One has in
 959 particular $\mathcal{R}^\emptyset = \mathcal{R}$.

960 Choosing for fundamental domain the collection of sheets \mathbb{C}_P with $P \cap \Delta = \emptyset$, the
 961 construction above defines the covering map $\Pi^\Delta : [v, P] \mapsto [v, P \setminus \Delta]$ from \mathcal{R} to \mathcal{R}^Δ ,
 962 and \mathcal{R}^Δ may be partitioned into sheets \mathbb{C}_P , $P \cap \Delta = \emptyset$, images of the sheets of \mathcal{R} by
 963 Π^Δ , see figure 16. The sheet \mathbb{C}_P of \mathcal{R}^Δ is glued to the sheet $\mathbb{C}_{P \ominus (B_n \setminus \Delta)}$ along the cut
 964 $v \in (2i\pi(n - 1/2), 2i\pi(n + 1/2))$.

965 The sheets \mathbb{C}_P may be further partitioned into pairs of half-infinite strips $\mathcal{S}_P^m = \mathcal{S}_P^{l,m} \cup$
 966 $\mathcal{S}_P^{r,m}$, $m \in \mathbb{Z}$ with the same notations (39) as in the previous section. Unlike for \mathcal{R} , we
 967 have not taken a quotient by translations of $2i\pi$ here, so that all values $m \in \mathbb{Z}$ must be
 968 taken in the partition. This defines the covering map $\rho^\Delta : [v, P] \mapsto v - 2i\pi \lfloor \frac{\text{Im} v}{2\pi} \rfloor$ from \mathcal{R}^Δ
 969 to the infinite cylinder \mathcal{C} , see figure 1 for a summary of useful covering maps.

970 3.8.4 Collection $\overline{\mathcal{R}}$ of Riemann surface \mathcal{R}^Δ

971 The Riemann surfaces \mathcal{R}^Δ and $\mathcal{R}^{\Delta+1}$ are isomorphic since changing Δ to $\Delta+1$ amounts to
 972 relabelling the sheets. For the application to KPZ in section 2, it is sometimes convenient,
 973 however, to consider sheets from all \mathcal{R}^Δ without the identification $\Delta \equiv \Delta+1$. In order to
 974 do this, we introduce bijective operators $\overline{T}_{l,r}$ acting on pairs of sets (P, Δ) , $P, \Delta \subset \mathbb{Z} + 1/2$
 975 by $\overline{T}_l(P, \Delta) = (P + 1, \Delta + 1)$ and $\overline{T}_r(P, \Delta) = ((P + 1) \ominus (\{1/2\} \setminus (\Delta + 1)), \Delta + 1)$. For
 976 any $m \in \mathbb{Z}$, the iterated composition of these operators is given by

$$\begin{aligned} \overline{T}_l^m(P, \Delta) &= (P + m, \Delta + m) \\ \overline{T}_r^m(P, \Delta) &= ((P + m) \ominus (B_m \setminus (\Delta + m)), \Delta + m). \end{aligned} \quad (42)$$

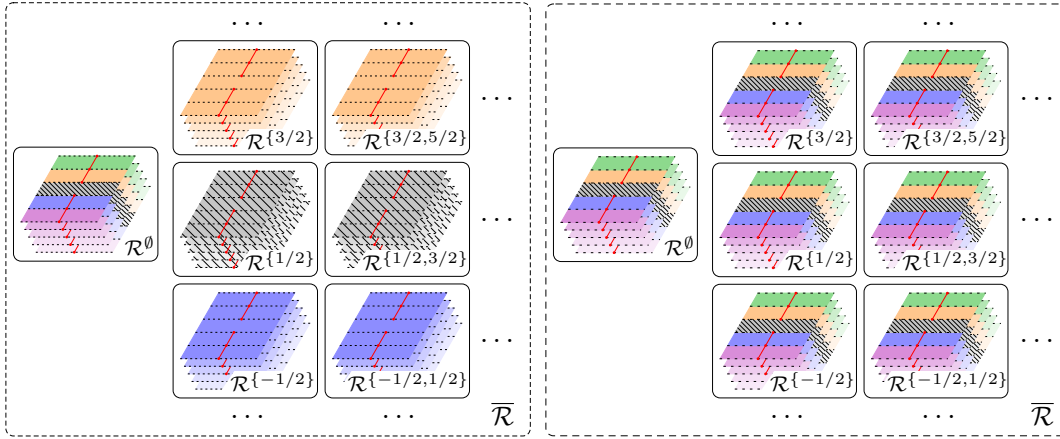


Figure 17: Two choices for the fundamental domain of the collection of Riemann surfaces $\overline{\mathcal{R}}$ under the action of $\overline{\mathfrak{g}}$. The fundamental domain is the hatched portion. How sheets are glued together is not represented for clarity. For the connected component $\mathcal{R}^\emptyset = \mathcal{R}$ of $\overline{\mathcal{R}}$, the fundamental domain $\tilde{\mathcal{R}}$ is chosen as in figure 13 left.

978 The operators $\overline{T}_{1|r}$ generate two groups $\overline{G}_{1|r} = \{\overline{T}_{1|r}^m, m \in \mathbb{Z}\}$ acting on subsets of $(\mathbb{Z} +$
 979 $1/2) \times (\mathbb{Z} + 1/2)$. The sector $\{(P, \emptyset), P \subset \mathbb{Z} + 1/2\}$ is an invariant subset under $\overline{G}_{1|r}$, which
 980 essentially reduce to the groups $G_{1|r}$ of the previous section there, and have in particular
 981 the same orbits. Outside of that sector, equivalence classes of pairs of sets in the same
 982 orbit under \overline{G}_1 may be labelled by pairs (P, Δ) with Δ arbitrary and P such that its
 983 smallest element is equal to e.g. $1/2$.

984 The situation is more complicated for \overline{G}_r . Introducing $\lambda_\pm(P, \Delta) = |P|_\pm - |P \ominus \Delta|_\mp$,
 985 one has for any $P, \Delta \subset \mathbb{Z} + 1/2$ the identity

$$(\lambda_\pm \circ \overline{T}_r^m)(P, \Delta) = \lambda_\pm(P, \Delta) \pm m, \quad (43)$$

986 which implies in particular that $|P| - |P \ominus \Delta|$ is invariant by \overline{T}_r^m . The equivalence classes
 987 of pairs of sets (P, Δ) in the same orbit under \overline{G}_r may thus be labelled by pairs (P, Δ) with
 988 $|P|_+ = |P \ominus \Delta|_-$. In the sector $|P| = |P \ominus \Delta|$, such pairs verify both $|P|_\pm = |P \ominus \Delta|_\mp$.

989 We consider the collection $\overline{\mathcal{R}}$ of all Riemann surfaces \mathcal{R}^Δ , $\Delta \subset \mathbb{Z} + 1/2$ and write
 990 $[v, (P, \Delta)] \in \overline{\mathcal{R}}$ for the point $[v, P] \in \mathcal{R}^\Delta$. The map $\overline{\mathcal{T}}$ whose iterated composition is given
 991 by

$$\overline{\mathcal{T}}^m[v, (P, \Delta)] = \begin{cases} [v + 2i\pi m, \overline{T}_1^m(P, \Delta)] & \text{Re } v < 0 \\ [v + 2i\pi m, \overline{T}_r^m(P, \Delta)] & \text{Re } v > 0 \end{cases} \quad (44)$$

992 with $\overline{T}_{1|r}^m$ defined in (42) is a holomorphic automorphism of $\overline{\mathcal{R}}$ generating a group $\overline{\mathfrak{g}}$. The
 993 map $\overline{\mathcal{T}}^m$ restricts to an isomorphism between \mathcal{R}^Δ and $\mathcal{R}^{\Delta+m}$ for any $\Delta \subset \mathbb{Z} + 1/2$. In
 994 particular, $\overline{\mathcal{T}}$ has the same action on $\mathcal{R}^\emptyset = \mathcal{R}$ as \mathcal{T} defined in (38).

995 The quotient $\overline{\mathcal{R}}/\overline{\mathfrak{g}}$ corresponds to the collection of Riemann surfaces containing $\tilde{\mathcal{R}}$
 996 and a representative \mathcal{R}^Δ from each equivalence class $\Delta \equiv \Delta + 1$ under isomorphism, see
 997 figure 17 left. Another choice of fundamental domain for the action of $\overline{\mathcal{T}}$ consists in taking
 998 $\tilde{\mathcal{R}}$ plus the infinite strips \mathcal{S}_p^0 , $P \cap \Delta = \emptyset$ from all \mathcal{R}^Δ without the identification $\Delta \equiv \Delta + 1$,
 999 see figure 17 right.

1000 **4 Functions on the Riemann surfaces \mathcal{R} , $\check{\mathcal{R}}$, \mathcal{R}^Δ**

1001 In this section, we study polylogarithms with half-integer index and several functions built
 1002 from them living on the Riemann surfaces \mathcal{R} , $\check{\mathcal{R}}$, \mathcal{R}^Δ defined in section 3.8, and used for
 1003 KPZ fluctuations in section 2. The results presented until section 4.6 are not new and
 1004 merely serve to introduce notations. The explicit analytic continuations performed from
 1005 section 4.7 on the specific functions needed for KPZ are presumably new.

1006 **4.1 $2i\pi(\mathbb{Z} + 1/2)$ -continuable functions, translation and analytic continu-**
 1007 **ations**

1008 Throughout section 4, we consider functions analytic in the domain

$$\mathbb{D} = \mathbb{C} \setminus ((-i\infty, -i\pi] \cup [i\pi, i\infty)), \quad (45)$$

1009 and which may be continued analytically along any path in \mathbb{C} avoiding the points in
 1010 $2i\pi(\mathbb{Z} + 1/2)$, i.e. such paths never encounter branch points, poles or essential singularities.
 1011 We borrow the terminology $2i\pi(\mathbb{Z} + 1/2)$ -continuable from the theory of resurgent function
 1012 for this class of functions. In the presence of branch points, which must necessarily belong
 1013 to $2i\pi(\mathbb{Z} + 1/2)$, new functions analytic in \mathbb{D} are generated by crossing branch cuts.

1014 We introduce the notation $A_n^l f$ (respectively $A_n^r f$) for the function obtained from a
 1015 $2i\pi(\mathbb{Z} + 1/2)$ -continuable function f after crossing the (potential) branch cut $(2i\pi(n -$
 1016 $1/2), 2i\pi(n + 1/2))$, $n \in \mathbb{Z}$ from left to right (resp. from right to left), i.e. when the
 1017 function f is continued analytically along the path $x + 2i\pi n$ with x increasing from 0^- to
 1018 0^+ (resp. decreasing from 0^+ to 0^-), see figure 18 right. Both $A_n^l f$ are understood as
 1019 analytic functions in \mathbb{D} . When the analytic continuation from both sides gives the same
 1020 result, which happens if the branch points of f are of square root type, we write A_n instead
 1021 of A_n^l or A_n^r . Since f is assumed to be analytic in \mathbb{D} , there is no branch cut between $-i\pi$
 1022 and $i\pi$, and one has $A_0^l f = f$. Furthermore, the operators A_n^l and A_n^r are inverse of each
 1023 other, $A_n^l A_n^r f = A_n^r A_n^l f = f$.

1024 We will be interested in the following in the interplay between analytic continuation
 1025 and translation by integer multiples of $2i\pi$. Since we are working with functions analytic
 1026 in \mathbb{D} , one has to distinguish the effect of translations on the left and on the right, as two
 1027 points apart of $2i\pi$ moved from the left side to the right side end up crossing distinct branch
 1028 cuts. We introduce translation operators $T_{l|r}$ acting on $2i\pi(\mathbb{Z} + 1/2)$ -continuable functions
 1029 f , such that $T_l f$ and $T_r f$ are analytic in \mathbb{D} and verify respectively $(T_l f)(v) = f(v + 2i\pi)$
 1030 when $\text{Re } v < 0$ and $(T_r f)(v) = f(v + 2i\pi)$ when $\text{Re } v > 0$, see figure 18 right.

1031 One has for any $m, n \in \mathbb{Z}$ the identities $A_{m+n}^l = T_r^{-m} A_n^l T_l^m$ and $A_{m+n}^r = T_l^{-m} A_n^r T_r^m$.
 1032 In particular, since A_0^l is the identity operator, we observe that the analytic continuation
 1033 can be deduced from translations on both sides:

$$\begin{aligned} A_n^l &= T_r^{-n} T_l^n \\ A_n^r &= T_l^{-n} T_r^n. \end{aligned} \quad (46)$$

1034 These identities are used in the following as a convenient way to derive analytic continu-
 1035 ations of functions defined as integrals of meromorphic differentials.

1036 **4.2 Polylogarithms**

1037 The polylogarithm of index $s \in \mathbb{C}$ is defined for $|z| < 1$ by the series

$$\text{Li}_s(z) = \sum_{k=1}^{\infty} \frac{z^k}{k^s}. \quad (47)$$

1038 When s is a non-positive integer, $s \in -\mathbb{N}$, $\text{Li}_s(z)$ reduces to a rational function of z with
 1039 a pole at $z = 1$. Otherwise, analytic continuation beyond the unit disk allows to extend
 1040 Li_s to an analytic function in $\mathbb{C} \setminus [1, \infty)$, the principal value of Li_s , with a branch point
 1041 at $z = 1$ and a branch cut traditionally chosen to be the real numbers larger than 1. For
 1042 $s = 1$, $\text{Li}_1(z) = -\log(1 - z)$, and the branch point is of logarithmic type. The function Li_1
 1043 can thus be extended to an analytic function on a Riemann surface built from infinitely
 1044 many sheets \mathbb{C}_k , $k \in \mathbb{Z}$, such that the top part of the cut in \mathbb{C}_k is glued to the bottom
 1045 part of the cut in \mathbb{C}_{k+1} .

1046 Analytic continuations in the variable z of $\text{Li}_s(z)$ when $s \neq 1$ is more involved [86].
 1047 Indeed, after analytic continuation from below the cut $[1, \infty)$, the function $\text{Li}_s(z)$ becomes
 1048 $\text{Li}_s(z) - \frac{2i\pi(\log z)^{s-1}}{\Gamma(s)}$ with Γ the Euler gamma function. The power $s - 1$ in the extra term
 1049 leads to the same branch point $z = 1$ as Li_s , while the logarithm gives an additional branch
 1050 point at $z = 0$, and makes the structure of the Riemann surface more complicated since
 1051 further analytic continuation must take into account how $(\log z)^{s-1}$ varies across branch
 1052 cuts.

1053 Because of the extra logarithm obtained from analytic continuation, it is useful to
 1054 consider instead ¹² the function $\text{Li}_s(-e^v)$. In terms of the variable v , this function has an
 1055 alternative expression as the complete Fermi-Dirac integral

$$\text{Li}_s(-e^v) = -\frac{1}{\Gamma(s)} \int_0^\infty du \frac{u^{s-1}}{e^{u-v} + 1} \quad (48)$$

1056 for $\text{Re } s > 0$, and in terms of the Hurwitz zeta function $\zeta(s, u) = \sum_{k=0}^\infty (u+k)^{-s}$ as

$$\text{Li}_s(-e^v) = \frac{\Gamma(1-s)}{(2\pi)^{1-s}} \left(i^{1-s} \zeta\left(1-s, \frac{1}{2} + \frac{v}{2i\pi}\right) + i^{s-1} \zeta\left(1-s, \frac{1}{2} - \frac{v}{2i\pi}\right) \right). \quad (49)$$

1057 The function $\text{Li}_s(-e^v)$ has the branch points $2i\pi a$, $a \in \mathbb{Z} + 1/2$. Crossing the branch cut
 1058 associated to $2i\pi a$ in the anti-clockwise direction relative to the branch point transforms
 1059 $\text{Li}_s(-e^v)$ into $\text{Li}_s(-e^v) - \frac{2i\pi(v-2i\pi a)^{s-1}}{\Gamma(s)}$, which has the same branch points as the principal
 1060 value: the function $v \mapsto \text{Li}_s(-e^v)$ thus belongs to the class of $2i\pi(\mathbb{Z} + 1/2)$ -continuable
 1061 functions defined in the previous section if the branch cut is chosen as $(-\infty, -i\pi] \cup [i\pi, \infty)$.

1062 In the much studied case where $s \geq 2$ is an integer, the extra terms obtained after
 1063 crossing branch cuts are polynomials in v , and are thus inert by analytic continuation:
 1064 crossing a branch cut twice in the same direction simply adds the same extra term once
 1065 more. All branch points are thus of logarithmic type. When s is not an integer, the
 1066 situation becomes more complicated since the extra terms are multiplied by a phase after
 1067 analytic continuation. After setting notations for square roots with specific branch cuts in
 1068 the next section, we focus in section 4.4 on the case where s is a half-integer, $s \in \mathbb{Z} + 1/2$,
 1069 which is the case of interest for KPZ.

1070 4.3 Square roots $\kappa_a(v)$

1071 Before considering polylogarithms with half-integer index, we introduce for convenience a
 1072 square root function κ_a , $a \in \mathbb{Z} + 1/2$ with branch point $2i\pi a$. We define

$$\kappa_a(v) = \sqrt{4i\pi a} \sqrt{1 - \frac{v}{2i\pi a}} = \sqrt{\text{sgn}(a)i} \sqrt{|4\pi a| + \text{sgn}(a)2iv}, \quad (50)$$

1073 with the usual branch cut $\mathbb{R}^- = (-\infty, 0]$ for the square roots so that the branch cut of
 1074 κ_a is the interval $\text{sgn}(a)2i\pi(|a|, \infty)$. In particular, κ_a is analytic in the domain \mathbb{D} defined

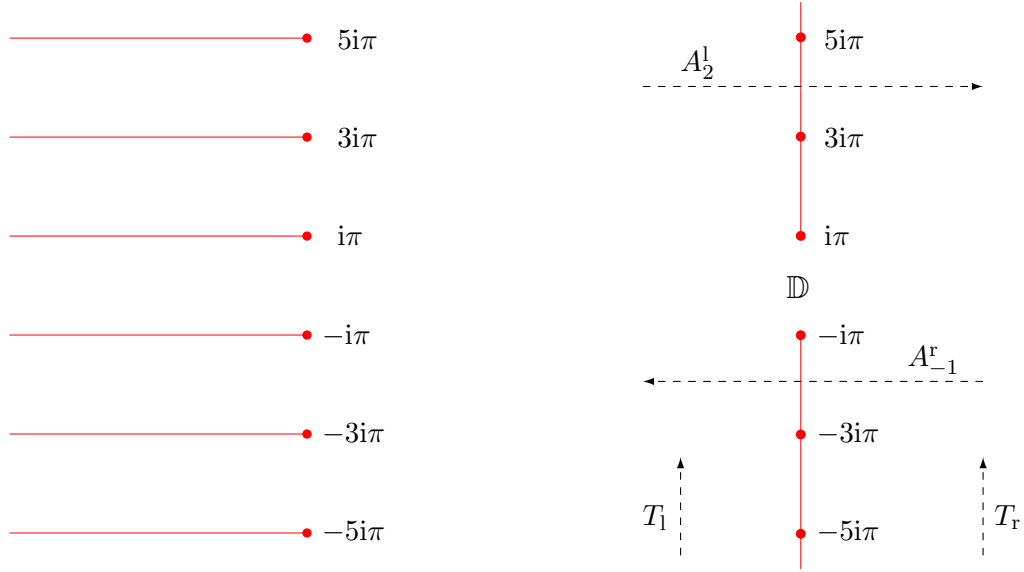


Figure 18: Two possible choices of branch cuts for the function χ_θ . The choice on the left, corresponding to the principal value of the polylogarithm $\text{Li}_{5/2}$ in (56), is not convenient because of the presence of symmetries $v \mapsto v + 2i\pi$. The choice on the right, which is the one actually used in the paper, defines by removing the cuts a space $\mathbb{D} = \mathbb{C} \setminus ((-\infty, -i\pi] \cup [i\pi, \infty))$ on which the chosen determination of χ_θ is analytic. Examples of paths of analytic continuation for the translation operators T_1 , T_r and the analytic continuation operators A_n^1 , A_n^r , $n \in \mathbb{Z}$ defined in section 4.1 are also indicated on the right with dashed arrows.

1075 in (45). The expression (50) for κ_a reduces to $\kappa_a(v) = \sqrt{4i\pi a - 2v}$ when $\text{Re } v < 0$ and
 1076 $\kappa_a(v) = \text{sgn}(a)i\sqrt{2v - 4i\pi a}$ when $\text{Re } v > 0$.

1077 We list a few useful properties of the functions κ_a . The derivative κ'_a , also analytic in
 1078 \mathbb{D} , is equal to

$$\kappa'_a = -\frac{1}{\kappa_a}. \tag{51}$$

1079 For $v \in \mathbb{D}$, the possible locations of $\kappa_a(v)$ in the complex plane are such that both $\log \kappa_a$
 1080 and $\log(\kappa_a + \kappa_b)$, $a, b \in \mathbb{Z} + 1/2$ are analytic in \mathbb{D} with the branch cut of the logarithm taken
 1081 as \mathbb{R}^- , see appendix C.1. Finally, shifting v by an integer multiple of $2i\pi$ is equivalent
 1082 to shifting a , up to a possible minus sign: $\kappa_a(v + 2i\pi n) = \kappa_{a-n}(v)$ when $\text{Re } v < 0$ and
 1083 $\kappa_a(v + 2i\pi n) = \sigma_a(B_n)\kappa_{a-n}(v)$ when $\text{Re } v > 0$, with σ_a given in (29) and B_n in (35). For
 1084 the logarithm of κ_a , using (180), one has instead $\log \kappa_a(v + 2i\pi n) = \log \kappa_{a-n}(v)$ when
 1085 $\text{Re } v < 0$ and $\log \kappa_a(v + 2i\pi n) = \log \kappa_{a-n}(v) + 1_{\{a \in B_n\}}i\pi \text{sgn}(n)$ when $\text{Re } v > 0$. In terms
 1086 of the translation operators of section 4.1, these identities can be written as

$$\begin{aligned} T_1^n \kappa_a &= \kappa_{a-n} \\ T_r^n \kappa_a &= \sigma_a(B_n)\kappa_{a-n}. \end{aligned} \tag{52}$$

1087 Using (46), this leads for the analytic continuation from either side of the cut to

$$A_n \kappa_a = \sigma_a(B_n)\kappa_a, \tag{53}$$

1088 which is already obvious from the definition of κ_a . The analytic continuation gives the
 1089 same result from both sides of the cut since the branch point of κ_a is of square root type.

¹²The minus sign in front of e^v is introduced to make formulas symmetric under complex conjugation.

1090 Similarly, one has for the logarithm of κ_a

$$\begin{aligned} T_1^n \log \kappa_a &= \log \kappa_{a-n} \\ T_r^n \log \kappa_a &= \log \kappa_{a-n} + 1_{\{a \in B_n\}} i\pi \operatorname{sgn}(n), \end{aligned} \quad (54)$$

1091 which using (46), leads to distinct analytic continuations from either side,

$$\begin{aligned} A_n^l \log \kappa_a &= \log \kappa_a - 1_{\{a \in B_n\}} i\pi \operatorname{sgn}(n) \\ A_n^r \log \kappa_a &= \log \kappa_a + 1_{\{a \in B_n\}} i\pi \operatorname{sgn}(n), \end{aligned} \quad (55)$$

1092 and the branch point of $\log \kappa_a$ is of logarithmic type.

1093 4.4 Half-integer polylogarithms and function χ on \mathcal{R}

1094 We introduce the function

$$\chi_\emptyset(v) = -\frac{\operatorname{Li}_{5/2}(-e^v)}{\sqrt{2\pi}}, \quad (56)$$

1095 The branch points of χ_\emptyset are the $2i\pi a$, $a \in \mathbb{Z} + 1/2$. If the principal value of $\operatorname{Li}_{5/2}$ is chosen
 1096 in (56), the branch cut associated to the branch point a is $2i\pi a + (-\infty, 0]$, see figure 18
 1097 left. We choose instead the branch cut $(-\infty, -i\pi] \cup [i\pi, \infty)$ in the following, see figure 18
 1098 right, so that χ_\emptyset is analytic in the domain \mathbb{D} defined in (45). Using (49), this can be done
 1099 explicitly by writing $\chi_\emptyset(v)$ as

$$\chi_\emptyset(v) = \frac{8\pi^{3/2}}{3} \left(e^{i\pi/4} \zeta\left(-\frac{3}{2}, \frac{1}{2} + \frac{v}{2i\pi}\right) + e^{-i\pi/4} \zeta\left(-\frac{3}{2}, \frac{1}{2} - \frac{v}{2i\pi}\right) \right), \quad (57)$$

1100 which is indeed analytic for $v \in \mathbb{D}$ if the usual branch cut \mathbb{R}^- is chosen for the Hurwitz ζ
 1101 function $\zeta(-3/2, \cdot)$.

1102 From (47), the polylogarithm expression (56) gives for large $|v|$, $\operatorname{Re} v < 0$ the convergent
 1103 expansion

$$\chi_\emptyset(v) \simeq -\frac{1}{\sqrt{2\pi}} \sum_{j=1}^{\infty} \frac{(-1)^j e^{jv}}{j^{5/2}} \simeq \frac{e^v}{\sqrt{2\pi}}. \quad (58)$$

1104 Using the asymptotic expansion for the Hurwitz zeta function in terms of Bernoulli num-
 1105 bers B_r ,

$$\zeta(s, u) \simeq -\frac{1}{1-s} \sum_{r=0}^{\infty} \binom{1-s}{r} \frac{B_r}{u^{r+s-1}} \quad (59)$$

1106 when $|u| \rightarrow \infty$ away from the negative real axis \mathbb{R}^- , the expression (57) for χ_\emptyset gives the
 1107 asymptotic expansion on the other side of the branch cut,

$$\chi_\emptyset(v) \simeq \frac{32\pi^{3/2}}{15} \sum_{r=0}^{\infty} \binom{5/2}{2r} \frac{(-1)^r (2^{1-2r} - 1) B_{2r}}{\left(\frac{v}{2\pi}\right)^{2r-5/2}} \simeq \frac{(2v)^{5/2}}{15\pi} + \frac{\pi\sqrt{2v}}{6} - \frac{7\pi^3}{360(2v)^{3/2}} \quad (60)$$

1108 when $|v| \rightarrow \infty$, $\operatorname{Re} v > 0$. The function χ_\emptyset has thus an essential singularity at infinity: on
 1109 the left side of the cut, the convergent expansion (58) for $\chi_\emptyset(v)$ is given as a series in e^v ,
 1110 while on the right side of the cut, the expansion (60) of $\chi_\emptyset(v)$ has a vanishing radius of
 1111 convergence in the variable $1/v$.

1112 From the Hurwitz zeta representation (57), it is possible to rewrite χ_\emptyset as an infinite
 1113 sum of powers $3/2$. In terms of the square root functions κ_a defined in (50), the identity

1114 $\zeta(s, u+1) = \zeta(s, u) - u^{-s}$, valid for any $s \in \mathbb{C} \setminus \{1\}$, even though $\zeta(s, u) = \sum_{k=0}^{\infty} (u+k)^{-s}$
 1115 only holds when $\text{Re } s > 1$, leads for any non-negative integer M to

$$\chi_{\emptyset}(v) = \frac{8\pi^{3/2}}{3} \left(e^{i\pi/4} \zeta\left(-\frac{3}{2}, M + \frac{1}{2} + \frac{v}{2i\pi}\right) + e^{-i\pi/4} \zeta\left(-\frac{3}{2}, M + \frac{1}{2} - \frac{v}{2i\pi}\right) \right) \quad (61)$$

$$- \sum_{a=-M+1/2}^{M-1/2} \frac{\kappa_a^3(v)}{3},$$

1116 where the sum is over half integers $a \in \mathbb{Z} + 1/2$ between $-M + 1/2$ and $M - 1/2$. In
 1117 the expression above, the first term containing the ζ functions is analytic in the strip
 1118 $-(M + 1/2)\pi < \text{Re } v < (M + 1/2)\pi$: the only branch points in the strip are contributed
 1119 by the sum. Our choice of branch cuts for the functions κ_a and $\zeta(-3/2, \cdot)$ then agrees
 1120 with the requirement that the expression (61) must be analytic in \mathbb{D} .

1121 Taking $M \rightarrow \infty$ and using the asymptotic expansion (59), we finally obtain χ_{\emptyset} as

$$\chi_{\emptyset}(v) = \lim_{M \rightarrow \infty} \left(-\frac{4(2\pi M)^{5/2}}{15\pi} - \frac{2v(2\pi M)^{3/2}}{3\pi} \quad (62)$$

$$+ \frac{(\pi^2 + 3v^2)\sqrt{2\pi M}}{6\pi} - \sum_{a=-M+1/2}^{M-1/2} \frac{\kappa_a^3(v)}{3} \right).$$

1122 In this expression, each term of the sum is analytic for $v \in \mathbb{D}$ with our choice of branch
 1123 cut for the functions κ_a . The two choices of branch cuts in figure 18 are thus analogous
 1124 to the ones in figure 5 for the finite sum of m square roots defined in (28).

1125 Analytic continuation of χ_{\emptyset} across the branch cut $(2i\pi(n-1/2), 2i\pi(n+1/2))$ changes
 1126 the signs of a finite number of terms in the infinite sum representation (62). After a finite
 1127 number of branch cut crossings, the function χ_{\emptyset} is replaced by

$$\chi_P(v) = \lim_{M \rightarrow \infty} \left(-\frac{4(2\pi M)^{5/2}}{15\pi} - \frac{2v(2\pi M)^{3/2}}{3\pi} + \frac{(\pi^2 + 3v^2)\sqrt{2\pi M}}{6\pi} \quad (63)$$

$$- \sum_{a=-M+1/2}^{M-1/2} \sigma_a(P) \frac{\kappa_a^3(v)}{3} \right),$$

1128 $P \subset \mathbb{Z} + 1/2$, where the sign $\sigma_a(P)$ is defined in (29). The set P contains the indices
 1129 $a \in \mathbb{Z} + 1/2$ for which the sign of $\kappa_a^3(v)$ has been flipped an odd number of times after
 1130 crossing branch cuts, and depends on the path along which the analytic continuation is
 1131 taken. When P is the empty set \emptyset , χ_P reduces to χ_{\emptyset} . The difference between χ_P and χ_{\emptyset}
 1132 is a finite sum,

$$\chi_P(v) = \chi_{\emptyset}(v) + \sum_{a \in P} \frac{2\kappa_a^3(v)}{3}. \quad (64)$$

1133 The expressions (63) and (64) for χ_P are manifestly analytic in \mathbb{D} with our choice of branch
 1134 cuts for χ_{\emptyset} and κ_a .

1135 In terms of the operators A_n defined in section 4.1, analytic continuations across branch
 1136 cuts of χ_P are simply given by

$$A_n \chi_P = \chi_{P \ominus B_n}, \quad (65)$$

1137 where the symmetric difference operator \ominus and the set B_n are defined in (30) and (35).
 1138 Since all the branch cuts of χ_P are of square root type, the analytic continuations are
 1139 independent of the side from which the branch cut is crossed.

1140 The functions χ_P on \mathbb{D} define a function χ analytic¹³ on the Riemann surface \mathcal{R} of
 1141 section 3.8.1 by

$$\chi([v, P]) = \chi_P(v) . \quad (66)$$

1142 Derivatives of χ_\emptyset can also be extended to functions on \mathcal{R} . The function χ' , defined by
 1143 $\chi'([v, P]) = \chi'_P(v)$ is still analytic on \mathcal{R} . The function χ'' , defined by $\chi''([v, P]) = \chi''_P(v)$
 1144 is only meromorphic on \mathcal{R} , as it has poles at the points $[(2i\pi a)_{1|r}, P]$.

1145 4.5 Symmetries of χ

1146 The expansion $\text{Li}_s(z) = \sum_{k=1}^{\infty} z^k/k^s$, valid for $|z| < 1$, indicates that $\chi_\emptyset(v)$ is periodic with
 1147 period $2i\pi$ in the sector $\text{Re } v < 0$. This is no longer true when $\text{Re } v > 0$ since the points v
 1148 and $v + 2i\pi$ end up in distinct sheets of \mathcal{R} when moved continuously from $\text{Re } v < 0$, which
 1149 leads to more complicated symmetries.

1150 The action of translations on χ_P can be deduced from its expression (63) as an infinite
 1151 sum. Recalling the translation operators $T_{1|r}$ from section 4.1 and using $\kappa_a(v) \simeq \sqrt{4i\pi a} -$
 1152 $v/\sqrt{4i\pi a}$ when $|a| \rightarrow \infty$, the identities (52) lead to

$$\begin{aligned} T_1^{-n} \chi_P &= \chi_{P+n} \\ T_r^{-n} \chi_P &= \chi_{(P+n) \ominus B_n} \end{aligned} \quad (67)$$

1153 for any $n \in \mathbb{Z}$, with B_n defined in (35). More explicitly, $\chi_P(v - 2i\pi n) = \chi_{P+n}(v)$ when
 1154 $\text{Re } v < 0$ and $\chi_P(v - 2i\pi n) = \chi_{(P+n) \ominus B_n}(v)$ when $\text{Re } v > 0$. The identities (67) are
 1155 compatible with analytic continuation (65) through (46) since $(P \ominus B_n) - n = (P - n) \ominus B_{-n}$.

1156 In terms of the map \mathcal{T} defined in (38), the identities (67) correspond to the symmetry
 1157 $\chi \circ \mathcal{T} = \chi$ for the function χ on \mathcal{R} . Since the Riemann surface $\tilde{\mathcal{R}}$ is defined as the quotient
 1158 of \mathcal{R} by the group generated by \mathcal{T} , this means that χ may also be defined as an analytic
 1159 function on $\tilde{\mathcal{R}}$. In the following, we use the same notation χ for both the function defined
 1160 on \mathcal{R} and on $\tilde{\mathcal{R}}$, and similarly for the functions χ' and χ'' built from the derivatives χ'_P
 1161 and χ''_P .

1162 4.6 Function I_0

1163 We consider for $\nu \in \mathbb{D}$ the function

$$I_0(\nu) = -\frac{1}{4} \int_{-\infty}^{\nu} \frac{dv}{1 + e^{-v}} = -\frac{1}{4} \int_{-\infty}^{\nu} dv \left(\frac{1}{2} + \sum_{a \in \mathbb{Z} + 1/2} \frac{1}{v - 2i\pi a} \right), \quad (68)$$

1164 with a path of integration contained in \mathbb{D} , see figure 19. Since the integrand is analytic in
 1165 \mathbb{D} , I_0 is independent from the path of integration. Because of the poles located at $2i\pi a$,
 1166 $a \in \mathbb{Z} + 1/2$, however, the function I_0 is defined with the branch cut $(-i\infty, -i\pi] \cup [i\pi, i\infty)$.
 1167 The integral can be performed explicitly, and one has the alternative expression

$$I_0(\nu) = \begin{cases} -\frac{1}{4} \log(1 + e^\nu) & \text{Re } \nu < 0 \\ -\frac{\nu}{4} - \frac{1}{4} \log(1 + e^{-\nu}) & \text{Re } \nu > 0 \end{cases} . \quad (69)$$

1168 An expression manifestly analytic in \mathbb{D} follows from the reflection formula for the Euler Γ
 1169 function $\Gamma(\frac{1}{2} - iz)\Gamma(\frac{1}{2} + iz) = \pi / \cosh(\pi z)$,

$$I_0(\nu) = -\frac{\log(2\pi)}{4} - \frac{\nu}{8} + \frac{1}{4} \log \Gamma\left(\frac{1}{2} - \frac{\nu}{2i\pi}\right) + \frac{1}{4} \log \Gamma\left(\frac{1}{2} + \frac{\nu}{2i\pi}\right) . \quad (70)$$

¹³We recall that the points at infinity, where χ_P has an essential singularity, are understood as punctures and do not belong to \mathcal{R} .

1170 Here, $\log \Gamma(z)$ is the principal value of the $\log \Gamma$ function ¹⁴, which is analytic for $z \in \mathbb{C} \setminus \mathbb{R}^-$.
 1171 Alternatively, the $\log \Gamma$ function may be written as an infinite sum of logarithms, and one
 1172 has

$$I_0(\nu) = -\frac{\log 2}{4} - \frac{\nu}{8} - \frac{1}{4} \sum_{a \in \mathbb{Z} + 1/2} \log \left(1 - \frac{\nu}{2i\pi a} \right). \quad (71)$$

1173 When $\operatorname{Re} \nu < 0$, the function I_0 verifies from (69) the identity $I_0(\nu + 2i\pi n) = I_0(\nu)$ for
 1174 $n \in \mathbb{Z}$. When $\operatorname{Re} \nu > 0$, one has instead $I_0(\nu + 2i\pi n) = I_0(\nu) - i\pi n/2$. In terms of the
 1175 translation operators defined in section 4.1, one can write

$$\begin{aligned} T_1^n I_0 &= I_0 \\ T_r^n I_0 &= I_0 - i\pi n/2. \end{aligned} \quad (72)$$

1176 The function I_0 is $2i\pi(\mathbb{Z} + 1/2)$ -continuable, as defined in section 4.1. Analytic con-
 1177 tinuations across the branch cut can then be written solely in terms of the translation
 1178 operators on both sides as (46), and we obtain

$$\begin{aligned} A_n^l I_0 &= I_0 + i\pi n/2 \\ A_n^r I_0 &= I_0 - i\pi n/2, \end{aligned} \quad (73)$$

1179 which can also be proved more directly from e.g. (69).

1180 We note that (73) implies that the domain of definition of the function I_0 may not
 1181 be extended to the Riemann surfaces \mathcal{R} or $\tilde{\mathcal{R}}$. This is a consequence of the presence of
 1182 logarithmic branch points, coming from the integration of poles, instead of the square root
 1183 branch points required for \mathcal{R} . The domain of definition of the function e^{2I_0} , studied below
 1184 in section 4.8, can on the other hand be extended to both \mathcal{R} and $\tilde{\mathcal{R}}$.

1185 4.7 Functions J_P

1186 We consider for $\nu \in \mathbb{D}$ and $P \subset \mathbb{Z} + 1/2$ the function

$$J_P(\nu) = \frac{1}{2} \int_{-\infty}^{\nu} dv \chi_P''(v)^2 = \lim_{\Lambda \rightarrow \infty} \left(-|P|^2 \log \Lambda + \frac{1}{2} \int_{-\Lambda}^{\nu} dv \chi_P''(v)^2 \right), \quad (74)$$

1187 with χ_P given in (64), (57) and a path of integration contained in \mathbb{D} , see figure 19. The
 1188 regularized integral \int is defined for convenience by subtracting the divergent logarithmic
 1189 term at $-\infty$ coming from (64), (58), with $|P|$ the cardinal of P . The integrand in (74)
 1190 is analytic in \mathbb{D} , and J_P is independent from the path of integration. The function J_P
 1191 has logarithmic singularities at $2i\pi a$, $a \in \mathbb{Z} + 1/2$ since $\chi_P''(v)^2 dv$ is a meromorphic differ-
 1192 ential of the third kind with simple poles at the $2i\pi a$. Additionally, J_\emptyset has the large $|\nu|$
 1193 asymptotics $J_\emptyset(\nu) \simeq \frac{e^{2\nu}}{4\pi}$ when $\operatorname{Re} \nu < 0$ and $J_\emptyset(\nu) \simeq \frac{\nu^2}{\pi^2} - \frac{\log \nu}{6}$ when $\operatorname{Re} \nu > 0$.

1194 From (67), the function J_P transforms under translations of $2i\pi$ as $J_P(\nu - 2i\pi n) =$
 1195 $J_{P+n}(\nu)$ when $\operatorname{Re} \nu < 0$, since the path of integration may be chosen such that $\operatorname{Re} v < 0$ ev-
 1196 erywhere along the path. The situation is more complicated on the other side. Shifting the
 1197 integration variable by $2i\pi n$ in (74), one has $J_P(\nu - 2i\pi n) = \frac{1}{2} \int_{-\infty}^{\nu} dv \chi_P''(v - 2i\pi n)^2$, where
 1198 the path of integration crosses the imaginary axis in the interval $(2i\pi(n-1/2), 2i\pi(n+1/2))$.
 1199 Introducing $\epsilon > 0$, $\epsilon \rightarrow 0$, the path of integration can be split into a path from $-\infty$ to $2i\pi n -$
 1200 ϵ with $\operatorname{Re} v < 0$ plus a path from $2i\pi n + \epsilon$ to ν with $\operatorname{Re} v > 0$. The translation identities
 1201 (67) for χ_P then imply $J_P(\nu - 2i\pi n) = \frac{1}{2} \int_{-\infty}^{2i\pi n - \epsilon} dv \chi_{P+n}''(v)^2 + \frac{1}{2} \int_{2i\pi n + \epsilon}^{\nu} dv \chi_{(P+n) \ominus B_n}''(v)^2$.
 1202 Completing the second term by adding the integral on a path from $-\infty$ to $2i\pi n + \epsilon$ crossing
 1203 the imaginary axis between $-i\pi$ and $i\pi$, we arrive according to (65) at the integral of the

¹⁴And not merely the logarithm of the Γ function for some choice of branch cut for the logarithm.

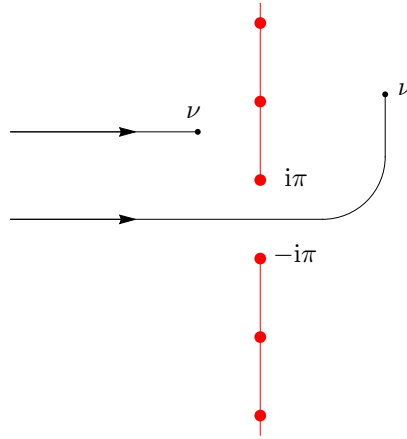


Figure 19: Examples of paths of integration in \mathbb{D} for $I_0(\nu)$ in (68) and for $J_P(\nu)$ in (74), so that the functions are analytic in \mathbb{D} . The vertical, red lines represent the branch cuts $\mathbb{C} \setminus \mathbb{D}$. The bigger, red dots are the branch points $2i\pi a$, $a \in \mathbb{Z} + 1/2$.

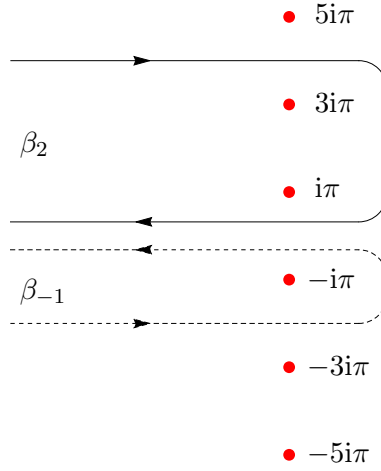


Figure 20: Paths β_2 (solid curve) and β_{-1} (dashed curve) from $-\infty$ to $-\infty$ in \mathbb{C} .

1204 meromorphic differential $\chi''(p)^2 dv$ on a path of the Riemann surface \mathcal{R} (or $\check{\mathcal{R}}$), from the
 1205 puncture $[-\infty, P+n]$ to the puncture $[-\infty, (P+n) \ominus B_n]$, regularized in the usual way
 1206 at both punctures:

$$J_P(\nu - 2i\pi n) = J_{(P+n) \ominus B_n}(\nu) + \frac{1}{2} \int_{\beta_n \cdot (P+n)} \chi''(p)^2 dv, \tag{75}$$

1207 with $\int_{\beta_n \cdot (P+n)} \chi''(p)^2 dv = \int_{-\infty}^{2i\pi n - \epsilon} dv \chi''_{P+n}(v)^2 - \int_{-\infty}^{2i\pi n + \epsilon} dv \chi''_{(P+n) \ominus B_n}(v)^2$. Here, β_n is a
 1208 path from $-\infty$ to $-\infty$ encircling the elements of $2i\pi B_n$ in the clockwise direction if $n > 0$
 1209 and in the anticlockwise direction if $n < 0$, see figure 20, while the path β_0 is empty. The
 1210 path $\beta_n \cdot Q$, $Q \subset \mathbb{Z} + 1/2$ lifting β_n to \mathcal{R} through the covering $[v, P] \mapsto v$ is contained in
 1211 the sheets $\mathbb{C}_Q \cup \mathbb{C}_{Q \ominus B_n}$ and links $[-\infty, Q]$ to $[-\infty, Q \ominus B_n]$.

1212 The integral $\int_{\beta_n \cdot (P+n)} \chi''(v)^2 dv$ is computed in appendix A. We find

$$\frac{1}{2} \int_{\beta_n \cdot P} \chi''(v)^2 dv = W_{P \ominus B_n} - W_{P-n} \tag{76}$$

1213 with

$$W_P = i\pi \left(|P|_+^2 - |P|_-^2 - \sum_{b \in P} b \right) - 2|P| \log 2 + \frac{1}{2} \sum_{\substack{b, c \in P \\ b \neq c}} \log \frac{\pi^2(b-c)^2}{4}. \quad (77)$$

1214 Here, $|P|_+$ (respectively $|P|_-$) denotes the number of positive (resp. negative) elements
1215 of P .

1216 The identity (76) leads to $J_P(\nu - 2i\pi n) = J_{(P+n) \ominus B_n}(\nu) + W_{(P+n) \ominus B_n} - W_P$ when
1217 $\text{Re } \nu > 0$. In terms of the translation operators defined in section 4.1, one has

$$\begin{aligned} T_1^{-n} J_P &= J_{P+n} \\ T_r^{-n} (J_P + W_P) &= J_{(P+n) \ominus B_n} + W_{(P+n) \ominus B_n}. \end{aligned} \quad (78)$$

1218 The function J_P has the same branch points $2i\pi a$, $a \in \mathbb{Z} + 1/2$ as χ_P . Analytic
1219 continuation across the branch cut $(-\infty, -i\pi) \cup (i\pi, \infty)$ can then be written solely in
1220 terms of the translation operators as in (46). Using $P \ominus B_n - n = (P - n) \ominus B_{-n}$, we
1221 obtain

$$\begin{aligned} A_n^1 J_P &= J_{P \ominus B_n} + W_{P \ominus B_n} - W_{P-n} \\ A_n^r J_P &= J_{P \ominus B_n} + W_{P \ominus B_n - n} - W_P. \end{aligned} \quad (79)$$

1222 Thus, J_P is related to $J_{P \ominus B_n}$ by analytic continuation across $(2i\pi(n-1/2), 2i\pi(n+1/2))$,
1223 just like the functions χ_P and $\chi_{P \ominus B_n}$. The extra terms $W_{P \ominus B_n} - W_{P-n}$ and $W_{P \ominus B_n - n} - W_P$
1224 are however distinct in general, as can be seen from the identity (205) in appendix E, and
1225 J_P may not be extended to an analytic function on \mathcal{R} . Since the difference between the
1226 extra terms is from (205) an integer multiple of $i\pi$, it is natural to consider the function
1227 e^{J_P} instead. This is done in the next section.

1228 4.8 Functions e^{2I} , e^{I+J} and e^{2J} defined on $\tilde{\mathcal{R}}$

1229 We consider in this section functions e^{2I} , e^{I+J} and e^{2J} ¹⁵ built from the functions I_0 and
1230 J_P defined respectively in (68) and (74), and which are shown below to be well defined on
1231 the Riemann surface $\tilde{\mathcal{R}}$. These functions are used as building blocks for KPZ fluctuations
1232 in section 2.

1233 We begin with the function I_0 from section 4.6. Equation (73) implies that the analytic
1234 continuation of the function e^{2I_0} across the cut is independent of the side from which
1235 the continuation is made, $A_n e^{2I_0} = (-1)^n e^{2I_0}$. It is then possible to extend e^{2I_0} to a
1236 meromorphic function e^{2I} on \mathcal{R} , defined as

$$e^{2I}([\nu, P]) = (-1)^{|P|} e^{2I_0(\nu)}. \quad (80)$$

1237 The relations $|P \ominus B_n| = |P| + |B_n| - 2|P \cap B_n|$ and $|B_n| = |n|$ indeed imply that the
1238 change of sign from A_n is equivalent to replacing P by $P \ominus B_n$ in (80). Furthermore, the
1239 function e^{2I} verifies the symmetry relation $e^{2I} \circ \mathcal{T} = e^{2I}$ with \mathcal{T} defined in (38), and is
1240 thus also well defined on the Riemann surface $\tilde{\mathcal{R}}$. In fact, since $e^{2I_0(\nu)} = \pm \sqrt{1 + e^\nu}$, the
1241 function e^{2I} can even be defined on the hyperelliptic-like Riemann surface with branch
1242 points $2i\pi a$, $a \in \mathbb{Z} + 1/2$.

1243 The function e^{2I} is meromorphic on $\tilde{\mathcal{R}}$, and has simple poles at the points $[(2i\pi a)_{|r}, P]$,
1244 $a \in \mathbb{Z} + 1/2$: for ν close to $2i\pi a$, $e^{2I}([\nu, P]) \simeq \pm i / \sqrt{\nu - 2i\pi a}$, which corresponds to a pole
1245 in the local coordinate $y = \sqrt{\nu - 2i\pi a}$. The differential defined at $p = [\nu, P] \in \tilde{\mathcal{R}}$ away

¹⁵We emphasize that only the combination of symbols e^{2I} , e^{I+J} and e^{2J} are defined here: I and J alone are not, as there is no meaningful way to extend I_0 and J_P to $\tilde{\mathcal{R}}$.

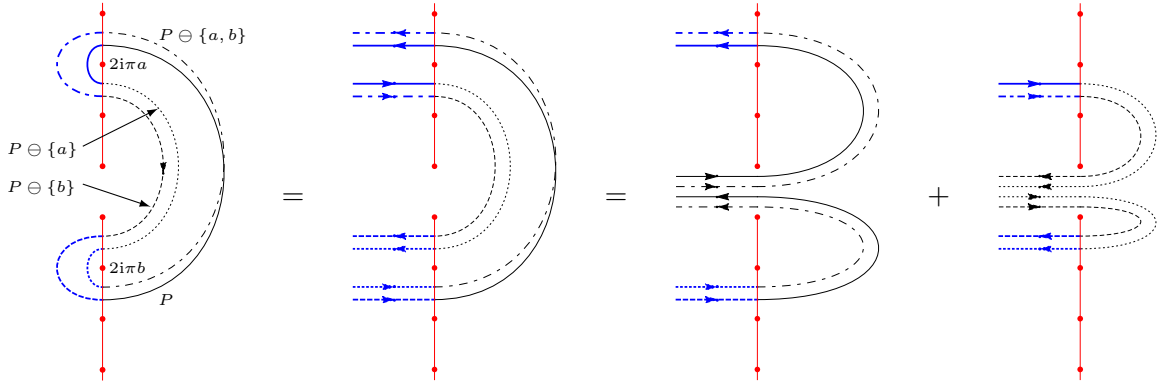


Figure 21: Decomposition of a loop $\ell_{a,b} \cdot P$, $b < 0 < a$ in terms of paths of the form $\beta_n \cdot Q$. Paths on various sheets \mathbb{C}_P are represented differently.

1246 from ramification points by $e^{2I}(p) d\nu$ is on the other hand holomorphic at $[(2i\pi a)_{\text{Irr}}, P]$,
 1247 $a \in \mathbb{Z} + 1/2$, since the differential $d\nu$ becomes proportional to $y dy$ in the local coordinate
 1248 above at $[(2i\pi a)_{\text{Irr}}, P]$ and compensates the pole of the function e^{2I} .

1249 We now consider the functions J_P from section 4.7. Using the identities (207), (211)
 1250 for the quantities W_P and the relation $|P \ominus B_n| = |P| + \sum_{a \in B_n} \sigma_a(P)$, we obtain after
 1251 some simplifications

$$A_n^l \left(\frac{(-1)^{|P|} V_P^2}{4^{|P|}} e^{J_P} \right) = i^{-n} \frac{(-1)^{|P \ominus B_n|} V_{P \ominus B_n}^2}{4^{|P \ominus B_n|}} e^{J_{P \ominus B_n}} \quad (81)$$

$$A_n^r \left(\frac{(-1)^{|P|} V_P^2}{4^{|P|}} e^{J_P} \right) = i^n \frac{(-1)^{|P \ominus B_n|} V_{P \ominus B_n}^2}{4^{|P \ominus B_n|}} e^{J_{P \ominus B_n}},$$

1252 where V_P is the Vandermonde determinant (5). Comparison with analytic continuations
 1253 (73) for I_0 implies that the function e^{I+J} , defined for $\nu \in \mathbb{D}$, $P \sqsubset \mathbb{Z} + 1/2$ by

$$e^{I+J}([\nu, P]) = \frac{(-1)^{|P|} V_P^2}{4^{|P|}} e^{I_0(\nu) + J_P(\nu)}, \quad (82)$$

1254 is well defined on the Riemann surface $\tilde{\mathcal{R}}$. Furthermore, using (72), (78) and (211), the
 1255 function e^{I+J} verifies the symmetry $e^{I+J} \circ \mathcal{T} = e^{I+J}$, so that e^{I+J} is also well defined on
 1256 $\tilde{\mathcal{R}}$.

1257 The function e^{I+J} is meromorphic on $\tilde{\mathcal{R}}$, with the same simple poles as e^{2I} at the
 1258 points $[(2i\pi a)_{\text{Irr}}, P]$, $a \in \mathbb{Z} + 1/2$. The poles come from logarithmic singularities at the
 1259 points $\nu = 2i\pi a$ in the integral representations (68) and (74) for the functions I_0 and J_P .
 1260 From the infinite sum representation (162) for χ_P'' , the functions I_0 and J_P contribute each
 1261 half of the logarithmic terms, and one has $e^{I+J}([\nu, P]) \propto 1/\sqrt{\nu - 2i\pi a}$ when $\nu \rightarrow 2i\pi a$.
 1262 The meromorphic differential defined at $p = [\nu, P] \in \tilde{\mathcal{R}}$ away from ramification points by
 1263 $e^{I+J}(p) d\nu$ is holomorphic at $[(2i\pi a)_{\text{Irr}}, P]$, $a \in \mathbb{Z} + 1/2$ for the same reason as for e^{2I} .

1264 Finally, the function $e^{2J} = (e^{I+J})^2 / e^{2I}$, more explicitly

$$e^{2J}([\nu, P]) = (-1)^{|P|} 2^{-4|P|} V_P^4 e^{2J_P(\nu)}, \quad (83)$$

1265 is also well defined and meromorphic on $\tilde{\mathcal{R}}$, with simple poles at the points $[(2i\pi a)_{\text{Irr}}, P]$,
 1266 $a \in \mathbb{Z} + 1/2$, while the differential $e^{2J}(p) d\nu$ is holomorphic.

1267 The functions e^{2I} , e^{2J} and e^{I+J} are defined through $I_0(\nu)$, $J_P(\nu)$ as integrals on a
 1268 path contained in \mathbb{D} between $-\infty$ and ν according to (68), (74). An alternative point

1269 of view, which takes into account from the start that ν lives on $\check{\mathcal{R}}$, consists instead in
 1270 writing directly $e^{2I}(p)$, $e^{2J}(p)$, $e^{I+J}(p)$ in terms of meromorphic differentials integrated
 1271 on a path of $\check{\mathcal{R}}$ between $[-\infty, \emptyset]$ and p . Defining a meromorphic function φ on $\check{\mathcal{R}}$ by
 1272 $\varphi([v, P]) = -\frac{1}{2} \frac{1}{1+e^{-v}}$ and the meromorphic differentials of the third kind ¹⁶

$$\begin{aligned} \Omega_{2I}(q) &= \varphi(q)d\nu \\ \Omega_{2J}(q) &= \chi''(q)^2 d\nu \\ \Omega_{I+J}(q) &= \left(\frac{\varphi(q)}{2} + \frac{\chi''(q)^2}{2} \right) d\nu, \end{aligned} \tag{84}$$

1273 at $q = [v, P]$ away from ramification points, one has

$$\begin{aligned} e^{2I}(p) &= \exp \left(\int_{[-\infty, \emptyset]}^p \Omega_{2I} \right) \\ e^{2J}(p) &= \exp \left(\int_{[-\infty, \emptyset]}^p \Omega_{2J} \right) \\ e^{I+J}(p) &= \exp \left(\int_{[-\infty, \emptyset]}^p \Omega_{I+J} \right). \end{aligned} \tag{85}$$

1274 The fact that the functions e^{2I} , e^{2J} and e^{I+J} are well defined on $\check{\mathcal{R}}$ imply that the integrals
 1275 on any loop in $\check{\mathcal{R}}$ of the meromorphic differentials Ω_{2I} , Ω_{2J} , Ω_{I+J} are integer multiples
 1276 of $2i\pi$. For small loops around a point $[(2i\pi a)_{1r}, P]$, this is a consequence of Cauchy's
 1277 residue theorem on the Riemann surface, both $\varphi(q)d\nu$ and $\chi''(q)^2 d\nu$ having a residue
 1278 -1 at that point ¹⁷. For non-contractible loops, this is a non-trivial statement. For
 1279 Ω_{2J} , it can be checked directly for a given loop by expressing its homology class as a
 1280 sum of paths of the form $\beta_n \cdot P$ from figure 20 and using (76) to compute the integrals.
 1281 For example, considering the loops $\ell_{a,b} \cdot P$ which generate all loops on $\check{\mathcal{R}}$ that are also
 1282 closed on \mathcal{R} and are defined in section 3.8.1, see also figure 21, we obtain after some
 1283 simplifications $\int_{\ell_{a,b}} \Omega_{2J} = 4i\pi(-1 + \sigma_a(P)\sigma_b(P)(\frac{\text{sgn } a - \text{sgn } b}{2} - \text{sgn}(a-b)\frac{1 + \text{sgn}(ab)}{2}))$, which is
 1284 an integer multiple of $4i\pi$. For loops on $\check{\mathcal{R}}$ corresponding to open paths on \mathcal{R} , the integral
 1285 is generally only an integer multiple of $2i\pi$: for instance, the integral of Ω_{2J} on the loop
 1286 $[v, \{1/2\}] \rightarrow [(4i\pi)_1, \{1/2\}] = [(4i\pi)_r, \{3/2\}] \rightarrow [v + 2i\pi, \{3/2\}]$, $\text{Re } v < 0$ is equal to $-2i\pi$.

1287 4.9 Functions on the Riemann surfaces \mathcal{R}^Δ

1288 In this section, we study functions on the Riemann surfaces \mathcal{R}^Δ built in section 3.8.3 by
 1289 quotienting \mathcal{R} by a group of involutions indexed by the elements of $\Delta \subset \mathbb{Z} + 1/2$. These
 1290 functions are used in sections 2.3 and 2.4 for KPZ fluctuations with sharp wedge and
 1291 stationary initial condition.

1292 4.9.1 Function χ^Δ

1293
 1294 Let $\Delta \subset \mathbb{Z} + 1/2$. The covering map $\Pi^\Delta : [v, P] \mapsto [v, P \setminus \Delta]$ from \mathcal{R} to \mathcal{R}^Δ allows to
 1295 define the function $\chi^\Delta = 2^{-|\Delta|} \text{tr}_{\Pi^\Delta} \chi$ analytic on \mathcal{R}^Δ , see section 3.4. More explicitly, for

¹⁶With additional essential singularities for the points at infinity.

¹⁷The function $v \mapsto -\frac{1}{2} \frac{1}{1+e^{-v}}$ has residues $-1/2$ in \mathbb{C} instead. The distinction with φ comes from the fact that the projection of a loop on $\check{\mathcal{R}}$ encircling $[(2i\pi a)_{1r}, P]$ to the complex plane by the covering map $[v, P] \mapsto v$ encircles $2i\pi a$ an even number of times, see figure 3. In terms of the local coordinate $y = \sqrt{v - 2i\pi a}$ at $[(2i\pi a)_{1r}, P]$, this is a consequence of $dv/(v - 2i\pi a) = 2dy/y$.

1296 any $v \in \mathbb{C}$ and $Q \sqsubset \mathbb{Z} + 1/2$, $Q \cap \Delta = \emptyset$, one has $\chi^\Delta([v, Q]) = 2^{-|\Delta|} \sum_{\substack{P \sqsubset \mathbb{Z} + 1/2 \\ P \setminus \Delta = Q}} \chi_P(v) =$
 1297 $2^{-|\Delta|} \sum_{A \subset \Delta} \chi_{Q \cup A}(v)$. Using (64), we find

$$\chi^\Delta([v, P]) = \chi_P^\Delta(v), \quad (86)$$

1298 where χ_P^Δ , given by¹⁸

$$\chi_P^\Delta(v) = \frac{\chi_P(v) + \chi_{P \ominus \Delta}(v)}{2}, \quad (87)$$

1299 generalizes the function χ_P of section 4.5. The function χ_P^Δ has the infinite sum represen-
 1300 tation

$$\chi_P^\Delta(v) = \lim_{M \rightarrow \infty} \left(-\frac{4(2\pi M)^{5/2}}{15\pi} - \frac{2v(2\pi M)^{3/2}}{3\pi} + \frac{(\pi^2 + 3v^2)\sqrt{2\pi M}}{6\pi} \right. \quad (88)$$

$$\left. - \sum_{a=-M+1/2}^{M-1/2} 1_{\{a \notin \Delta\}} \sigma_a(P) \frac{\kappa_a^3(v)}{3} \right)$$

1301 with σ_a defined in (29) and κ_a in (50), and verifies $\chi_P^\Delta = \chi_{P \setminus \Delta}^\Delta$.

1302 Since χ^Δ is analytic on \mathcal{R}^Δ , the function χ_P^Δ defined on \mathbb{D} has the analytic continuation
 1303

$$A_n \chi_P^\Delta = \chi_{P \ominus (B_n \setminus \Delta)}^\Delta \quad (89)$$

1304 across branch cuts. Alternatively, (89) can be proved directly from (65) using the general
 1305 identity $\chi_P^\Delta = \chi_{P \ominus A}^\Delta$, $A \subset \Delta$ with $A = B_n \cap \Delta$. From (67), the functions χ_P^Δ also verify
 1306 the shift identities

$$T_1^{-n} \chi_P^\Delta = \chi_{P+n}^{\Delta+n} \quad (90)$$

$$T_r^{-n} \chi_P^\Delta = \chi_{(P+n) \ominus (B_n \setminus (\Delta+n))}^{\Delta+n},$$

1307 where we used again $\chi_P^\Delta = \chi_{P \ominus A}^\Delta$, $A \subset \Delta$ for the second line. In terms of the collection $\overline{\mathcal{R}}$
 1308 of all Riemann surfaces \mathcal{R}^Δ of section 3.8.3, of the function $\overline{\chi}([v, (P, \Delta)]) = \chi_P^\Delta(v)$ defined
 1309 on $\overline{\mathcal{R}}$, and of the holomorphic map $\overline{\mathcal{T}}$ on $\overline{\mathcal{R}}$ defined in (44), the identity (90) simply rewrites
 1310 as $\overline{\chi} \circ \overline{\mathcal{T}} = \overline{\chi}$.

1311 Finally, we also define functions χ'^Δ , χ''^Δ from derivatives of χ_P^Δ as

$$\chi'^\Delta([v, P]) = \chi_P'^\Delta(v) \quad (91)$$

$$\chi''^\Delta([v, P]) = \chi_P''^\Delta(v).$$

1312 The function χ'^Δ is analytic on \mathcal{R}^Δ while χ''^Δ is meromorphic on \mathcal{R}^Δ . Both verify the
 1313 same translation symmetries as χ^Δ .

1314 4.9.2 Functions J_P^Δ

1315
 1316 We now consider J_P^Δ generalizing the function J_P of section 4.7, defined from the second
 1317 derivative $\chi_P''^\Delta$ of χ_P^Δ as

$$J_P^\Delta(v) = \frac{1}{2} \int_{-\infty}^v dv \chi_P''^\Delta(v)^2 \quad (92)$$

$$= \lim_{\Lambda \rightarrow \infty} \left(-\frac{(|P| + |P \ominus \Delta|)^2}{4} \log \Lambda + \frac{1}{2} \int_{-\Lambda}^v dv \chi_P''^\Delta(v)^2 \right),$$

¹⁸For later convenience, we define χ_P^Δ in (87) in terms of $P \ominus \Delta$ instead of $P \cup \Delta$ when $P \cap \Delta \neq \emptyset$.

1318 for $\nu \in \mathbb{D}$, with a path of integration contained in \mathbb{D} . One has $J_P^\Delta = J_{P \setminus \Delta}^\Delta$.

1319 The same reasoning as in section 4.7 gives for any $n \in \mathbb{Z}$ the identities $J_P^\Delta(\nu - 2i\pi n) =$
 1320 $J_{P+n}^{\Delta+n}(\nu)$ when $\text{Re } \nu < 0$ and $J_P^\Delta(\nu - 2i\pi n) = J_{(P+n) \ominus (B_n \setminus (\Delta+n))}(\nu) + \frac{1}{2} \int_{\beta_n \cdot (P+n)} \chi''^{\Delta+n}(p) d\nu$
 1321 with $\beta_n \cdot (P+n)$ the lift to the sheet $P+n$ of $\mathcal{R}^{\Delta+n}$ of the path in the complex plane β_n
 1322 from figure 20. The integral over $\beta_n \cdot (P+n)$ can be computed similarly as in appendix A.
 1323 We obtain eventually

$$\begin{aligned} T_1^{-n} J_P^\Delta &= J_{P+n}^{\Delta+n} & (93) \\ T_r^{-n} J_P^\Delta &= J_{(P+n) \ominus (B_n \setminus (\Delta+n))}^{\Delta+n} + W_{(P+n) \ominus (B_n \setminus (\Delta+n))}^{\Delta+n} - W_P^\Delta, \end{aligned}$$

1324 where

$$\begin{aligned} W_P^\Delta &= \frac{i\pi}{4} \left((|P|_+ + |P \ominus \Delta|_+)^2 - (|P|_- + |P \ominus \Delta|_-)^2 \right) - \frac{i\pi}{2} \left(\sum_{b \in P} b + \sum_{b \in P \ominus \Delta} b \right) & (94) \\ &\quad - (|P| + |P \ominus \Delta|) \log 2 + \frac{1}{4} \sum_{\substack{b, c \in P \\ b \neq c}} \log \frac{\pi^2(b-c)^2}{4} + \frac{1}{4} \sum_{\substack{b, c \in P \ominus \Delta \\ b \neq c}} \log \frac{\pi^2(b-c)^2}{4} \end{aligned}$$

1325 generalizes the constants $W_P = W_P^\emptyset$ of (77). Using (46), the analytic continuation of J_P^Δ
 1326 across branch cuts is given by

$$\begin{aligned} A_n^l J_P^\Delta &= J_{P \ominus (B_n \setminus \Delta)}^\Delta + W_{P \ominus (B_n \setminus \Delta)}^\Delta - W_{P-n}^{\Delta-n} & (95) \\ A_n^r J_P^\Delta &= J_{P \ominus (B_n \setminus \Delta)}^\Delta + W_{P \ominus (B_n \setminus \Delta) - n}^{\Delta-n} - W_P^\Delta. \end{aligned}$$

1327 As in section 4.7, the analytic continuation from each side of the branch cuts does not give
 1328 the same result, so that J_P^Δ may not be extended to \mathcal{R}^Δ . For the application to KPZ in
 1329 sections 2.3 and 2.4, however, only $e^{2J_P^\Delta}$ is needed. Using the identity (213), we find that
 1330 the function e^{2J^Δ} generalizing $e^{2J} = e^{2J^\emptyset}$ and defined by

$$e^{2J^\Delta}([\nu, P]) = (i/4)^{2|P \setminus \Delta|} \left(\prod_{a \in P \setminus \Delta} \prod_{\substack{b \in P \cup \Delta \\ b \neq a}} \left(\frac{2i\pi a}{4} - \frac{2i\pi b}{4} \right)^2 \right) e^{2J_P^\Delta(\nu)} \quad (96)$$

1331 is well defined on \mathcal{R}^Δ . The prefactor of $e^{2J_P^\Delta(\nu)}$, which depends on P and Δ only through
 1332 Δ and $P \setminus \Delta$ since $P \cup \Delta = (P \setminus \Delta) \cup \Delta$, has been chosen equal to 1 when $P = \emptyset$. The
 1333 function e^{2J^Δ} can then be expressed alternatively as

$$e^{2J^\Delta}(p) = \exp \left(\int_{[-\infty, \emptyset]}^p \Omega_{2J}^\Delta \right), \quad (97)$$

1334 independently from the path between $[-\infty, \emptyset]$ and p in \mathcal{R}^Δ , with Ω_{2J}^Δ the meromorphic
 1335 differential of the third kind

$$\Omega_{2J}^\Delta([\nu, P]) = \chi''^\Delta([\nu, P])^2 d\nu. \quad (98)$$

1336 The function e^{2J^Δ} has the simple poles $[(2i\pi a)_{|r}, P]$, $a \in (\mathbb{Z} + 1/2) \setminus \Delta$, $P \subset (\mathbb{Z} + 1/2) \setminus \Delta$,
 1337 while the differential $e^{2J^\Delta}([\nu, P]) d\nu$ is holomorphic on \mathcal{R}^Δ .

1338 Additionally, for any $m \in \mathbb{Z}$, the function e^{2J^Δ} verifies from (93), (212)

$$e^{2J^\Delta}([\nu - 2i\pi m, P]) = \begin{cases} e^{2J^{\Delta+m}}([\nu, P + m]) & \text{Re } \nu < 0 \\ e^{2J^{\Delta+m}}([\nu, (P + m) \ominus (B_m \setminus (\Delta + m))]) & \text{Re } \nu > 0 \end{cases}. \quad (99)$$

1339 Extending e^{2J^Δ} to the collection $\overline{\mathcal{R}}$ of all \mathcal{R}^Δ by $\overline{e^{2J}}([\nu, (P, \Delta)]) = e^{2J^\Delta}([\nu, P])$, the identity
 1340 (99) is equivalent to the symmetry $\overline{e^{2J}} \circ \overline{\mathcal{T}} = e^{2J}$ with $\overline{\mathcal{T}}$ defined in (44).

1341 **4.10 Functions $K_{P,Q}$, $K_{P,Q}^{\Delta,\Gamma}$ and $e^{2K^{\Delta,\Gamma}}$**

1342 In this section, we study functions on products of Riemann surfaces needed for joint
 1343 statistics of the KPZ height at multiple times.

1344 **4.10.1 Functions $K_{P,Q}$**

1345
 1346 Given two finite sets of half-integers P and Q , and (ν, μ) in the simply connected domain

$$\mathbb{D}_2 = \{(\nu, \mu) \in \mathbb{D} \times \mathbb{D}, (\operatorname{Re} \nu \neq \operatorname{Re} \mu) \text{ or } (\operatorname{Re} \nu = \operatorname{Re} \mu \text{ and } \operatorname{Im}(\nu - \mu) \in (0, 2\pi))\}, \quad (100)$$

1347 we consider the functions

$$\begin{aligned} K_{P,Q}(\nu, \mu) &= \frac{1}{2} \int_{-\infty}^0 du \chi''_P(u + \nu) \chi''_Q(u + \mu) \\ &= \lim_{\Lambda \rightarrow \infty} \left(-|P||Q| \log \Lambda + \frac{1}{2} \int_{-\Lambda}^0 du \chi''_P(u + \nu) \chi''_Q(u + \mu) \right). \end{aligned} \quad (101)$$

1348 The path of integration is chosen such that $u + \nu$ and $u + \mu$ both stay in \mathbb{D} , which is
 1349 possible¹⁹ if $(\nu, \mu) \in \mathbb{D}_2$, see figure 22, and $K_{P,Q}$ is thus analytic in \mathbb{D}_2 . When $P = Q$,
 1350 one recovers $J_P(\nu) = \lim_{\mu \rightarrow \nu} K_{P,P}(\nu, \mu)$.

1351 Crossing the branch cuts $\mu, \nu \in (-i\infty, -i\pi) \cup (i\pi, i\infty)$, $\nu - \mu \in (-i\infty, 0) \cup (i\pi, i\infty)$
 1352 produces new functions analytic in \mathbb{D}_2 . In order to obtain explicit formulas for the various
 1353 analytic continuations of $K_{P,Q}(\nu, \mu)$, it is useful to study first shifts by integer multiples
 1354 of $2i\pi$ in the variables ν and μ . When both $\operatorname{Re} \nu < 0$ and $\operatorname{Re} \mu < 0$, the path of in-
 1355 tegration in (101) can be chosen such that $\operatorname{Re}(u + \nu) < 0$, $\operatorname{Re}(u + \mu) < 0$ everywhere,
 1356 see figure 22 top left, and one has from (67) the identity $K_{P,Q}(\nu - 2i\pi n, \mu - 2i\pi m) =$
 1357 $K_{P+n, Q+m}(\nu, \mu)$. Similar reasonings leads to $K_{P,Q}(\nu - 2i\pi n, \mu) = K_{P+n, Q}(\nu, \mu)$ when
 1358 $\operatorname{Re} \nu < 0$ and $K_{P,Q}(\nu, \mu - 2i\pi m) = K_{P, Q+m}(\nu, \mu)$ when $\operatorname{Re} \mu < 0$. Shifting variables with a
 1359 positive real part is more complicated. Indeed, the argument of the functions χ''_P, χ''_Q has
 1360 then a positive real part on some portions of the path of integration in (101) and a negative
 1361 real part on other portions of the path, so that (67) gives several distinct expressions for
 1362 the shifts along the path. After some rewriting, one finds in all cases the identity

$$\begin{aligned} K_{P,Q}(\nu - 2i\pi n, \mu - 2i\pi m) &= K_{\tilde{P}, \tilde{Q}}(\nu, \mu) \\ &\quad + \frac{1}{2} \int_{\gamma_{n,m}} du \mathcal{A}_u(\chi''_{P+n}(\cdot + \nu) \chi''_{Q+m}(\cdot + \mu)) \end{aligned} \quad (102)$$

1363 with $\tilde{P} = P + n$ when $\operatorname{Re} \nu < 0$, $\tilde{P} = (P + n) \ominus B_n$ when $\operatorname{Re} \nu > 0$ and $\tilde{Q} = Q + m$ when
 1364 $\operatorname{Re} \mu < 0$, $\tilde{Q} = (Q + m) \ominus B_m$ when $\operatorname{Re} \mu > 0$. We used the notation $\int_{\gamma} du \mathcal{A}_u f$ for the
 1365 integral of the analytic continuation of a function f along a path γ . The path $\gamma_{n,m}$ in the
 1366 complex plane depends on the real parts of ν and μ , see figure 23. When $\operatorname{Re} \nu$ and $\operatorname{Re} \nu$
 1367 are both negative, the path is empty and the integral in (102) is equal to zero. When $\operatorname{Re} \nu$
 1368 and $\operatorname{Re} \nu$ do not have the same sign, the path reduces to $\gamma_{n,m} = \beta_n - \nu$ if $\operatorname{Re} \mu < 0 < \operatorname{Re} \nu$
 1369 and $\gamma_{n,m} = \beta_m - \mu$ if $\operatorname{Re} \nu < 0 < \operatorname{Re} \mu$, with β_n defined in section 4.7, compare with
 1370 figure 20. Finally, when $\operatorname{Re} \nu$ and $\operatorname{Re} \mu$ are both positive, the path goes from $-\infty$ to $-\infty$
 1371 and crosses the lines $\operatorname{Re}(u + \nu) = 0$ and $\operatorname{Re}(u + \mu) = 0$ along the path at successive points
 1372 $2i\pi n - \nu, 2i\pi m - \mu, -\mu, -\nu$ (respectively $2i\pi m - \mu, 2i\pi n - \nu, -\nu, -\mu$) if $\operatorname{Re} \nu > \operatorname{Re} \mu$
 1373 (resp. $\operatorname{Re} \nu < \operatorname{Re} \mu$).

¹⁹At this point, $K_{P,Q}(\nu, \mu)$ is in fact analytic in a domain larger than \mathbb{D}_2 : in the sector $\operatorname{Re} \nu = \operatorname{Re} \mu$, $\operatorname{Im}(\nu - \mu)$ need not be restricted when the real parts are negative, and one requires only $\operatorname{Im}(\nu - \mu) \in (-2\pi, 2\pi)$ when the real parts are positive. Additional terms contributed later on by analytic continuation are however only analytic in \mathbb{D}_2 , and it is thus convenient to add this restriction from the beginning.

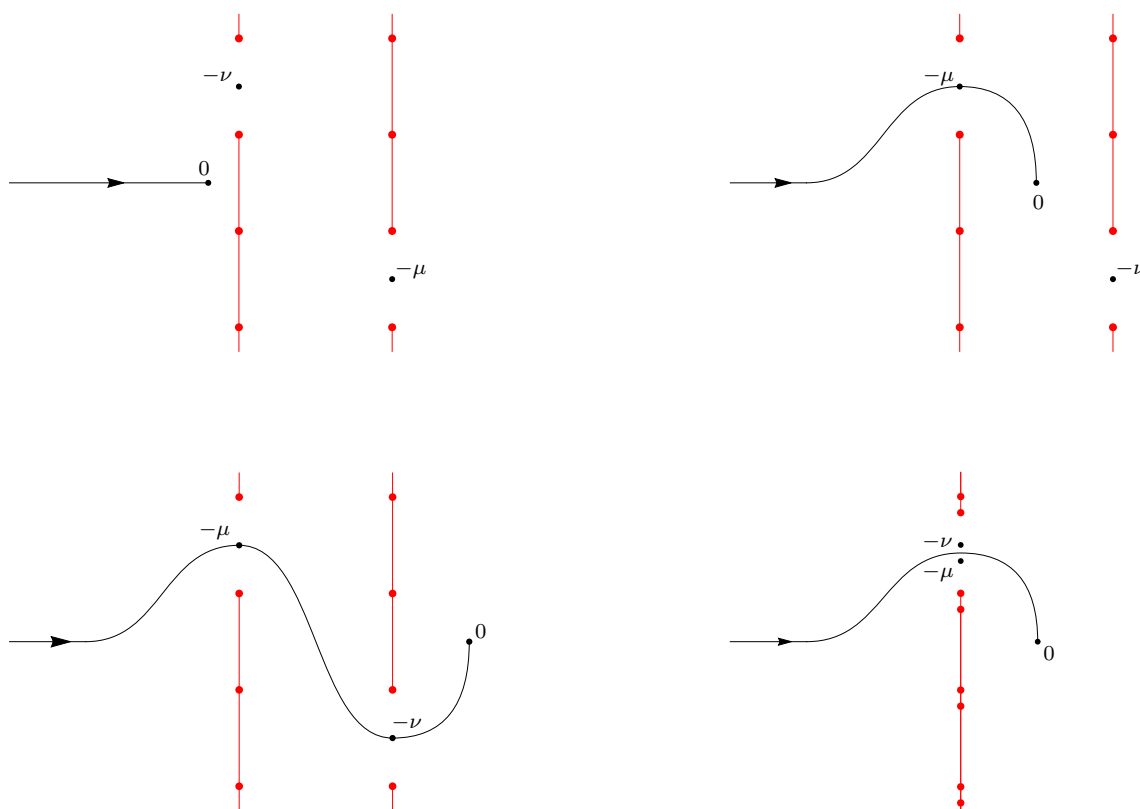


Figure 22: Possible choices for the path of integration in the definition (101) for $K_{P,Q}$. The red, vertical lines are the branch cuts in the variable u of $\chi_P''(u+\nu)$ and $\chi_Q''(u+\mu)$, and the red dots on the cuts are the associated branch points $-\nu + 2i\pi a$, $-\mu + 2i\pi a$, $a \in \mathbb{Z} + 1/2$. The black curves, ending at $u = 0$, represent the path for the variable u . From left to right, top to bottom, the four graphs represent respectively the situations $\text{Re } \mu < \text{Re } \nu < 0$; $\text{Re } \nu < 0 < \text{Re } \mu$; $\text{Re } \mu > \text{Re } \nu > 0$; $\text{Re } \nu = \text{Re } \mu > 0$ with $-\pi < \text{Im}(\nu - \mu) < \pi$.

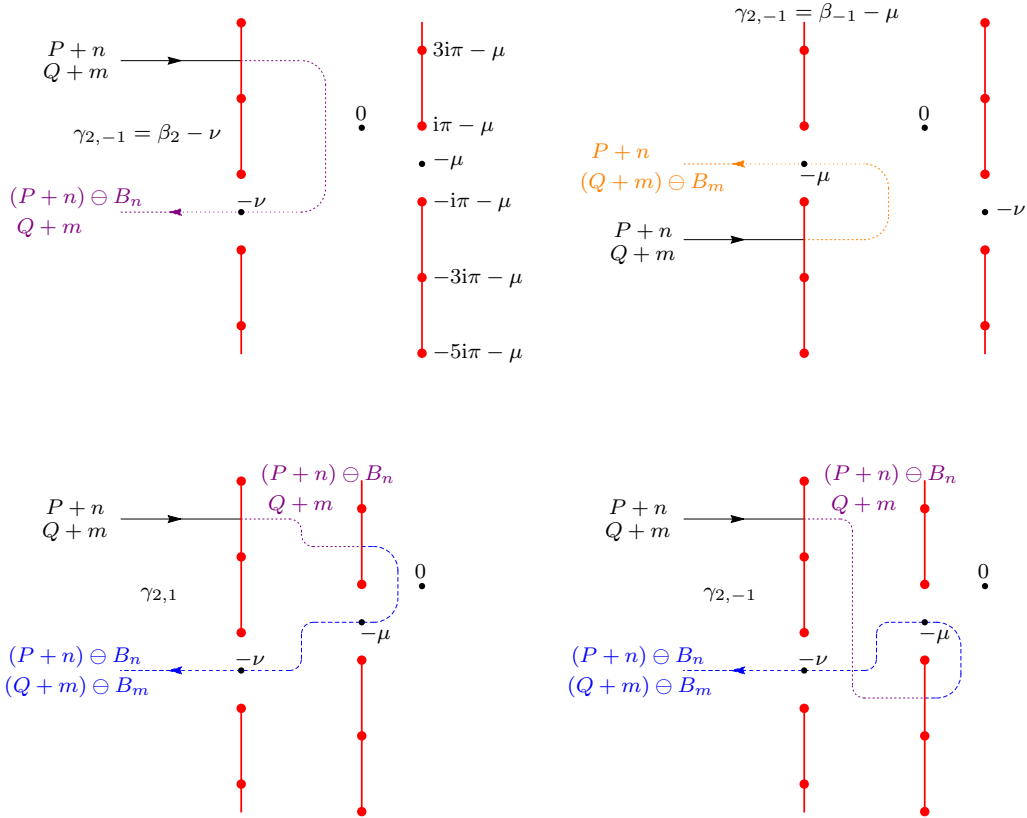


Figure 23: Path $\gamma_{n,m}$ in (102) plotted for some choices of $\nu, \mu \in \mathbb{D}$, $n, m \in \mathbb{Z}$. From left to right, top to bottom, the graphs represent $\gamma_{2,-1} = \beta_2 - \nu$ for $\text{Re } \mu < 0 < \text{Re } \nu$, $\gamma_{2,-1} = \beta_{-1} - \mu$ for $\text{Re } \nu < 0 < \text{Re } \mu$, $\gamma_{2,1}$ for $0 < \text{Re } \mu < \text{Re } \nu$, and $\gamma_{2,-1}$ for $0 < \text{Re } \mu < \text{Re } \nu$. The smaller, black dots represent the points $0, -\nu, -\mu$. The bigger, red dots represent the branch points $-\nu + 2i\pi a, -\mu + 2i\pi a$, $a \in \mathbb{Z} + 1/2$ of $\chi''_{P+n}(\cdot + \nu)\chi''_{Q+m}(\cdot + \mu)$, and the vertical, red lines the associated branch cuts. The solid / dotted / dashed portions of the path $\gamma_{n,m}$ correspond to distinct values of the sets \hat{P}, \hat{Q} in $\chi''_{\hat{P}}(u + \nu)\chi''_{\hat{Q}}(u + \mu) = \mathcal{A}_u(\chi''_{P+n}(\cdot + \nu)\chi''_{Q+m}(\cdot + \mu))$ which are indicated next to the paths.

1374 It is sufficient for the following to consider shifts of ν and μ separately, and compute
 1375 the integrals over the paths $\gamma_{n,0}$ and $\gamma_{0,m}$ only. Anticipating the result, we define the
 1376 function

$$W_{P,Q}(z) = 2|P| I_0(z) + 2 \sum_{a \in P} \sum_{b \in Q} \log \left(\frac{\kappa_{b-a+1/2}(z)}{\sqrt{8}} \right), \quad (103)$$

1377 and the coefficients

$$Z_{P,Q} = \sum_{a \in P} \left(-i\pi(a-1/2) + 2i\pi \operatorname{sgn}(a) |Q \cap B_{a-1/2}| \right). \quad (104)$$

1378 The function $W_{P,Q}$ is analytic in \mathbb{D} so that $(\nu, \mu) \mapsto W_{P,Q}(\mu - \nu + i\pi)$ and $(\nu, \mu) \mapsto$
 1379 $W_{P,Q}(\nu - \mu - i\pi)$ are both analytic in \mathbb{D}_2 . Additionally, using (54), (72) and $\operatorname{sgn}(n)|(Q -$
 1380 $a + 1/2) \cap B_n| = \operatorname{sgn}(n+a)|Q \cap B_{n+a-1/2}| - \operatorname{sgn}(a)|Q \cap B_{a-1/2}|$, one has

$$W_{P,Q}(z + 2i\pi n) = W_{P+n,Q}(z) + \mathbf{1}_{\{\operatorname{Re} z > 0\}}(Z_{P+n,Q} - Z_{P,Q}). \quad (105)$$

1381 The integral over $\gamma_{n,0}$ is computed in appendix B. There, one finds

$$\begin{aligned} & \frac{1}{2} \int_{\gamma_{n,0}} du \mathcal{A}_u(\chi_{P+n}''(\cdot + \nu) \chi_Q''(\cdot + \mu)) \\ &= \mathbf{1}_{\{\operatorname{Re} \nu > 0\}} \left(W_{(P+n) \ominus B_n, Q}(\mu - \nu + i\pi) - W_{P+n, Q}(\mu - \nu + i\pi) \right. \\ & \quad \left. + \mathbf{1}_{\{\operatorname{Re} \mu > \operatorname{Re} \nu\}} (Z_{(P+n) \ominus B_n, Q} - Z_{P+n, Q}) \right) \end{aligned} \quad (106)$$

1382 and

$$\begin{aligned} & \frac{1}{2} \int_{\gamma_{0,m}} du \mathcal{A}_u(\chi_P''(\cdot + \nu) \chi_{Q+m}''(\cdot + \mu)) \\ &= \mathbf{1}_{\{\operatorname{Re} \mu > 0\}} \left(W_{(Q+m) \ominus B_m+1, P}(\nu - \mu - i\pi) - W_{Q+m+1, P}(\nu - \mu - i\pi) \right. \\ & \quad \left. + \mathbf{1}_{\{\operatorname{Re} \nu > \operatorname{Re} \mu\}} (Z_{(Q+m) \ominus B_m+1, P} - Z_{Q+m+1, P}) \right). \end{aligned} \quad (107)$$

1383 As usual, it is useful to interpret (102), (106), (107) in terms of translation operators
 1384 mapping $K_{P,Q}$ to other functions analytic in \mathbb{D}_2 . We define the operators $T_{i \uparrow r}^n$ with $i = 1$
 1385 corresponding to translation in the first variable, $i = 2$ to translation in the second variable,
 1386 and the indices $\uparrow r, \pm$ indicating the sector for $(\operatorname{Re} \nu, \operatorname{Re} \mu)$ in which the translation is
 1387 initially applied before reconstructing functions defined in \mathbb{D}_2 by analytic continuation, see
 1388 table 1. All eight operators are in principle distinct, even though some of them coincide
 1389 on $K_{P,Q}$. Writing ν for the first variable and μ for the second variable of the function
 1390 $K_{P,Q}$, one has

$$T_{1 \pm}^{-n} K_{P,Q} = K_{P+n, Q} \quad (108)$$

$$T_{1r}^{-n} K_{P,Q} = K_{(P+n) \ominus B_n, Q} + W_{(P+n) \ominus B_n, Q}(\mu - \nu + i\pi) - W_{P+n, Q}(\mu - \nu + i\pi) \\ + Z_{(P+n) \ominus B_n, Q} - Z_{P+n, Q}$$

$$T_{1\uparrow}^{-n} K_{P,Q} = K_{(P+n) \ominus B_n, Q} + W_{(P+n) \ominus B_n, Q}(\mu - \nu + i\pi) - W_{P+n, Q}(\mu - \nu + i\pi)$$

1391 for translations in the first variable and

$$T_{2 \pm}^{-m} K_{P,Q} = K_{P, Q+m} \quad (109)$$

$$T_{2r}^{-m} K_{P,Q} = K_{P, (Q+m) \ominus B_m} + W_{(Q+m) \ominus B_m+1, P}(\nu - \mu - i\pi) - W_{Q+m+1, P}(\nu - \mu - i\pi) \\ + Z_{(Q+m) \ominus B_m+1, P} - Z_{Q+m+1, P}$$

$$T_{2\uparrow}^{-m} K_{P,Q} = K_{P, (Q+m) \ominus B_m} + W_{(Q+m) \ominus B_m+1, P}(\nu - \mu - i\pi) - W_{Q+m+1, P}(\nu - \mu - i\pi)$$

Operators		Sector
$T_{1^-}^n$	$A_n^{1^-}$	$\text{Re } \nu < \min(0, \text{Re } \mu)$
$T_{1^+}^n$	$A_n^{1^+}$	$\text{Re } \mu < \text{Re } \nu < 0$
$T_{1_r^-}^n$	$A_n^{1_r^-}$	$0 < \text{Re } \nu < \text{Re } \mu$
$T_{1_r^+}^n$	$A_n^{1_r^+}$	$\max(0, \text{Re } \mu) < \text{Re } \nu$
$T_{2^-}^m$	$A_m^{2^-}$	$\text{Re } \mu < \min(0, \text{Re } \nu)$
$T_{2^+}^m$	$A_m^{2^+}$	$\text{Re } \nu < \text{Re } \mu < 0$
$T_{2_r^-}^m$	$A_m^{2_r^-}$	$0 < \text{Re } \mu < \text{Re } \nu$
$T_{2_r^+}^m$	$A_m^{2_r^+}$	$\max(0, \text{Re } \nu) < \text{Re } \mu$

Table 1: Translation operators T^n, T^m and analytic continuation operators A_n, A_m defined on functions f analytic in \mathbb{D}_2 . The translation operators verify $(T^n f)(\nu, \mu) = f(\nu + 2i\pi n, \mu)$ (first four operators) or $(T^m f)(\nu, \mu) = f(\nu, \mu + 2i\pi m)$ (last four operators) in the specified sector for $(\text{Re } \nu, \text{Re } \mu)$. The operators A_n (first four operators) correspond to analytic continuation in the first variable across the cut $\nu \in (2i\pi(n - 1/2), 2i\pi(n + 1/2))$ and the operators A_m (last four operators) correspond to analytic continuation in the second variable across the cut $\mu \in (2i\pi(m - 1/2), 2i\pi(m + 1/2))$, starting from the specified sector for $(\text{Re } \nu, \text{Re } \mu)$.

1392 for translations in the second variable.

1393 Analytic continuation for the first and second variable across the branch cuts $(2i\pi(n -$
 1394 $1/2), 2i\pi(n + 1/2))$ can be expressed in terms of operators $A_n^{i\pm}$, with $i = 1$ and $i = 2$
 1395 corresponding to analytic continuation respectively in the first and in the second vari-
 1396 able, and the indices $l|r, \pm$ indicating the sector for $(\text{Re } \nu, \text{Re } \mu)$ from which the analytic
 1397 continuation is performed, see table 1. The same reasoning as in section 4.1 gives

$$A_n^{i\pm} = T_{i_r^\pm}^{-n} T_{i_r^\pm}^n \quad (110)$$

$$A_n^{i\pm} = T_{i^\pm}^{-n} T_{i^\pm}^n \quad (111)$$

1398 for $i = 1, 2$. Using (108), (109), we observe that the analytic continuation for $K_{P,Q}$ is
 1399 in fact independent of the side $l|r$ from which the analytic continuation is made, and we
 1400 simply write $A_n^{i\pm}$ instead of $A_n^{i_l r \pm}$. Writing ν for the first variable and μ for the second
 1401 variable of $K_{P,Q}$, we obtain

$$\begin{aligned} A_n^{1^-} (K_{P,Q} + W_{P,Q}(\mu - \nu + i\pi) + Z_{P,Q}) &= K_{P \ominus B_n, Q} + W_{P \ominus B_n, Q}(\mu - \nu + i\pi) + Z_{P \ominus B_n, Q} \\ A_n^{1^+} (K_{P,Q} + W_{P,Q}(\mu - \nu + i\pi)) &= K_{P \ominus B_n, Q} + W_{P \ominus B_n, Q}(\mu - \nu + i\pi) \end{aligned} \quad (112)$$

1402 for analytic continuations in the first variable and

$$\begin{aligned} A_n^{2^-} (K_{P,Q} + W_{Q+1,P}(\nu - \mu - i\pi) + Z_{Q+1,P}) &= K_{P, Q \ominus B_n} + W_{Q \ominus B_n+1, P}(\nu - \mu - i\pi) + Z_{Q \ominus B_n+1, P} \\ A_n^{2^+} (K_{P,Q} + W_{Q+1,P}(\nu - \mu - i\pi)) &= K_{P, Q \ominus B_n} + W_{Q \ominus B_n+1, P}(\nu - \mu - i\pi) \end{aligned} \quad (113)$$

1403 for analytic continuations in the second variable. In particular, one has $(A_n^{1^-})^2 K_{P,Q} =$
 1404 $(A_n^{1^+})^2 K_{P,Q} = (A_n^{2^-})^2 K_{P,Q} = (A_n^{2^+})^2 K_{P,Q} = K_{P,Q}$, and the branch points $\nu = 2i\pi a,$
 1405 $\mu = 2i\pi a, a \in \mathbb{Z} + 1/2$ of $K_{P,Q}$ are of square root type.

1406 Analytic continuation for ν across $(\mu + 2i\pi n, \mu + 2i\pi(n + 1))$ is represented by the
 1407 operator $D_n^{l,\pm}$ (respectively $D_n^{r,\pm}$) if the analytic continuation is made from the sector
 1408 $\text{Re } \nu < 0$ (resp. $\text{Re } \nu > 0$), the sign $-$ corresponding to ν crossing the cut from the left
 1409 and the sign $+$ from the right. Analytic continuation for μ across $(\nu + 2i\pi(n - 1), \nu + 2i\pi n)$
 1410 is represented by the operator $D_{-n}^{l,\pm}$ (respectively $D_{-n}^{r,\pm}$) if the analytic continuation is made
 1411 from the sector $\text{Re } \mu < 0$ (resp. $\text{Re } \mu > 0$). In terms of translation operators, one has

$$\begin{aligned} D_n^{l,\pm} &= T_{1_{\mp}^{\mp}}^{-n} T_{1_{\pm}^{\pm}}^n \\ D_n^{r,\pm} &= T_{1_{\mp}^{\mp}}^{-n} T_{1_{\pm}^{\pm}}^n, \end{aligned} \quad (114)$$

1412 and one finds

$$\begin{aligned} D_n^{l,\pm} K_{P,Q} &= K_{P,Q} \\ D_n^{r,-} K_{P,Q} &= K_{P,Q} + Z_{P \ominus B_n - n, Q} - Z_{P - n, Q} \\ D_n^{r,+} K_{P,Q} &= K_{P,Q} - Z_{P \ominus B_n - n, Q} + Z_{P - n, Q}. \end{aligned} \quad (115)$$

1413

1414 4.10.2 Functions $K_{P,Q}^{\Delta,\Gamma}$

1415 We now introduce a generalization of $K_{P,Q}$ depending on two finite sets $\Delta, \Gamma \sqsubset \mathbb{Z} + 1/2$
 1416 similar to the generalization from J_P to J_P^{Δ} in section 4.9.2. We define
 1417

$$K_{P,Q}^{\Delta,\Gamma}(\nu, \mu) = \frac{1}{2} \int_{-\infty}^0 du \chi_P^{\Delta}(u + \nu) \chi_Q^{\Gamma}(u + \mu), \quad (116)$$

1418 with χ_P^{Δ} defined in (87). We show in the following that $e^{2K_{P,Q}^{\Delta,\Gamma}}$ can be extended to a
 1419 meromorphic function on $\mathcal{R}^{\Delta} \times \mathcal{R}^{\Gamma}$. More precisely, introducing the function

$$\begin{aligned} \Upsilon_{P,Q}^{\Delta,\Gamma}(\nu, \mu) &= \frac{e^{2K_{P,Q}^{\Delta,\Gamma}(\nu, \mu)}}{(1 - e^{\mu - \nu})^{|P \setminus \Delta|} (1 - e^{\nu - \mu})^{|Q \setminus \Gamma|}} \\ &\times \frac{\left(\prod_{a \in P \setminus \Delta} \prod_{b \in Q \setminus \Gamma} \left(\frac{2i\pi b - \mu}{4} - \frac{2i\pi a - \nu}{4} \right) \right) \left(\prod_{a \in P \cup \Delta} \prod_{b \in Q \cup \Gamma} \left(\frac{2i\pi b - \mu}{4} - \frac{2i\pi a - \nu}{4} \right) \right)}{\left(\prod_{a \in \Delta} \prod_{b \in \Gamma} \left(\frac{2i\pi b - \mu}{4} - \frac{2i\pi a - \nu}{4} \right) \right)}, \end{aligned} \quad (117)$$

1420 which verifies $\Upsilon_{P,Q}^{\Delta,\Gamma}(\nu, \mu) = \Upsilon_{P \setminus \Delta, Q \setminus \Gamma}^{\Delta,\Gamma}(\nu, \mu)$, the function $e^{2K^{\Delta,\Gamma}}$ defined by

$$(e^{2K^{\Delta,\Gamma}})([\nu, P], [\mu, Q]) = \Upsilon_{P,Q}^{\Delta,\Gamma}(\nu, \mu) \quad (118)$$

1421 is shown below to be meromorphic on $\mathcal{R}^{\Delta} \times \mathcal{R}^{\Gamma}$ when $|\Delta| \in 2\mathbb{N}$ and $|\Gamma| \in 2\mathbb{N}$, which is the
 1422 case needed for KPZ fluctuations.

1423 The function $K_{P,Q}^{\Delta,\Gamma}$ can be expressed in terms of $K_{P,Q}$ as

$$K_{P,Q}^{\Delta,\Gamma}(\nu, \mu) = \frac{K_{P,Q}(\nu, \mu)}{4} + \frac{K_{P \ominus \Delta, Q}(\nu, \mu)}{4} + \frac{K_{P, Q \ominus \Gamma}(\nu, \mu)}{4} + \frac{K_{P \ominus \Delta, Q \ominus \Gamma}(\nu, \mu)}{4}, \quad (119)$$

1424 and verifies $K_{P,Q}^{\Delta,\Gamma}(\nu, \mu) = K_{P \setminus \Delta, Q \setminus \Gamma}^{\Delta,\Gamma}(\nu, \mu)$. Tedious computations using (108), (109), (112),
 1425 (113), (115) then lead for shifts by integer multiples of $2i\pi$ to

$$\begin{aligned} T_{1_{\pm}}^{-n} \Upsilon_{P,Q}^{\Delta,\Gamma} &= \Upsilon_{P+n,Q}^{\Delta+n,\Gamma} \\ T_{1_{\pm}}^{-n} \Upsilon_{P,Q}^{\Delta,\Gamma} &= \Upsilon_{(P+n) \ominus (B_n \setminus (\Delta+n)), Q}^{\Delta+n,\Gamma} \\ T_{2_{\pm}}^{-n} \Upsilon_{P,Q}^{\Delta,\Gamma} &= \Upsilon_{P, Q+n}^{\Delta,\Gamma+n} \\ T_{2_{\pm}}^{-n} \Upsilon_{P,Q}^{\Delta,\Gamma} &= (-1)^{|\Delta| |B_n \setminus \Gamma|} \Upsilon_{P, (Q+n) \ominus (B_n \setminus (\Gamma+n))}^{\Delta,\Gamma+n} \end{aligned} \quad (120)$$

1426 and for the analytic continuations to ²⁰

$$\begin{aligned} A_n^1 \Upsilon_{P,Q}^{\Delta,\Gamma} &= \Upsilon_{P \ominus (B_n \setminus \Delta), Q}^{\Delta,\Gamma} \\ A_n^2 \Upsilon_{P,Q}^{\Delta,\Gamma} &= (-1)^{|\Delta| |B_n \setminus \Gamma|} \Upsilon_{P, Q \ominus (B_n \setminus \Gamma)}^{\Delta,\Gamma} \\ D_n \Upsilon_{P,Q}^{\Delta,\Gamma} &= \Upsilon_{P,Q}^{\Delta,\Gamma}. \end{aligned} \quad (121)$$

1427 The signs above disappear when $|\Delta|$ and $|\Gamma|$ are even numbers, and thus $\Upsilon_{P,Q}^{\Delta,\Gamma}$ can indeed
 1428 be extended to a function meromorphic on $\mathcal{R}^{\Delta} \times \mathcal{R}^{\Gamma}$ in that case.

1429 Additionally, extending $e^{2K^{\Delta,\Gamma}}$ to the collection $\overline{\mathcal{R}}^2$ of all $\mathcal{R}^{\Delta} \times \mathcal{R}^{\Gamma}$ by $\overline{e^{2K}}([\nu, (P, \Delta)],$
 1430 $[\mu, (Q, \Gamma)]) = e^{2K^{\Delta,\Gamma}}([\nu, P], [\mu, Q])$, see section 3.8.4, the function $\overline{e^{2K}}$ verifies from (120)
 1431 the symmetries $e^{2K} \circ (\overline{\mathcal{T}} \otimes 1) = e^{2K} \circ (1 \otimes \overline{\mathcal{T}}) = \overline{e^{2K}}$ with $\overline{\mathcal{T}}$ defined in (44).

1432 5 Relation with known formulas for KPZ

1433 In this section, we show that several known results about KPZ fluctuations in finite volume
 1434 with periodic boundary conditions are equivalent to the results given in section 2 in terms
 1435 of the Riemann surfaces introduced in section 3.8 and meromorphic functions on them from
 1436 section 4. For flat initial condition considered in section 2.2, only the Riemann surface $\tilde{\mathcal{R}}$
 1437 is needed. For sharp wedge and stationary initial conditions, discussed in sections 2.3, 2.4
 1438 and 2.5, a summation over the Riemann surfaces \mathcal{R}^{Δ} , $\Delta \sqsubset \mathbb{Z} + 1/2$ is needed.

1439 5.1 Flat initial condition

1440 In this section, we show that the expression (4) for the probability of the KPZ height with
 1441 flat initial condition is equivalent to exact results from [39, 40].

1442 5.1.1 Relation with the generating function of the height

1443
 1444 The expression (4) follows directly from that of the generating function $\langle e^{sh(x,t)} \rangle_{\text{flat}}$, $s > 0$
 1445 obtained in [39], equation (8) ²¹, based on earlier works [44, 45, 53, 54, 87–90] on the Bethe
 1446 ansatz solution of TASEP with periodic boundaries. One has

$$\langle e^{sh(x,t)} \rangle_{\text{flat}} = s \sum_{\substack{P \sqsubset \mathbb{Z} + 1/2 \\ |P|_+ = |P|_-}} \frac{V_P^2}{4^{|P|}} \frac{e^{t\chi_P(\nu_P(s))} e^{\frac{1}{2} f_{-\infty}^{\nu_P(s)} dv \chi_P''(v)^2}}{\chi_P''(\nu_P(s)) e^{\nu_P(s)/4} (1 + e^{-\nu_P(s)})^{1/4}}, \quad (122)$$

²⁰We write A_n^i instead of $A_n^{i_{\pm}}$ and D_n instead of $D_n^{l_{r,\pm}}$ when analytic continuations depends neither on the signs of the real parts of the variables nor on the sign of the real part of their difference.

²¹The function κ_a was called ω_a in [39].

1447 where $\nu_P(s)$ is the solution of the equation $\chi'_P(\nu_P(s)) = s$, conjectured to be unique and to
 1448 verify $\text{Re } \nu_P(s) > 0$ when $s > 0$. The probability density $p_{\text{flat}}(u) = -\partial_u \mathbb{P}_{\text{flat}}(h(x, t) > u)$ is
 1449 related by Fourier transform to the generating function as $p_{\text{flat}}(u) = \int_{-\infty}^{\infty} \frac{ds}{2\pi} e^{-isu} \langle e^{ish(x,t)} \rangle_{\text{flat}}$.
 1450 Making the change of variables $s = -i\chi'_P(\nu)$ and integrating with respect to u then gives
 1451 for $c > 0$

$$\mathbb{P}_{\text{flat}}(h(x, t) > u) = \sum_{\substack{P \subset \mathbb{Z} + 1/2 \\ |P|_+ = |P|_-}} \frac{V_P^2}{4^{|P|}} \int_{c-i\infty}^{c+i\infty} \frac{d\nu}{2i\pi} \frac{e^{t\chi_P(\nu) - u\chi'_P(\nu) + \frac{1}{2} \int_{-\infty}^{\nu} dv \chi''_P(v)^2}}{e^{\nu/4} (1 + e^{-\nu})^{1/4}}. \quad (123)$$

1452 At this stage, there are two differences between (123) and (4): the constraint $|P|_+ = |P|_-$
 1453 that P has as many positive and negative elements, and the integration range $(c - i\infty, c +$
 1454 $i\infty)$ instead of $(c - i\pi, c + i\pi)$. These differences correspond simply to distinct ways to
 1455 label the sheets of $\tilde{\mathcal{R}}$, or equivalently to the choice of a fundamental domain in \mathcal{R} for the
 1456 group action $\tilde{\mathfrak{g}}$ when writing $\tilde{\mathcal{R}} = \mathcal{R}/\tilde{\mathfrak{g}}$, compare the two representations of \mathcal{R} in figure 13
 1457 on the right side $\text{Re } \nu > 0$ of the branch cuts. Using (69), the expressions (123) and (4)
 1458 are equivalent explicit representations of (1) when $c > 0$ since $|P|_+ = |P|_-$ implies that
 1459 $|P|$ is even.

1460 5.1.2 Relation with Fredholm determinants

1461

1462 The probability distribution $\mathbb{P}_{\text{flat}}(h(x, t) > u)$ was also expressed in [39] as the integral
 1463 over ν , $\text{Re } \nu > 0$ of a Fredholm determinant, using the Cauchy determinant identity (21),
 1464 see section 2.6.3. Another Fredholm determinant expression for $\mathbb{P}_{\text{flat}}(h(x, t) > u)$ was
 1465 proved by Baik and Liu in [40] using the propagator approach [91, 92], but with a slightly
 1466 different kernel and an integral over ν , $\text{Re } \nu < 0$ instead. Although it had been checked
 1467 numerically that both expressions do agree, a proper derivation was missing. We show
 1468 below that the expression in [40] agrees with (4) when $c < 0$. The analyticity on the
 1469 cylinder, consequence of the trace in (1), justifies that (4) gives the same result for $c < 0$
 1470 and $c > 0$, and shows that the expressions in [39] and [40] for flat initial condition are
 1471 indeed equivalent.

1472 We start with equation (4.2) of [40]. In our notations, Baik and Liu prove that the
 1473 height function $h(x, t)$ for the totally asymmetric simple exclusion process with flat ini-
 1474 tial condition, appropriately rescaled according to KPZ universality, has the cumulative
 1475 distribution function $\mathbb{P}_{\text{flat}}(h(x, t) > u) = F_1(-u; t)$, with

$$F_1(-u; t) = \oint_{|z|<1} \frac{dz}{2i\pi z} e^{-uA_1(z) + tA_2(z) + A_3(z) + B(z)} \det(1 - \mathcal{K}_z^{(1)}). \quad (124)$$

1476 The contour of integration encircles 0 once in the anti-clockwise direction. Writing $z =$
 1477 $-e^\nu$, $\text{Re } \nu < 0$, one has in terms of the functions of section 4 the identifications $A_1(-e^\nu) =$
 1478 $\chi'_\emptyset(\nu)$, $A_2(-e^\nu) = \chi_\emptyset(\nu)$, $A_3(-e^\nu) = I_0(\nu)$ and $B(-e^\nu) = J_\emptyset(\nu)$. After some harmless
 1479 changes of notations using the fact that any $\xi \in S_{z, \text{left}}$ in [40] is of the form $-\kappa_a(\nu)$ for
 1480 some $a \in \mathbb{Z} + 1/2$, the discrete operator $\mathcal{K}_z^{(1)}$ has for kernel

$$\mathcal{K}_z^{(1)}(a, b) = \frac{\exp(\frac{2t}{3} \kappa_a(\nu)^3 + 2u\kappa_a(\nu) + 2 \int_{-\infty}^{\nu} dv \frac{\chi''_\emptyset(v)}{\kappa_a(v)})}{\kappa_a(\nu)(\kappa_a(\nu) + \kappa_b(\nu))}, \quad (125)$$

1481 with $a, b \in \mathbb{Z} + 1/2$ and a path of integration contained in \mathbb{D} . The rest of the section
 1482 is essentially a more detailed version of the derivation of equation (22), run backwards.

1483 Expanding the Fredholm determinant in (124) as

$$\det(1 - \mathcal{K}_z^{(1)}) = \sum_{P \sqsubset \mathbb{Z} + 1/2} (-1)^{|P|} \det(\mathcal{K}_z^{(1)}(a, b))_{a, b \in P}, \quad (126)$$

1484 using the Cauchy determinant identity (21) and making the change of variable $z = -e^\nu$,
 1485 one finds for any real number $c < 0$

$$F_1(-u; t) = \int_{c-i\pi}^{c+i\pi} \frac{d\nu}{2i\pi} e^{t\chi_\emptyset(\nu) - u\chi'_\emptyset(\nu) + I_0(\nu) + J_\emptyset(\nu)} \sum_{P \sqsubset \mathbb{Z} + 1/2} (-1)^{|P|} \quad (127)$$

$$\times \left(\prod_{a \in P} \frac{\exp(\frac{2t}{3} \kappa_a(\nu)^3 + 2u\kappa_a(\nu) + 2 \int_{-\infty}^{\nu} dv \frac{\chi''_\emptyset(v)}{\kappa_a(v)})}{\kappa_a(\nu)} \right) \frac{\prod_{\substack{a, b \in P \\ a > b}} (\kappa_a(\nu) - \kappa_b(\nu))^2}{\prod_{a, b \in P} (\kappa_a(\nu) + \kappa_b(\nu))}.$$

1486 In terms of the functions χ_P , we obtain from (64), (51)

$$F_1(-u; t) = \int_{c-i\pi}^{c+i\pi} \frac{d\nu}{2i\pi} \sum_{P \sqsubset \mathbb{Z} + 1/2} (-1)^{|P|} e^{t\chi_P(\nu) - u\chi'_P(\nu) + I_0(\nu) + J_\emptyset(\nu) + \int_{-\infty}^{\nu} dv \chi''_\emptyset(v) (\chi''_P(v) - \chi''_\emptyset(v))}$$

$$\times \left(\prod_{a \in P} \frac{1}{\kappa_a(\nu)} \right) \frac{\prod_{\substack{a, b \in P \\ a > b}} (\kappa_a(\nu) - \kappa_b(\nu))^2}{\prod_{a, b \in P} (\kappa_a(\nu) + \kappa_b(\nu))}. \quad (128)$$

1487 In terms of the regularized integral $\mathcal{f}_{-\infty}^{\nu} = \lim_{\Lambda \rightarrow \infty} (\dots) \log \Lambda + \int_{-\infty}^{\nu}$ subtracting appro-
 1488 priately logarithmic divergences used in the definition (74) for the functions J_P , one has

$$J_\emptyset(\nu) + \int_{-\infty}^{\nu} dv \chi''_\emptyset(v) (\chi''_P(v) - \chi''_\emptyset(v)) \quad (129)$$

$$= J_P(\nu) - \frac{1}{2} \mathcal{f}_{-\infty}^{\nu} dv (\chi''_P(v) - \chi''_\emptyset(v))^2$$

$$= J_P(\nu) - 2 \sum_{a, b \in P} \mathcal{f}_{-\infty}^{\nu} \frac{dv}{\kappa_a(v) \kappa_b(v)}$$

$$= J_P(\nu) + \sum_{a, b \in P} \log \left(\frac{(\kappa_a(\nu) + \kappa_b(\nu))^2}{8} \right),$$

1489 where the first equality comes from (74), the second from (161) and the third from (184)
 1490 using the fact that $2 \log(\kappa_a(\nu) + \kappa_b(\nu)) = \log((\kappa_a(\nu) + \kappa_b(\nu))^2)$ when $\text{Re } \nu < 0$. We obtain

$$F_1(-u; t) = \int_{c-i\pi}^{c+i\pi} \frac{d\nu}{2i\pi} \sum_{P \sqsubset \mathbb{Z} + 1/2} \frac{(-1)^{|P|}}{4^{|P|}} e^{t\chi_P(\nu) - u\chi'_P(\nu) + I_0(\nu) + J_P(\nu)}$$

$$\times \prod_{\substack{a, b \in P \\ a > b}} \left(\frac{\kappa_a(\nu)^2 - \kappa_b(\nu)^2}{8} \right)^2. \quad (130)$$

1491 From the definition (50) of $\kappa_a(\nu)$, one has $(\kappa_a(\nu)^2 - \kappa_b(\nu)^2)/8 = 2i\pi a/4 - 2i\pi b/4$, which
 1492 finally gives (4) with $c < 0$.

1493 5.2 Sharp wedge initial condition

1494 In this section, we show that the expression (10) for the probability of the KPZ height
 1495 with sharp wedge initial condition is equivalent to exact results from [39, 40].

1496 **5.2.1 Relation with the generating function of the height from [39]**

1497

1498 The expression (6) for sharp wedge initial condition is a consequence of the generating
1499 function obtained in [39], equation (9), and given for $s > 0$ by

$$\begin{aligned} \langle e^{sh(x,t)} \rangle_{\text{sw}} = s \sum_{\substack{P,H \subset \mathbb{Z}+1/2 \\ |P|_{\pm}=|H|_{\mp}}} \frac{i^{|P|+|H|} V_P^2 V_H^2}{4^{|P|+|H|}} e^{2i\pi x(\sum_{a \in P} a - \sum_{a \in H} a)} \quad (131) \\ \times \frac{e^{t\chi_{P,H}(\nu_{P,H}(s))} \lim_{\Lambda \rightarrow \infty} \Lambda^{-|P|^2-|H|^2} e^{\int_{-\Lambda}^{\nu_{P,H}(s)} dv \chi''_{P,H}(v)^2}}{\chi''_{P,H}(\nu_{P,H}(s))}, \end{aligned}$$

1500 with Vandermonde determinants V_P, V_H defined in (5),

$$\chi_{P,H}(v) = \frac{\chi_P(v) + \chi_H(v)}{2} \quad (132)$$

1501 and $\nu_{P,H}(s)$ the solution of $\chi'_{P,H}(\nu_{P,H}(s)) = s$, conjectured to be unique when $\text{Re } s > 0$.
1502 The restrictions $|P|_+ = |H|_-$, $|P|_- = |H|_+$ on the number of positive and negative
1503 elements of P and H imply in particular that we are summing only over sets P and H
1504 with $|P| = |H|$.

1505 As in section 2.2, the cumulative distribution function of the height can be derived
1506 from the generating function by Fourier transform, and we obtain in terms of $\chi_P^\Delta, J_P^\Delta$
1507 defined in (87), (74)

$$\begin{aligned} \mathbb{P}_{\text{sw}}(h(x,t) > u) = \sum_{\substack{P,H \subset \mathbb{Z}+1/2 \\ |P|_{\pm}=|H|_{\mp}}} \frac{i^{|P|+|H|} V_P^2 V_H^2}{4^{|P|+|H|}} e^{2i\pi x(\sum_{a \in P} a - \sum_{a \in H} a)} \quad (133) \\ \times \int_{c-i\infty}^{c+i\infty} \frac{d\nu}{2i\pi} e^{t\chi_P^\Delta(\nu) - u\chi'_P(\nu) + 2J_P^\Delta(\nu)}, \end{aligned}$$

1508 with $c > 0$ and $\Delta = P \ominus H$.

1509 One has $|P| + |H| = 2|P \setminus \Delta| + |\Delta|$, $\sum_{a \in P} a - \sum_{a \in H} a = \sum_{a \in A} a - \sum_{a \in \Delta \setminus A} a$ and

$$V_P^2 V_H^2 = V_A^2 V_{\Delta \setminus A}^2 \prod_{a \in P \setminus \Delta} \prod_{\substack{b \in P \cup \Delta \\ b \neq a}} \left(\frac{2i\pi a}{4} - \frac{2i\pi b}{4} \right)^2, \quad (134)$$

1510 where $\Delta = P \ominus H$ and $A = P \cap \Delta$. These identities allow to rewrite (133) as

$$\begin{aligned} \mathbb{P}_{\text{sw}}(h(x,t) > u) = \sum_{\Delta \subset \mathbb{Z}+1/2} \sum_{A \subset \Delta} \sum_{\substack{Q \subset \mathbb{Z}+1/2 \\ Q \cap \Delta = \emptyset}} 1_{\{|P|_{\pm}=|P \ominus \Delta|_{\mp}\}} (i/4)^{2|P \setminus \Delta|+|\Delta|} V_A^2 V_{\Delta \setminus A}^2 \\ \times \left(\prod_{a \in P \setminus \Delta} \prod_{\substack{b \in P \cup \Delta \\ b \neq a}} \left(\frac{2i\pi a}{4} - \frac{2i\pi b}{4} \right)^2 \right) e^{2i\pi x(\sum_{a \in A} a - \sum_{a \in \Delta \setminus A} a)} \\ \times \int_{c-i\infty}^{c+i\infty} \frac{d\nu}{2i\pi} e^{t\chi_P^\Delta(\nu) - u\chi'_P(\nu) + 2J_P^\Delta(\nu)}, \quad (135) \end{aligned}$$

1511 where the sum over $P = Q \cup A$ and $H = P \cup (\Delta \setminus A)$ has been replaced by a sum over
1512 Δ, A, Q . Since $A \subset \Delta$ and the function χ_P^Δ verifies $\chi_P^\Delta = \chi_{P \setminus \Delta}^\Delta$, all χ_P^Δ in the integral
1513 can be replaced by χ_Q^Δ . Additionally, $P \setminus \Delta = Q$ and $P \cup \Delta = Q \cup \Delta$ shows that further
1514 factors are independent of A . Finally $|P|_{\pm} = |Q|_{\pm} + |A|_{\pm}$, $|P \ominus \Delta|_{\mp} = |Q|_{\mp} + |\Delta \setminus A|_{\mp} =$

1515 $|Q|_{\mp} + |\Delta|_{\mp} - |A|_{\mp}$, and the constraints $|P|_{\pm} = |P \ominus \Delta|_{\mp}$ can be replaced by $|A| = |\Delta \setminus A|$,
 1516 implying that $|\Delta|$ is necessarily even, and $|Q|_{+} - |Q \ominus \Delta|_{-} = -|\Delta|/2$, equivalent to
 1517 $\lambda_{+}(Q, \Delta) = -|\Delta|/2$ with λ_{+} defined above (43).

1518 In terms of Ξ_x^{Δ} defined in (7) and of the functions χ^{Δ} , χ'^{Δ} , $e^{2J^{\Delta}}$ on the Riemann
 1519 surface \mathcal{R}^{Δ} defined in (86), (91), (96), we obtain

$$\mathbb{P}_{\text{sw}}(h(x, t) > u) = \sum_{\Delta \in \mathbb{Z} + 1/2} \Xi_x^{\Delta} \sum_{\substack{Q \in \mathbb{Z} + 1/2 \\ Q \cap \Delta = \emptyset}} 1_{\{\lambda_{+}(Q, \Delta) = -|\Delta|/2\}} \quad (136)$$

$$\times \int_{c-i\infty}^{c+i\infty} \frac{d\nu}{2i\pi} (e^{t\chi^{\Delta} - u\chi'^{\Delta} + 2J^{\Delta}})([\nu, Q]).$$

1520 We split $\int_{c-i\infty}^{c+i\infty}$ into $\sum_{m=-\infty}^{\infty} \int_{c-2i\pi(m-1/2)}^{c+2i\pi(m+1/2)}$ and shift ν by $-2i\pi m$. We then use the
 1521 symmetry by $\overline{\mathcal{T}}$ defined in (44) of the extension to $\overline{\mathcal{R}}$ of χ^{Δ} and $e^{2J^{\Delta}}$, i.e. we replace
 1522 $[\nu - 2i\pi m, (Q, \Delta)]$ by $[\nu, ((Q + m) \ominus (B_m \setminus (\Delta + m)), \Delta + m)]$ everywhere since $c > 0$.
 1523 Making the change of variable $Q \rightarrow P \ominus (B_m \setminus (\Delta + m)) - m = (P - m) \ominus (B_{-m} \setminus \Delta)$
 1524 followed by $\Delta \rightarrow \Delta - m$, the constraint $Q \cap \Delta = \emptyset$ becomes $P \cap \Delta = \emptyset$. Using $\Xi_x^{\Delta - m} = \Xi_x^{\Delta}$
 1525 then leads to

$$\mathbb{P}_{\text{sw}}(h(x, t) > u) = \sum_{\Delta \in \mathbb{Z} + 1/2} \Xi_x^{\Delta} \sum_{\substack{P \in \mathbb{Z} + 1/2 \\ P \cap \Delta = \emptyset}} \sum_{m=-\infty}^{\infty} 1_{\{\lambda_{+}((P-m) \ominus (B_{-m} \setminus (\Delta - m)), \Delta - m) = -|\Delta|/2\}} \quad (137)$$

$$\times \int_{c-i\pi}^{c+i\pi} \frac{d\nu}{2i\pi} (e^{t\chi^{\Delta} - u\chi'^{\Delta} + 2J^{\Delta}})([\nu, P]).$$

1526 Using (43), the condition $\lambda_{+}((P - m) \ominus (B_{-m} \setminus (\Delta - m)), \Delta - m) = -|\Delta|/2$ is equivalent
 1527 to $\lambda_{+}(P, \Delta) = m - |\Delta|/2$. We observe that there exists a unique $m \in \mathbb{Z}$ such that the
 1528 constraint is verified when $|\Delta|$ is even, and that no $m \in \mathbb{Z}$ satisfies the constraint when
 1529 $|\Delta|$ is odd. Since $\Xi_x^{\Delta} = 0$ when $|\Delta|$ is odd, this leads to (10), using the definitions (86),
 1530 (96) of χ^{Δ} and $e^{2J^{\Delta}}$.

1531 The slightly tedious derivation of (10) from (135) in this section can be understood
 1532 more directly, but at the price of heavier formalism, by considering a collection $\overline{\overline{\mathcal{R}}}$ of
 1533 copies of \mathcal{R} and a covering map from $\overline{\overline{\mathcal{R}}}$ to $\overline{\mathcal{R}}$ projecting each copy of \mathcal{R} in $\overline{\overline{\mathcal{R}}}$ to a distinct
 1534 \mathcal{R}^{Δ} in $\overline{\mathcal{R}}$. The functions appearing in (135) can then be interpreted as functions on the
 1535 components \mathcal{R} of $\overline{\overline{\mathcal{R}}}$, equal at $[\nu, P] \in \mathcal{R}$ to the product of a constant depending only on
 1536 $A = P \cap \Delta$, which is eventually gathered into Ξ_x^{Δ} , and a function of $[\nu, P \setminus \Delta] \in \mathcal{R}^{\Delta}$.

1537 5.2.2 Relation with the expression from Baik and Liu [40]

1538
 1539 In this section, we show that our result (6) for the cumulative distribution function of
 1540 KPZ fluctuations with sharp wedge initial condition agrees with the alternative formula
 1541 by Baik and Liu [40], with an integration on the left side of the branch cuts.

1542 We start with equation (4.10) of [40]. In our notations, Baik and Liu prove that the
 1543 height function $h(x, t)$ for the totally asymmetric simple exclusion process with domain
 1544 wall initial condition, appropriately rescaled according to KPZ universality, has the cu-
 1545 mulative distribution function $\mathbb{P}_{\text{sw}}(h(x, t) > u) = F_2(-u; t, x)$, with

$$F_2(-u; t, x) = \oint_{|z|<1} \frac{dz}{2i\pi z} e^{-uA_1(z) + tA_2(z) + 2B(z)} \det(1 - \mathcal{K}_z^{(2)}). \quad (138)$$

1546 The contour of integration encircles 0 once in the anti-clockwise direction. Writing $z =$
 1547 $-e^{\nu}$, $\text{Re } \nu < 0$, one has in terms of the functions of section 4 the identifications $A_1(-e^{\nu}) =$

1548 $\chi'_\theta(\nu)$, $A_2(-e^\nu) = \chi_\theta(\nu)$ and $B(-e^\nu) = J_\theta(\nu)$. After some harmless changes of notations
 1549 using the fact that any $\xi \in \mathcal{S}_{z,\text{left}}$ in [40] is of the form $-\kappa_a(\nu)$ for some $a \in \mathbb{Z} + 1/2$, the
 1550 discrete operator $\mathcal{K}_z^{(2)}$ has for kernel

$$\begin{aligned} \mathcal{K}_z^{(2)}(a, b) &= \frac{\exp(\frac{t}{3} \kappa_a(\nu)^3 + u\kappa_a(\nu) + 2i\pi ax + 2 \int_{-\infty}^\nu dv \frac{\chi''_\theta(v)}{\kappa_a(v)})}{\kappa_a(\nu)} \\ &\times \sum_{c \in \mathbb{Z} + 1/2} \frac{\exp(\frac{t}{3} \kappa_c(\nu)^3 + u\kappa_c(\nu) - 2i\pi cx + 2 \int_{-\infty}^\nu dv \frac{\chi''_\theta(v)}{\kappa_c(v)})}{\kappa_c(\nu)(\kappa_a(\nu) + \kappa_c(\nu))(\kappa_b(\nu) + \kappa_c(\nu))}, \end{aligned} \quad (139)$$

1551 with $a, b \in \mathbb{Z} + 1/2$. The rest of the section is essentially a more detailed version of the
 1552 derivation of (25), run backwards. Expanding the Fredholm determinant in (124) as

$$\det(1 - \mathcal{K}_z^{(2)}) = \sum_{P \sqsubset \mathbb{Z} + 1/2} (-1)^{|P|} \det(\mathcal{K}_z^{(2)}(a, b))_{a, b \in P}, \quad (140)$$

1553 using

$$\det \left(\sum_{c \in \mathbb{Z} + 1/2} \mathcal{K}_{a, b, c} \right)_{a, b \in P} = \left(\prod_{a \in P} \sum_{c_a \in \mathbb{Z} + 1/2} \right) \det \left(\mathcal{K}_{a, b, c_a} \right)_{a, b \in P}, \quad (141)$$

1554 the Cauchy determinant identity

$$\det \left(\frac{1}{\kappa_a + \kappa_b} \right)_{a, b \in P} = \frac{\left(\prod_{\substack{a, b \in P \\ a > b}} (\kappa_a - \kappa_b) \right) \left(\prod_{\substack{a, b \in P \\ a > b}} (\kappa_{c_a} - \kappa_{c_b}) \right)}{\prod_{a, b \in P} (\kappa_{c_a} + \kappa_b)}, \quad (142)$$

1555 and making the change of variable $z = -e^\nu$, one finds for any real number $c < 0$

$$\begin{aligned} F_2(-u; t, x) &= \int_{c-i\pi}^{c+i\pi} \frac{d\nu}{2i\pi} e^{t\chi_\theta(\nu) - u\chi'_\theta(\nu) + 2J_\theta(\nu)} \sum_{P \sqsubset \mathbb{Z} + 1/2} \left(\prod_{a \in P} \sum_{c_a \in \mathbb{Z} + 1/2} \right) (-1)^{|P|} \\ &\times \left(\prod_{a \in P} \frac{\exp(\frac{t}{3} \kappa_a(\nu)^3 + u\kappa_a(\nu) + 2i\pi ax + 2 \int_{-\infty}^\nu dv \frac{\chi''_\theta(v)}{\kappa_a(v)})}{\kappa_a(\nu)} \right) \\ &\times \left(\prod_{a \in P} \frac{\exp(\frac{t}{3} \kappa_{c_a}(\nu)^3 + u\kappa_{c_a}(\nu) - 2i\pi c_a x + 2 \int_{-\infty}^\nu dv \frac{\chi''_\theta(v)}{\kappa_{c_a}(v)})}{\kappa_{c_a}(\nu)} \right) \\ &\times \frac{\left(\prod_{\substack{a, b \in P \\ a > b}} (\kappa_a(\nu) - \kappa_b(\nu)) \right) \left(\prod_{\substack{a, b \in P \\ a > b}} (\kappa_{c_a}(\nu) - \kappa_{c_b}(\nu)) \right)}{\left(\prod_{a \in P} (\kappa_a(\nu) + \kappa_{c_a}(\nu)) \right) \left(\prod_{a, b \in P} (\kappa_{c_a}(\nu) + \kappa_b(\nu)) \right)}. \end{aligned} \quad (143)$$

1556 Because of the factor $\prod_{\substack{a, b \in P \\ a > b}} (\kappa_{c_a}(\nu) - \kappa_{c_b}(\nu))$, only the tuples c_a , $a \in P$ with distinct
 1557 elements contribute, and one can replace these tuples by finite sets $H \sqsubset \mathbb{Z} + 1/2$ with
 1558 $|H| = |P|$ up to permutations. Using the identity

$$\begin{aligned} &\left(\prod_{a \in P} \sum_{c_a \in \mathbb{Z} + 1/2} \right) 1_{\{\{c_a, a \in P\} = H\}} \frac{\left(\prod_{\substack{a, b \in P \\ a > b}} (\kappa_{c_a} - \kappa_{c_b}) \right)}{\left(\prod_{a \in P} (\kappa_a + \kappa_{c_a}) \right) \left(\prod_{a, b \in P} (\kappa_{c_a} + \kappa_b) \right)} \\ &= \frac{\left(\prod_{\substack{a, b \in P \\ a > b}} (\kappa_a - \kappa_b) \right) \left(\prod_{\substack{a, b \in H \\ a > b}} (\kappa_a - \kappa_b)^2 \right)}{\prod_{a \in P} \prod_{b \in H} (\kappa_a + \kappa_b)^2} \end{aligned} \quad (144)$$

1559 for $P, H \subset \mathbb{Z} + 1/2$, $|P| = |H|$, (132), (64) and (161), this leads to

$$\begin{aligned}
 F_2(-u; t, x) &= \int_{c-i\pi}^{c+i\pi} \frac{d\nu}{2i\pi} \sum_{\substack{P, H \subset \mathbb{Z} + 1/2 \\ |P|=|H|}} (-1)^{|P|} e^{t\chi_{P,H}(\nu) - u\chi'_{P,H}(\nu)} e^{2i\pi x (\sum_{a \in P} a - \sum_{a \in H} a)} \\
 &\quad \times e^{2J_\emptyset(\nu) + 2 \int_{-\infty}^{\nu} dv \chi''_\emptyset(v) (\chi''_{P,H}(v) - \chi''_\emptyset(v))} \left(\prod_{a \in P} \frac{1}{\kappa_a(\nu)} \right) \left(\prod_{a \in H} \frac{1}{\kappa_a(\nu)} \right) \\
 &\quad \times \frac{\left(\prod_{\substack{a, b \in P \\ a > b}} (\kappa_a(\nu) - \kappa_b(\nu)) \right)^2 \left(\prod_{\substack{a, b \in H \\ a > b}} (\kappa_a(\nu) - \kappa_b(\nu)) \right)^2}{\left(\prod_{a \in P} \prod_{b \in H} (\kappa_a(\nu) + \kappa_b(\nu)) \right)^2}. \quad (145)
 \end{aligned}$$

1560 In terms of the regularized integral $f_{-\infty}^{\nu} = \lim_{\Lambda \rightarrow \infty} (\dots) \log \Lambda + \int_{-\infty}^{\nu}$ subtracting appro-
 1561 priately logarithmic divergences used in the definition (74) for the functions J_P , one has

$$\begin{aligned}
 &J_\emptyset(\nu) + \int_{-\infty}^{\nu} dv \chi''_\emptyset(v) (\chi''_{P,H}(v) - \chi''_\emptyset(v)) \quad (146) \\
 &= \frac{1}{2} \int_{-\infty}^{\nu} dv \chi''_{P,H}(v)^2 - \frac{1}{2} \int_{-\infty}^{\nu} dv (\chi''_{P,H}(v) - \chi''_\emptyset(v))^2 \\
 &= \frac{1}{2} \int_{-\infty}^{\nu} dv \chi''_{P,H}(v)^2 - \frac{1}{2} \sum_{a, b \in P} \int_{-\infty}^{\nu} \frac{dv}{\kappa_a(v) \kappa_b(v)} - \frac{1}{2} \sum_{a, b \in H} \int_{-\infty}^{\nu} \frac{dv}{\kappa_a(v) \kappa_b(v)} \\
 &\quad - \sum_{a \in P} \sum_{b \in H} \int_{-\infty}^{\nu} \frac{dv}{\kappa_a(v) \kappa_b(v)} \\
 &= \frac{1}{2} \int_{-\infty}^{\nu} dv \chi''_{P,H}(v)^2 + \frac{1}{2} \sum_{a, b \in P} \log \left(\frac{\kappa_a(\nu) + \kappa_b(\nu)}{\sqrt{8}} \right) \\
 &\quad + \frac{1}{2} \sum_{a, b \in H} \log \left(\frac{\kappa_a(\nu) + \kappa_b(\nu)}{\sqrt{8}} \right) + \sum_{a \in P} \sum_{b \in H} \log \left(\frac{\kappa_a(\nu) + \kappa_b(\nu)}{\sqrt{8}} \right),
 \end{aligned}$$

1562 where the first equality comes from (74), the second from (132), (161) and the third from
 1563 (184). We obtain

$$\begin{aligned}
 F_2(-u; t, x) &= \int_{c-i\pi}^{c+i\pi} \frac{d\nu}{2i\pi} \sum_{\substack{P, H \subset \mathbb{Z} + 1/2 \\ |P|=|H|}} \frac{i^{|P|+|H|}}{4^{|P|+|H|}} e^{t\chi_{P,H}(\nu) - u\chi'_{P,H}(\nu) + f_{-\infty}^{\nu} dv \chi''_{P,H}(v)^2} \quad (147) \\
 &\quad \times e^{2i\pi x (\sum_{a \in P} a - \sum_{a \in H} a)} \left(\prod_{\substack{a, b \in P \\ a > b}} \frac{\kappa_a(\nu)^2 - \kappa_b(\nu)^2}{8} \right)^2 \left(\prod_{\substack{a, b \in H \\ a > b}} \frac{\kappa_a(\nu)^2 - \kappa_b(\nu)^2}{8} \right)^2.
 \end{aligned}$$

1564 From the definition (50) of $\kappa_a(\nu)$, one has $(\kappa_a(\nu)^2 - \kappa_b(\nu)^2)/8 = 2i\pi a/4 - 2i\pi b/4$, which
 1565 gives

$$\begin{aligned}
 F_2(-u; t, x) &= \int_{c-i\pi}^{c+i\pi} \frac{d\nu}{2i\pi} \sum_{\substack{P, H \subset \mathbb{Z} + 1/2 \\ |P|=|H|}} \frac{i^{|P|+|H|} V_P^2 V_H^2}{4^{|P|+|H|}} e^{2i\pi x (\sum_{a \in P} a - \sum_{a \in H} a)} \\
 &\quad \times e^{t\chi_{P,H}(\nu) - u\chi'_{P,H}(\nu) + f_{-\infty}^{\nu} dv \chi''_{P,H}(v)^2}. \quad (148)
 \end{aligned}$$

1566 with V_P the Vandermonde determinant defined in (5). Introducing $\Delta = P \ominus H$ and the

1567 functions χ_P^Δ and J_P^Δ from (87), (92), we finally obtain

$$\mathbb{P}_{\text{sw}}(h(x, t) > u) = \sum_{\substack{P, H \subset \mathbb{Z} + 1/2 \\ |P|=|H|}} \frac{i^{|P|+|H|} V_P^2 V_H^2}{4^{|P|+|H|}} e^{2i\pi x (\sum_{a \in P} a - \sum_{a \in H} a)} \quad (149)$$

$$\times \int_{c-i\pi}^{c+i\pi} \frac{d\nu}{2i\pi} e^{t\chi_P^\Delta(\nu) - u\chi_P^\Delta(\nu) + 2J_P^\Delta(\nu)},$$

1568 with $\Delta = P \ominus H$ and $V_P, \chi_P^\Delta, J_P^\Delta$ defined in (5), (87), (92). The sign of c , the integration
 1569 range and the constraint on the sets P and H differ from (133). This corresponds simply
 1570 to another choice of fundamental domain for the Riemann surfaces \mathcal{R}^Δ . Indeed, writing
 1571 $P = Q \cup A$ with $A \subset \Delta, Q \cap \Delta = \emptyset$ and using (134) as in the previous section leads to

$$\mathbb{P}_{\text{sw}}(h(x, t) > u) = \sum_{\Delta \subset \mathbb{Z} + 1/2} \sum_{A \subset \Delta} \sum_{\substack{Q \subset \mathbb{Z} + 1/2 \\ Q \cap \Delta = \emptyset}} 1_{\{|P|=|P \ominus \Delta|\}} (i/4)^{2|P \setminus \Delta| + |\Delta|} V_A^2 V_{\Delta \setminus A}^2$$

$$\times \left(\prod_{a \in P \setminus \Delta} \prod_{\substack{b \in P \cup \Delta \\ b \neq a}} \left(\frac{2i\pi a}{4} - \frac{2i\pi b}{4} \right)^2 \right) e^{2i\pi x (\sum_{a \in A} a - \sum_{a \in \Delta \setminus A} a)}$$

$$\times \int_{c-i\pi}^{c+i\pi} \frac{d\nu}{2i\pi} e^{t\chi_P^\Delta(\nu) - u\chi_P^\Delta(\nu) + 2J_P^\Delta(\nu)}, \quad (150)$$

1572 which parallels (135). Since $|P| = |P \ominus \Delta|$ is equivalent to $|A| = |\Delta \setminus A|$, the same reasoning
 1573 as from (135) to (136) finally gives

$$\mathbb{P}_{\text{sw}}(h(x, t) > u) = \sum_{\Delta \subset \mathbb{Z} + 1/2} \Xi_x^\Delta \sum_{\substack{Q \subset \mathbb{Z} + 1/2 \\ Q \cap \Delta = \emptyset}} \int_{c-i\pi}^{c+i\pi} \frac{d\nu}{2i\pi} (e^{t\chi^\Delta - u\chi'^\Delta + 2J^\Delta})([\nu, Q]), \quad (151)$$

1574 which is precisely (10).

1575 5.3 Multiple-time statistics with sharp wedge initial condition

1576 In this section, we derive (13) starting with a result by Baik and Liu [42]. We also discuss
 1577 the pole structure on the Riemann surfaces $\mathcal{R}^{\Delta_\ell}$ of the final expression.

1578 5.3.1 Derivation of (13) from Baik-Liu [42]

1579
 1580 The joint distribution of the height at multiple times $0 < t_1 < \dots < t_m$ and positions
 1581 x_j was obtained by Baik and Liu in [42], equation (2.15), with the expression (2.21) for
 1582 $C(\mathbf{z})$, and (2.51), (2.55) for $D(\mathbf{z})$. Under the replacements $\tau_j \rightarrow t_j, \gamma_j \rightarrow x_j, x_j \rightarrow -u_j$,

1583 one has $\mathbb{P}_{\text{sw}}(h(x_1, t_1) > u_1, \dots, h(x_m, t_m) > u_m) = F(\vec{t}, \vec{x}, \vec{u})$ where

$$\begin{aligned}
 & F(\vec{t}, \vec{x}, \vec{u}) \\
 &= \oint \frac{dz_1}{2i\pi z_1} \cdots \frac{dz_m}{2i\pi z_m} \left(\prod_{\ell=1}^m \left(\frac{z_\ell}{z_\ell - z_{\ell+1}} \frac{e^{-u_\ell A_1(z_\ell) + t_\ell A_2(z_\ell)}}{e^{-u_\ell A_1(z_{\ell+1}) + t_\ell A_2(z_{\ell+1})}} e^{2B(z_\ell, z_\ell) - 2B(z_{\ell+1}, z_\ell)} \right) \right) \\
 & \quad \times \sum_{n_1, \dots, n_m=0}^{\infty} \left(\prod_{\ell=1}^m \frac{1}{(n_\ell!)^2} \right) \left(\prod_{\ell=2}^m \left(\left(1 - \frac{z_{\ell-1}}{z_\ell}\right)^{n_\ell} \left(1 - \frac{z_\ell}{z_{\ell-1}}\right)^{n_{\ell-1}} \right) \right) \quad (152) \\
 & \quad \times \left(\prod_{\ell=1}^m \sum_{\mathcal{P}_\ell, \mathcal{H}_\ell \in (\mathbb{Z} + 1/2)^{n_\ell}} \right) \left(\prod_{\ell=1}^m \left(\frac{\Delta(U^{(\ell)})^2 \Delta(V^{(\ell)})^2}{\Delta(U^{(\ell)}; V^{(\ell)})^2} \hat{f}_\ell(U^{(\ell)}) \hat{f}_\ell(V^{(\ell)}) \right) \right) \\
 & \quad \times \left(\prod_{\ell=2}^m \left(\frac{\Delta(U^{(\ell)}; V^{(\ell-1)}) \Delta(V^{(\ell)}; U^{(\ell-1)}) e^{-h(V^{(\ell)}, z_{\ell-1}) - h(V^{(\ell-1)}, z_\ell)}}{\Delta(U^{(\ell)}; U^{(\ell-1)}) \Delta(V^{(\ell)}; V^{(\ell-1)}) e^{h(U^{(\ell)}, z_{\ell-1}) + h(U^{(\ell-1)}, z_\ell)}} \right) \right),
 \end{aligned}$$

1584 with $|z_m| < \dots < |z_1| < 1$, $\nu_{m+1} = -\infty$, $x_0 = x_{m+1} = t_0 = t_{m+1} = u_0 = u_{m+1} =$
 1585 0 . In terms of $z_\ell = -e^{\nu_\ell}$, $\text{Re } \nu_\ell < 0$, $-\pi < \text{Im } \nu_\ell < \pi$, one has $A_1(z_\ell) = \chi'_\emptyset(\nu_\ell)$
 1586 and $A_2(z_\ell) = \chi_\emptyset(\nu_\ell)$ with χ_\emptyset given by (56) and $B(z_{\ell_1}, z_{\ell_2}) = K_{\emptyset, \emptyset}(\nu_{\ell_1}, \nu_{\ell_2})$ with $K_{\emptyset, \emptyset}$
 1587 given by (101). The n_ℓ -uples $U^{(\ell)}$, $V^{(\ell)}$ are defined in terms of the n_ℓ -uples \mathcal{P}_ℓ , \mathcal{H}_ℓ as
 1588 $U^{(\ell)} = (\kappa_a(\nu_\ell), a \in \mathcal{P}_\ell)$, $V^{(\ell)} = (-\kappa_a(\nu_\ell), a \in \mathcal{H}_\ell)$. The quantities $\Delta(W)$, $\Delta(W; W')$ for
 1589 tuples $W = (w_1, \dots, w_n)$, $W' = (w'_1, \dots, w'_n)$ are defined as $\Delta(W) = \prod_{1 \leq i < j \leq n} (w_j - w_i)$,
 1590 $\Delta(W; W') = \prod_{i=1}^n \prod_{i'=1}^{n'} (w_i - w'_{i'})$. The remaining factors are given by $h(U^{(\ell_1)}, z_{\ell_2}) =$
 1591 $\sum_{a \in \mathcal{P}_{\ell_1}} \int_{-\infty}^0 du \chi''_\emptyset(u + \nu_{\ell_2}) / \kappa_a(u + \nu_{\ell_2})$, $h(V^{(\ell_1)}, z_{\ell_2}) = \sum_{a \in \mathcal{H}_{\ell_1}} \int_{-\infty}^0 du \chi''_\emptyset(u + \nu_{\ell_2}) / \kappa_a(u +$
 1592 $\nu_{\ell_2})$ and

$$\begin{aligned}
 \hat{f}_\ell(U^{(\ell)}) &= (-1)^{n_\ell} e^{2 \sum_{a \in \mathcal{P}_\ell} \int_{-\infty}^{\nu_\ell} dv \frac{\chi''_\emptyset(v)}{\kappa_a(v)}} \prod_{a \in \mathcal{P}_\ell} \frac{e^{(t_\ell - t_{\ell-1}) \frac{\kappa_a(\nu_\ell)^3}{3} + (x_\ell - x_{\ell-1}) \frac{\kappa_a(\nu_\ell)^2}{2} + (u_\ell - u_{\ell-1}) \kappa_a(\nu_\ell)}}{\kappa_a(\nu_\ell)} \\
 \hat{f}_\ell(V^{(\ell)}) &= e^{2 \sum_{a \in \mathcal{H}_\ell} \int_{-\infty}^{\nu_\ell} dv \frac{\chi''_\emptyset(v)}{\kappa_a(v)}} \prod_{a \in \mathcal{H}_\ell} \frac{e^{(t_\ell - t_{\ell-1}) \frac{\kappa_a(\nu_\ell)^3}{3} - (x_\ell - x_{\ell-1}) \frac{\kappa_a(\nu_\ell)^2}{2} + (u_\ell - u_{\ell-1}) \kappa_a(\nu_\ell)}}{\kappa_a(\nu_\ell)}. \quad (153)
 \end{aligned}$$

1593 Because of the Vandermonde determinants $\Delta(U^{(\ell)})$, $\Delta(V^{(\ell)})$, only tuples \mathcal{P}_ℓ , \mathcal{H}_ℓ with
 1594 distinct elements contribute to (152). Since the summand is invariant under permutations
 1595 of the elements of \mathcal{P}_ℓ , \mathcal{H}_ℓ , one can sum over subsets P_ℓ , H_ℓ of $\mathbb{Z} + 1/2$ instead, up to a
 1596 factor $\prod_{\ell=1}^m (n_\ell!)^2$ counting the number of permutations. Making the changes of variables
 1597 $z_\ell = -e^{\nu_\ell}$, one finds after some simplifications

$$\begin{aligned}
 & F(\vec{t}, \vec{x}, \vec{u}) = \int_{c_1 - i\pi}^{c_1 + i\pi} \frac{d\nu_1}{2i\pi} \cdots \int_{c_m - i\pi}^{c_m + i\pi} \frac{d\nu_m}{2i\pi} \left(\prod_{\ell=1}^m \sum_{\substack{P_\ell, H_\ell \subset \mathbb{Z} + 1/2 \\ |P_\ell| = |H_\ell|}} \right) \quad (154) \\
 & \quad \times \left(\prod_{\ell=1}^m \left((i/4)^{2n_\ell} V_{P_\ell}^2 V_{H_\ell}^2 e^{2i\pi(x_\ell - x_{\ell-1})(\sum_{a \in P_\ell} a - \sum_{a \in H_\ell} a)} \right. \right. \\
 & \quad \quad \quad \left. \left. \times e^{(t_\ell - t_{\ell-1}) \chi_{P_\ell}^{\Delta_\ell}(\nu_\ell) - (u_\ell - u_{\ell-1}) \chi_{P_\ell}^{\Delta_\ell}(\nu_\ell) + 2J_{P_\ell}^{\Delta_\ell}(\nu_\ell)} \right) \right) \\
 & \quad \times \prod_{\ell=1}^{m-1} \frac{(1 - e^{\nu_{\ell+1} - \nu_\ell})^{-1 + n_\ell} (1 - e^{\nu_\ell - \nu_{\ell+1}})^{n_{\ell+1}} e^{-2K_{P_\ell, P_{\ell+1}}^{\Delta_\ell, \Delta_{\ell+1}}(\nu_\ell, \nu_{\ell+1})}}{\left(\prod_{a \in P_\ell} \prod_{b \in P_{\ell+1}} \left(\frac{2i\pi b - \nu_{\ell+1}}{4} - \frac{2i\pi a - \nu_\ell}{4} \right) \right) \left(\prod_{a \in H_\ell} \prod_{b \in H_{\ell+1}} \left(\frac{2i\pi b - \nu_{\ell+1}}{4} - \frac{2i\pi a - \nu_\ell}{4} \right) \right)}
 \end{aligned}$$

1598 with $c_m < \dots < c_1 < 0$, $n_\ell = |P_\ell| = |H_\ell|$ and $\Delta_\ell = P_\ell \ominus H_\ell$.

1599 Using $2n_\ell = 2|P_\ell \setminus \Delta_\ell| + |\Delta_\ell|$ and (134), the general factor of the first product in (154)
 1600 rewrites in terms of the functions χ^Δ , χ'^Δ , e^{2J^Δ} on the Riemann surface \mathcal{R}^Δ defined in
 1601 (86), (91), (96) as

$$\begin{aligned} & (i/4)^{2n_\ell} V_{P_\ell}^2 V_{H_\ell}^2 e^{(t_\ell - t_{\ell-1})\chi_{P_\ell}^{\Delta_\ell}(\nu_\ell) - (u_\ell - u_{\ell-1})\chi_{P_\ell}^{\prime\Delta_\ell}(\nu_\ell) + 2J_{P_\ell}^{\Delta_\ell}(\nu_\ell)} \\ & = (i/4)^{|\Delta_\ell|} V_{A_\ell}^2 V_{\Delta_\ell \setminus A_\ell}^2 \left(e^{(t_\ell - t_{\ell-1})\chi^{\Delta_\ell} - (u_\ell - u_{\ell-1})\chi'^{\Delta_\ell} + 2J^{\Delta_\ell}} \right) ([\nu_\ell, P_\ell]) \end{aligned} \quad (155)$$

1602 with $A_\ell = P_\ell \cap \Delta_\ell$. Furthermore, one has $1 - e^{\nu_{\ell+1} - \nu_\ell} = e^{-4I_0(\nu_{\ell+1} - \nu_\ell + i\pi)}$, $1 - e^{\nu_\ell - \nu_{\ell+1}} =$
 1603 $e^{-4I_0(\nu_\ell - \nu_{\ell+1} - i\pi)}$ with I_0 defined in (68), and the identities $n_\ell = |P_\ell \setminus \Delta_\ell| + |\Delta_\ell|/2$,

$$\begin{aligned} & \frac{\left(\prod_{a \in P \setminus \Delta} \prod_{b \in Q \setminus \Gamma} \left(\frac{2i\pi b - \mu}{4} - \frac{2i\pi a - \nu}{4} \right) \right) \left(\prod_{a \in P \cup \Delta} \prod_{b \in Q \cup \Gamma} \left(\frac{2i\pi b - \mu}{4} - \frac{2i\pi a - \nu}{4} \right) \right)}{\left(\prod_{a \in P} \prod_{b \in Q} \left(\frac{2i\pi b - \mu}{4} - \frac{2i\pi a - \nu}{4} \right) \right) \left(\prod_{a \in P \ominus \Delta} \prod_{b \in Q \ominus \Gamma} \left(\frac{2i\pi b - \mu}{4} - \frac{2i\pi a - \nu}{4} \right) \right)} \\ & = \prod_{a \in \Delta} \prod_{b \in \Gamma} \left(\frac{2i\pi b - \mu}{4} - \frac{2i\pi a - \nu}{4} \right)^{\frac{1 - \sigma_a(P)\sigma_b(Q)}{2}} \end{aligned} \quad (156)$$

1604 lead for the general factor of the second product in (154) to

$$\begin{aligned} & \frac{(1 - e^{\nu_{\ell+1} - \nu_\ell})^{n_\ell} (1 - e^{\nu_\ell - \nu_{\ell+1}})^{n_{\ell+1}} e^{-2K_{P_\ell, P_{\ell+1}}^{\Delta_\ell, \Delta_{\ell+1}}(\nu_\ell, \nu_{\ell+1})}}{\left(\prod_{a \in P_\ell} \prod_{b \in P_{\ell+1}} \left(\frac{2i\pi b - \nu_{\ell+1}}{4} - \frac{2i\pi a - \nu_\ell}{4} \right) \right) \left(\prod_{a \in H_\ell} \prod_{b \in H_{\ell+1}} \left(\frac{2i\pi b - \nu_{\ell+1}}{4} - \frac{2i\pi a - \nu_\ell}{4} \right) \right)} \quad (157) \\ & = \frac{(1 - e^{\nu_{\ell+1} - \nu_\ell})^{|\Delta_\ell|/2} (1 - e^{\nu_\ell - \nu_{\ell+1}})^{|\Delta_{\ell+1}|/2}}{\left(\prod_{a \in \Delta_\ell} \prod_{b \in \Delta_{\ell+1}} \left(\frac{2i\pi b - \nu_{\ell+1}}{4} - \frac{2i\pi a - \nu_\ell}{4} \right)^{\frac{1 + \sigma_a(A_\ell)\sigma_b(A_{\ell+1})}{2}} \right)} \times \left(e^{-2K^{\Delta_\ell, \Delta_{\ell+1}}(p_\ell, p_{\ell+1})} \right), \end{aligned}$$

1605 where $A_\ell = P_\ell \cap \Delta_\ell$, $p_\ell = [\nu_\ell, P_\ell]$ is a point on the Riemann surface $\mathcal{R}^{\Delta_\ell}$ and $e^{2K^{\Delta_\ell, \Delta_{\ell+1}}$
 1606 a function meromorphic on $\mathcal{R}^{\Delta_\ell} \times \mathcal{R}^{\Delta_{\ell+1}}$ defined in (118). Writing $P_\ell = Q_\ell \cup A_\ell$ with
 1607 $Q_\ell \cap \Delta_\ell = \emptyset$ and $A_\ell \subset \Delta_\ell$ and using that $\chi^\Delta([\nu, P]) = \chi^\Delta([\nu, P \setminus \Delta])$, $e^{2J^\Delta}([\nu, P]) =$
 1608 $e^{2J^\Delta}([\nu, P \setminus \Delta])$, $e^{2K^{\Delta, \Gamma}}([\nu, P], [\mu, Q]) = e^{2K^{\Delta, \Gamma}}([\nu, P \setminus \Delta], [\mu, Q \setminus \Gamma])$ are independent of
 1609 $P \cap \Delta$ and $Q \cap \Gamma$, we obtain

$$\begin{aligned} F(\vec{t}, \vec{x}, \vec{u}) & = \int_{c_1 - i\pi}^{c_1 + i\pi} \frac{d\nu_1}{2i\pi} \cdots \int_{c_m - i\pi}^{c_m + i\pi} \frac{d\nu_m}{2i\pi} \left(\prod_{\ell=1}^m \sum_{\Delta_\ell \subset \mathbb{Z} + 1/2} \sum_{\substack{A_\ell \subset \Delta_\ell \\ |A_\ell| = |\Delta_\ell \setminus A_\ell|}} \sum_{\substack{Q_\ell \subset \mathbb{Z} + 1/2 \\ Q_\ell \cap \Delta_\ell = \emptyset}} \right) \quad (158) \\ & \times \left(\prod_{\ell=1}^m \left((i/4)^{|\Delta_\ell|} V_{A_\ell}^2 V_{\Delta_\ell \setminus A_\ell}^2 e^{2i\pi(x_\ell - x_{\ell-1})(\sum_{a \in A_\ell} a - \sum_{a \in \Delta_\ell \setminus A_\ell} a)} \right. \right. \\ & \quad \left. \left. \times \left(e^{(t_\ell - t_{\ell-1})\chi^{\Delta_\ell} - (u_\ell - u_{\ell-1})\chi'^{\Delta_\ell} + 2J^{\Delta_\ell}} \right) (p_\ell) \right) \right) \\ & \times \left(\prod_{\ell=1}^{m-1} \left(\frac{(1 - e^{\nu_{\ell+1} - \nu_\ell})^{|\Delta_\ell|/2} (1 - e^{\nu_\ell - \nu_{\ell+1}})^{|\Delta_{\ell+1}|/2}}{1 - e^{\nu_{\ell+1} - \nu_\ell}} \right. \right. \\ & \quad \left. \left. \times \frac{e^{-2K^{\Delta_\ell, \Delta_{\ell+1}}(p_\ell, p_{\ell+1})}}{\prod_{a \in \Delta_\ell} \prod_{b \in \Delta_{\ell+1}} \left(\frac{2i\pi b - \nu_{\ell+1}}{4} - \frac{2i\pi a - \nu_\ell}{4} \right)^{\frac{1 + \sigma_a(A_\ell)\sigma_b(A_{\ell+1})}{2}}} \right) \right), \end{aligned}$$

1610 where $p_\ell = [\nu_\ell, Q_\ell]$. This is essentially (13).

1611 5.3.2 Pole structure of (16)

1612

1613 The integrand in (16) has potential poles and zeroes at $\nu_{\ell+1} = \nu_\ell + 2i\pi m$, $m \in \mathbb{Z}$. More
1614 precisely defining from (14), (15) and (118) the integer

$$\begin{aligned} \alpha_\ell = -1 + & \left(\frac{|\Delta_\ell|}{2} + \frac{|\Delta_{\ell+1}|}{2} - |A_\ell \cap (A_{\ell+1} - m)| - |(\Delta_\ell \setminus A_\ell) \cap ((\Delta_{\ell+1} \setminus A_{\ell+1}) - m)| \right) \\ & + \left(|P_\ell| + |P_{\ell+1}| + |\Delta_\ell \cap (\Delta_{\ell+1} - m)| \right. \\ & \left. - |P_\ell \cap (P_{\ell+1} - m)| - |(P_\ell \cup \Delta_\ell) \cap ((P_{\ell+1} \cup \Delta_{\ell+1}) - m)| \right) \end{aligned} \quad (159)$$

1615 with $P_\ell \cap \Delta_\ell = \emptyset$, $A_\ell \subset \Delta_\ell$ and $|A_\ell| = |\Delta_\ell|/2$ as in (13), the integrand has at the point
1616 $\nu_{\ell+1} = \nu_\ell + 2i\pi m$ a zero of order α_ℓ if $\alpha_\ell > 0$ and a pole of order $-\alpha_\ell$ if $\alpha_\ell < 0$. We show
1617 below that for any choice of the integer m and of the sets Δ_ℓ , A_ℓ , P_ℓ , $\Delta_{\ell+1}$, $A_{\ell+1}$, $P_{\ell+1}$
1618 as in (13), one has $\alpha_\ell \geq -1$, with $\alpha_\ell = -1$ if and only if $\Delta_{\ell+1} = \Delta_\ell + m$, $A_{\ell+1} = A_\ell + m$
1619 and $P_{\ell+1} = P_\ell + m$.

1620 We consider first the terms of (159) in the first line within the parenthesis. Using
1621 $|A_\ell \cap (A_{\ell+1} - m)| \leq \min(|A_\ell|, |A_{\ell+1}|) = \min(|\Delta_\ell|, |\Delta_{\ell+1}|)/2$, and similarly for $|(\Delta_\ell \setminus A_\ell) \cap$
1622 $((\Delta_{\ell+1} \setminus A_{\ell+1}) - m)|$, the first parenthesis of (159) is non-negative, and equal to zero if
1623 and only if $\Delta_{\ell+1} = \Delta_\ell + m$ and $A_{\ell+1} = A_\ell + m$.

1624 We consider then the terms in the second and third line of (159). After some manipu-
1625 lations, we observe that the sum of these terms is equal to $|P_\ell| - |P_\ell \cap ((P_{\ell+1} - m) \cup (\Delta_{\ell+1} -$
1626 $m))| + |P_{\ell+1}| - |(P_\ell \cup \Delta_\ell) \cap (P_{\ell+1} - m)|$, which is manifestly non-negative. The integrand
1627 in (13) may thus have a pole only if both parentheses in (159) are equal to zero. Provided
1628 that $\Delta_{\ell+1} = \Delta_\ell + m$, the second parenthesis is equal to zero if and only if $P_{\ell+1} = P_\ell + m$,
1629 which concludes the proof.

1630 A Derivation of the identity (76)

1631 In this appendix, we derive the identity (76) for the integral $\oint_{\beta_n \cdot P} \chi''(v)^2 dv$, $n \in \mathbb{Z}$. The
1632 identity is obviously true for $n = 0$ since $\beta_0 \cdot P$ is homotopic to an empty loop. We consider
1633 first the case $n = 1$, for which a detailed calculation is needed, and then generalize to
1634 arbitrary $n \in \mathbb{Z}$ by using translation properties of the functions J_P .

1635 A.1 Case $n = 1$

1636 We introduce positive numbers ϵ , δ , $0 < \epsilon \ll \delta \ll 1$. By definition of the path $\beta_1 \cdot P$, one
1637 has

$$\oint_{\beta_1 \cdot P} \chi''(v)^2 dv = \int_{-\infty}^{i(\pi+\delta)-\epsilon} dv \chi''_P(v)^2 - \int_{-\infty}^{i(\pi+\delta)+\epsilon} dv \chi''_{P \ominus \{1/2\}}(v)^2, \quad (160)$$

1638 with both paths of integration contained in \mathbb{D} on the right hand side. The path for the
1639 second integral on the right has to cross the imaginary axis in the interval $-\pi < \text{Im } v < \pi$,
1640 see figure 20. At this point, δ need not be infinitesimal (we only require that $0 < \delta < 2\pi$),
1641 but it will be convenient in the following in order to compute some integrals by expanding
1642 close to the singularity at $v = i\pi$.

1643 From (64), (63), (50) and $\kappa_b'' = 3/\kappa_b$, the function $\chi''_P(v)$ verifies

$$\chi''_P(v) = \chi''_\emptyset(v) + \sum_{b \in P} \frac{2}{\kappa_b(v)} \quad (161)$$

1644 and

$$\chi_P''(v) = \lim_{M \rightarrow \infty} \left(\sqrt{\frac{2M}{\pi}} - \sum_{b=-M+1/2}^{M-1/2} \frac{\sigma_b(P)}{\kappa_b(v)} \right). \quad (162)$$

1645 Since $\sigma_{1/2}(P) = -\sigma_{1/2}(P \ominus \{1/2\})$, the function $\chi_P''(v) + \sigma_{1/2}(P)/\kappa_{1/2}(v) = \chi_{P \ominus \{1/2\}}''(v) -$
 1646 $\sigma_{1/2}(P)/\kappa_{1/2}(v)$ does not have a branch point at $v = i\pi$, so that

$$\int_{-\infty}^{i(\pi+\delta)-\epsilon} dv \left(\chi_P''(v) + \frac{\sigma_{1/2}(P)}{\kappa_{1/2}(v)} \right)^2 - \int_{-\infty}^{i(\pi+\delta)+\epsilon} dv \left(\chi_{P \ominus \{1/2\}}''(v) - \frac{\sigma_{1/2}(P)}{\kappa_{1/2}(v)} \right)^2 = 0. \quad (163)$$

1647 This leads to

$$\begin{aligned} \int_{\beta_1 \cdot P} \chi''(v)^2 dv &= \int_{-\infty}^{i(\pi+\delta)-\epsilon} dv \left(-\frac{1}{\kappa_{1/2}(v)^2} - 2\sigma_{1/2}(P) \frac{\chi_P''(v)}{\kappa_{1/2}(v)} \right) \\ &\quad - \int_{-\infty}^{i(\pi+\delta)+\epsilon} dv \left(-\frac{1}{\kappa_{1/2}(v)^2} + 2\sigma_{1/2}(P) \frac{\chi_{P \ominus \{1/2\}}''(v)}{\kappa_{1/2}(v)} \right), \end{aligned} \quad (164)$$

1648 which, using (161), gives

$$\begin{aligned} \int_{\beta_1 \cdot P} \chi''(v)^2 dv &= \sigma_{1/2}(P) \int_{-\infty}^{i(\pi+\delta)-\epsilon} dv \left(\frac{\sigma_{1/2}(P) - 2}{\kappa_{1/2}(v)^2} - \frac{2\chi_\emptyset''(v)}{\kappa_{1/2}(v)} - \sum_{b \in P \setminus \{1/2\}} \frac{4}{\kappa_{1/2}(v)\kappa_b(v)} \right) \\ &\quad - \sigma_{1/2}(P) \int_{-\infty}^{i(\pi+\delta)+\epsilon} dv \left(\frac{\sigma_{1/2}(P) + 2}{\kappa_{1/2}(v)^2} + \frac{2\chi_\emptyset''(v)}{\kappa_{1/2}(v)} + \sum_{b \in P \setminus \{1/2\}} \frac{4}{\kappa_{1/2}(v)\kappa_b(v)} \right). \end{aligned} \quad (165)$$

1649 The integrals needed are computed in appendix C. Using (184) and (185), we obtain after
 1650 some simplifications

$$\begin{aligned} \frac{1}{2} \int_{\beta_1 \cdot P} \chi''(v)^2 dv &= i\pi + \sigma_{1/2}(P) \left(i\pi(|P|_+ - |P|_- - 1/2) - 2 \log 2 \right. \\ &\quad \left. + \sum_{b \in P \setminus \{1/2\}} \log \frac{\pi^2(b - 1/2)^2}{4} \right), \end{aligned} \quad (166)$$

1651 which is equivalent to (76) with $n = 1$.

1652 A.2 Extension to $n > 1$

1653 For $n \geq 2$, we write the telescopic sum

$$\begin{aligned} J_{P-n}(\nu - 2i\pi n) - J_{P \ominus B_n}(\nu) &= \sum_{m=1}^n \left(J_{(P-m) \ominus B_{n-m}}(\nu - 2i\pi m) \right. \\ &\quad \left. - J_{(P-m+1) \ominus B_{n-m+1}}(\nu - 2i\pi(m-1)) \right). \end{aligned} \quad (167)$$

1654 Noting that $(P-m+1) \ominus B_{n-m+1} = ((P-m) \ominus B_{n-m} + 1) \ominus \{1/2\}$, see the group identity
 1655 (36), one has from (75)

$$\frac{1}{2} \int_{\beta_n \cdot P} \chi''(v)^2 dv = \frac{1}{2} \sum_{m=1}^n \int_{\beta_1 \cdot ((P-m) \ominus B_{n-m} + 1)} \chi''(v)^2 dv. \quad (168)$$

1656 Using the identity (76) with $n = 1$ derived previously, we arrive at

$$\frac{1}{2} \int_{\beta_n \cdot P} \chi''(v)^2 dv = \frac{1}{2} \sum_{m=1}^n \left(W_{(P-m+1) \ominus B_{n-m+1}} - W_{(P-m) \ominus B_{n-m}} \right), \quad (169)$$

1657 whose right hand side telescopically reduces to $(W_{P \ominus B_n} - W_{P-n})/2$. This proves (76) for
 1658 $n \geq 2$.

1659 A.3 Extension to $n < 0$

1660 Let n be a positive integer. The replacements $\nu \rightarrow \nu + 2i\pi n$ and $P \rightarrow (P \ominus B_n) - n$ in
 1661 (75) give

$$J_{P \ominus B_n - n}(\nu) = J_P(\nu + 2i\pi n) + \frac{1}{2} \int_{\beta_n \cdot (P \ominus B_n)} \chi''(v)^2 dv . \quad (170)$$

1662 Changing the order of the terms and using $P \ominus B_n - n = (P - n) \ominus B_{-n}$, one has

$$J_P(\nu + 2i\pi n) = J_{(P-n) \ominus B_{-n}}(\nu) - \frac{1}{2} \int_{\beta_n \cdot (P \ominus B_n)} \chi''(v)^2 dv , \quad (171)$$

1663 which, from (75) with n replaced by $-n$, gives

$$\frac{1}{2} \int_{\beta_{-n} \cdot (P-n)} \chi''(v)^2 dv = -\frac{1}{2} \int_{\beta_n \cdot (P \ominus B_n)} \chi''(v)^2 dv . \quad (172)$$

1664 Using the identity (76) for $n > 0$ derived previously, this leads to

$$\frac{1}{2} \int_{\beta_{-n} \cdot (P-n)} \chi''(v)^2 dv = -W_P + W_{P \ominus B_n - n} . \quad (173)$$

1665 Replacing P by $P + n$ finally leads to (76) with n replaced by $-n < 0$.

1666 B Derivation of the identities (106) and (107)

1667 In this appendix, we derive the identities (106) and (107) for some integrals over the paths
 1668 $\gamma_{n,0}$ and $\gamma_{0,m}$. The identities are obviously true for $n = 0$ or $m = 0$ since the paths are
 1669 then homotopic to empty loops. We start with the identity (106), which is proved first for
 1670 $n = 1$, where a detailed calculation is needed, and then generalized to arbitrary $n \in \mathbb{Z}$ by
 1671 using translation properties of the functions $K_{P,Q}$. The identity (107) is then obtained by
 1672 exchanging μ with ν and P with Q .

1673 B.1 Case $n = 1$ for (106)

1674 The integral $\int_{\gamma_{1,0}} du \mathcal{A}_u(\chi_P''(\cdot + \nu)\chi_Q''(\cdot + \mu))$ is equal to zero if $\text{Re } \nu < 0$ since the path $\gamma_{1,0}$
 1675 is empty then. Therefore, we restrict to $\text{Re } \nu > 0$ in the rest of this section. We introduce
 1676 positive numbers ϵ, δ , $0 < \epsilon \ll \delta \ll 1$. We want to compute the integral

$$\begin{aligned} & \int_{\gamma_{1,0}} du \mathcal{A}_u(\chi_P''(\cdot + \nu)\chi_Q''(\cdot + \mu)) \\ &= \int_{-\infty}^{i(\pi+\delta)-\nu-\epsilon} du \chi_P''(u + \nu)\chi_Q''(u + \mu) - \int_{-\infty}^{i(\pi+\delta)-\nu+\epsilon} du \chi_{P \ominus \{1/2\}}''(u + \nu)\chi_Q''(u + \mu) , \end{aligned} \quad (174)$$

1677 where the paths of integration in the second line are contained in \mathbb{D} . The path for the last
 1678 integral in the second line has to cross the imaginary axis in the interval $-\pi < \text{Im } v < \pi$,
 1679 see figure 20. Additionally, if $\text{Re } \mu > \text{Re } \nu$, the paths of both integrals in the second line
 1680 must cross the line $\text{Re}(u + \mu) = 0$ in the interval $-\pi < \text{Im}(u + \mu) < \pi$. At this point, δ
 1681 need not be infinitesimal (we only require that $0 < \delta < 2\pi$), but it will be convenient in
 1682 the following in order to compute some integrals by expanding close to the singularity at
 1683 $u = i\pi - \nu$.

1684 Because of (162), the function $\chi''_P(v) + \sigma_{1/2}(P)/\kappa_{1/2}(v) = \chi''_{P \ominus \{1/2\}}(v) - \sigma_{1/2}(P)/\kappa_{1/2}(v)$
 1685 does not have a branch point at $v = i\pi$, so that

$$\begin{aligned} & \int_{-\infty}^{i(\pi+\delta)-\nu-\epsilon} du \left(\chi''_P(u+\nu) + \frac{\sigma_{1/2}(P)}{\kappa_{1/2}(u+\nu)} \right) \chi''_Q(u+\mu) \\ &= \int_{-\infty}^{i(\pi+\delta)-\nu+\epsilon} du \left(\chi''_P(u+\nu) - \frac{\sigma_{1/2}(P)}{\kappa_{1/2}(u+\nu)} \right) \chi''_Q(u+\mu) = 0. \end{aligned} \quad (175)$$

1686 This leads to

$$\begin{aligned} & \int_{\gamma_{1,0}} du \mathcal{A}_u(\chi''_P(\cdot+\nu)\chi''_Q(\cdot+\mu)) \\ &= -\sigma_{1/2}(P) \left(\int_{-\infty}^{i(\pi+\delta)-\nu-\epsilon} du \frac{\chi''_Q(u+\mu)}{\kappa_{1/2}(u+\nu)} + \int_{-\infty}^{i(\pi+\delta)-\nu+\epsilon} du \frac{\chi''_Q(u+\mu)}{\kappa_{1/2}(u+\nu)} \right). \end{aligned} \quad (176)$$

1687 Using (161), one has

$$\begin{aligned} & \int_{\gamma_{1,0}} du \mathcal{A}_u(\chi''_P(\cdot+\nu)\chi''_Q(\cdot+\mu)) \\ &= -\sigma_{1/2}(P) \left(\int_{-\infty}^{i(\pi+\delta)-\nu-\epsilon} du \frac{\chi''_\emptyset(u+\mu)}{\kappa_{1/2}(u+\nu)} + \int_{-\infty}^{i(\pi+\delta)-\nu+\epsilon} du \frac{\chi''_\emptyset(u+\mu)}{\kappa_{1/2}(u+\nu)} \right. \\ & \quad \left. + 2 \sum_{b \in Q} \left(\int_{-\infty}^{i(\pi+\delta)-\nu-\epsilon} \frac{du}{\kappa_{1/2}(u+\nu)\kappa_b(u+\mu)} + \int_{-\infty}^{i(\pi+\delta)-\nu+\epsilon} \frac{du}{\kappa_{1/2}(u+\nu)\kappa_b(u+\mu)} \right) \right). \end{aligned} \quad (177)$$

1688 The remaining integrals are computed in appendix D. Using (194) and (201), we find

$$\frac{1}{2} \int_{\gamma_{1,0}} du \mathcal{A}_u(\chi''_P(\cdot+\nu)\chi''_Q(\cdot+\mu)) = 2\sigma_{1/2}(P) \left(I_0(\mu-\nu+i\pi) + \sum_{b \in Q} \log \frac{\kappa_b(\mu-\nu+i\pi)}{\sqrt{8}} \right). \quad (178)$$

1689 Noting from (103) that $W_{P \ominus \{1/2\}, Q}(z) - W_{P, Q}(z) = 2\sigma_{1/2}(P)(I_0(z) + \sum_{b \in Q} \log \frac{\kappa_b(z)}{\sqrt{8}})$ and
 1690 from (104) that $Z_{P \ominus \{1/2\}, Q} - Z_{P, Q} = 0$, we finally obtain (106) for $n = 1$ after replacing
 1691 P by $P + 1$ in (178).

1692 B.2 Extension to $n > 1$ and $n < 0$

1693 The extension of (106) from $n = 1$ to all $n \in \mathbb{Z}$ works essentially the same as in appendix A.

1694 B.3 Proof of (107)

1695 Exchanging ν with μ and replacing n by m transforms the path $\gamma_{n,0}$ to $\gamma_{0,m}$. Replacing
 1696 also P with Q in (106) gives

$$\begin{aligned} & \frac{1}{2} \int_{\gamma_{0,m}} du \mathcal{A}_u(\chi''_{Q+m}(\cdot+\mu)\chi''_P(\cdot+\nu)) \\ &= 1_{\{\text{Re } \mu > 0\}} \left(W_{(Q+m) \ominus B_m, P}(\nu-\mu+i\pi) - W_{Q+m, P}(\nu-\mu+i\pi) \right. \\ & \quad \left. + 1_{\{\text{Re } \nu > \text{Re } \mu\}} (Z_{(Q+m) \ominus B_m, P} - Z_{Q+m, P}) \right). \end{aligned} \quad (179)$$

1697 Using (105) then leads to (107).

1698 C Calculations of some integrals between $-\infty$ and $\nu \in \mathbb{D}$

1699 In this appendix, we compute some integrals between $-\infty$ and $\nu \in \mathbb{D}$, with a path of
 1700 integration contained in \mathbb{D} . For some integrals, indicated by the symbol \int , a regularization
 1701 at $-\infty$ is needed due to the presence of logarithmic divergences.

1702 C.1 The functions $\log \kappa_a$ and $\log(\kappa_a + \kappa_b)$ are analytic in \mathbb{D}

1703 For any $a \in \mathbb{Z} + 1/2$, the function κ_a defined in (50) is analytic in \mathbb{D} . When $\operatorname{Re} v = 0$,
 1704 $-\pi < \operatorname{Im} v < \pi$ and $\arg(\kappa_a(v)) = \operatorname{sgn}(a)\pi/4$. Otherwise, $\operatorname{Re} v$ is non-zero and one has

$$\arg(\kappa_a(v)) \in \begin{cases} (-3\pi/4, -\pi/4) & \operatorname{Re} v > 0 \text{ and } a < 0 \\ (\pi/4, 3\pi/4) & \operatorname{Re} v > 0 \text{ and } a > 0 \\ (-\pi/4, \pi/4) & \operatorname{Re} v < 0 \end{cases}, \quad (180)$$

1705 which implies in particular that $\log \kappa_a$ is analytic in \mathbb{D} if the branch cut of the logarithm
 1706 is chosen as \mathbb{R}^- .

1707 For $a, b \in \mathbb{Z} + 1/2$ and $v \in \mathbb{D}$, the discussion above imply constraints on the argument of
 1708 $\kappa_a(v) + \kappa_b(v)$, $a, b \in \mathbb{Z} + 1/2$. When $\operatorname{Re} v = 0$, $-\pi < \operatorname{Im} v < \pi$, one has $\arg(\kappa_a(v) + \kappa_b(v)) =$
 1709 $(\operatorname{sgn}(a) + \operatorname{sgn}(b))i\pi/4$. Otherwise, $\operatorname{Re} v$ is non-zero and (180) implies

$$\arg(\kappa_a(v) + \kappa_b(v)) \in \begin{cases} (-3\pi/4, -\pi/4) & \operatorname{Re} v > 0, a < 0 \text{ and } b < 0 \\ (\pi/4, 3\pi/4) & \operatorname{Re} v > 0, a > 0 \text{ and } b > 0 \\ (-\pi/4, \pi/4) & \operatorname{Re} v > 0, ab < 0 \\ (-\pi/4, \pi/4) & \operatorname{Re} v < 0 \end{cases}, \quad (181)$$

1710 In the case $\operatorname{Re} v > 0$, $ab < 0$, we have used $\kappa_a(v) + \kappa_b(v) = 4i\pi(a - b)/(\kappa_a(v) - \kappa_b(v))$.
 1711 We observe in particular from (181) that $\arg(\kappa_a(v) + \kappa_b(v))$ always stays between $-3\pi/4$
 1712 and $3\pi/4$, and thus $\kappa_a(v) + \kappa_b(v)$ never reaches the negative real axis \mathbb{R}^- . The function
 1713 $\log(\kappa_a(v) + \kappa_b(v))$ is thus analytic in \mathbb{D} for any $a, b \in \mathbb{Z} + 1/2$ with the branch cut of the
 1714 logarithm chosen as \mathbb{R}^- .

1715 C.2 Integral of $\kappa_a(v)^{-1}\kappa_b(v)^{-1}$

1716 Let $a, b \in \mathbb{Z} + 1/2$ and $\nu \in \mathbb{D}$. We consider the integral $\int_{-\Lambda}^{\nu} dv \kappa_a(v)^{-1}\kappa_b(v)^{-1}$ with a path
 1717 of integration staying in \mathbb{D} and $|\Lambda| \rightarrow \infty$, $\operatorname{Re} \Lambda > 0$. The identity

$$\frac{1}{\kappa_a(v)\kappa_b(v)} = -\partial_v \log(\kappa_a(v) + \kappa_b(v)) \quad (182)$$

1718 allows to compute the integral explicitly since $\log(\kappa_a(v) + \kappa_b(v))$ is analytic in \mathbb{D} when the
 1719 branch cut of the logarithm is chosen as \mathbb{R}^- , as showed in appendix C.1. Taking $|\Lambda| \rightarrow \infty$,
 1720 $\operatorname{Re} \Lambda > 0$, one finds

$$\int_{-\Lambda}^{\nu} \frac{dv}{\kappa_a(v)\kappa_b(v)} \simeq \log \sqrt{8\Lambda} - \log(\kappa_a(\nu) + \kappa_b(\nu)). \quad (183)$$

1721 For any $\nu \in \mathbb{D}$, the regularized integral is then equal to

$$\int_{-\infty}^{\nu} \frac{dv}{\kappa_a(v)\kappa_b(v)} = -\log\left(\frac{\kappa_a(\nu) + \kappa_b(\nu)}{\sqrt{8}}\right). \quad (184)$$

1722

1723 **C.3 Integral of $\chi''_\theta(v)/\kappa_a(v)$ between $-\infty$ and a branch point**

1724 Let δ be a positive real number and $\theta \neq 0$, $-\pi < \theta < \pi$. In the limit $\delta \rightarrow 0$ one has

$$\int_{-\infty}^{i(2\pi a + e^{i\theta}\delta)} dv \frac{\chi''_\theta(v)}{\kappa_a(v)} \simeq \log \sqrt{4\delta} + \frac{i\theta}{2} - \operatorname{sgn}(\theta) \frac{i\pi}{4} + 1_{\{\theta < 0\}} i\pi a, \quad (185)$$

1725 which can be derived by taking $\mu = \nu = 0$ and $v = i(2\pi a + e^{i\theta}\delta)$ in (200), after rather
 1726 tedious simplifications using $\kappa_a(i(2\pi a + e^{i\theta}\delta)) = e^{\frac{i\theta}{2} - (1-4)^{-1}\{ \theta < 0 \} 1_{\{a > 0\}} \frac{i\pi}{4}} \sqrt{2\delta}$, $\kappa_b(i(2\pi a +$
 1727 $e^{i\theta}\delta)) \simeq \operatorname{sgn}(\theta) e^{-\operatorname{sgn}(a-b) \frac{i\pi}{4}} \sqrt{|4\pi(a-b)|}$ if $\operatorname{sgn}(a) = \operatorname{sgn}(b)$ and $|b| < |a|$, and $\kappa_b(i(2\pi a +$
 1728 $e^{i\theta}\delta)) \simeq e^{-\operatorname{sgn}(a-b) \frac{i\pi}{4}} \sqrt{|4\pi(a-b)|}$ otherwise.

1729 **C.4 Integral of $\chi''_\theta(v)/\kappa_a(v)$ as an infinite sum**

1730 The indefinite integral of $\chi''_\theta(v)/\kappa_a(v)$ can be rewritten as an infinite sum by expanding
 1731 $\chi''_\theta(v)$ as in (162) and computing the integrals using (51) and (184). After careful treatment
 1732 of the exchange between the integral and the infinite sum, one has

$$\int_{-\infty}^{\nu} dv \frac{\chi''_\theta(v)}{\kappa_a(v)} = \lim_{M \rightarrow \infty} \left(-2I_0(\nu) - \sqrt{\frac{2M}{\pi}} \kappa_a(\nu) + \frac{\kappa_a^2(\nu)}{8} \right. \quad (186)$$

$$\left. + \sum_{b=-M+1/2}^{M-1/2} \log \left(1 + \frac{\kappa_a(\nu)}{\kappa_b(\nu)} \right) \right),$$

1733 with I_0 defined in (68). When $\kappa_a(\nu)$ is small enough, i.e. when ν is in the vicinity of $2i\pi a$,
 1734 the logarithm can be expanded. Using $2I_0^{(m)}(\nu) = -\delta_{m,1}/4 + (2m-2)!! \sum_{b \in \mathbb{Z}+1/2} \kappa_b(\nu)^{-2m}$
 1735 and $\chi_\theta^{(m+2)}(\nu) = -(2m-1)!! \sum_{b \in \mathbb{Z}+1/2} \kappa_b(\nu)^{-2m-1}$ for $m \geq 1$, we obtain the identity

$$\int_{-\infty}^{\nu} dv \frac{\chi''_\theta(v)}{\kappa_a(v)} = - \sum_{m=0}^{\infty} \left(\frac{\kappa_a(\nu)^{2m}}{(2m)!!} 2I_0^{(m)}(\nu) + \frac{\kappa_a(\nu)^{2m+1}}{(2m+1)!!} \chi_\theta^{(m+2)}(\nu) \right). \quad (187)$$

1736

1737 **D Calculations of some integrals depending on $(\nu, \mu) \in \mathbb{D}_2$**

1738 In this appendix, we compute some integrals depending on two variables ν and μ .

1739 **D.1 Domain of analyticity of functions $\log(e^{i\theta}(\kappa_a(\nu) + \kappa_b(\mu)))$**

1740 Let $a, b \in \mathbb{Z} + 1/2$ and $(\nu, \mu) \in \mathbb{D}_2$. We are interested in the position in the complex plane
 1741 of $\kappa_a(\nu) + \kappa_b(\mu)$. Using (180), we obtain

$$\arg \left(i^{\frac{\operatorname{sgn}(a) - \operatorname{sgn}(b)}{2}} (\kappa_a(\nu) + \kappa_b(\mu)) \right) \in \begin{cases} (-3\pi/4, \pi/4) & a < 0 \quad b < 0 \\ (-\pi/4, 3\pi/4) & a > 0 \quad b > 0 \\ (-3\pi/4, 3\pi/4) & ab < 0 \end{cases} \quad (188)$$

1742 for $\operatorname{Re} \nu < \operatorname{Re} \mu$,

$$\arg \left(i^{\frac{\operatorname{sgn}(b) - \operatorname{sgn}(a)}{2}} (\kappa_a(\nu) + \kappa_b(\mu)) \right) \in \begin{cases} (-3\pi/4, \pi/4) & a < 0 \quad b < 0 \\ (-\pi/4, 3\pi/4) & a > 0 \quad b > 0 \\ (-3\pi/4, 3\pi/4) & ab < 0 \end{cases} \quad (189)$$

1743 for $\text{Re } \nu > \text{Re } \mu$, and

$$\arg(\kappa_a(\nu) + \kappa_b(\mu)) \in \begin{cases} (-3\pi/4, \pi/4) & a < 0 \quad b < 0 \\ (-\pi/4, 3\pi/4) & a > 0 \quad b > 0 \\ (-\pi/4, +\pi/4) & ab < 0 \end{cases} \quad (190)$$

1744 for $\text{Re } \nu = \text{Re } \mu$, $0 < \text{Im}(\nu - \mu) < 2\pi$.

1745 This implies in particular that the function $(\nu, \mu) \mapsto \log\left(i^{\frac{\text{sgn}(a) - \text{sgn}(b)}{2}}(\kappa_a(\nu) + \kappa_b(\mu))\right)$
 1746 is analytic in the domain $\{(\nu, \mu) \in \mathbb{D} \times \mathbb{D}, \text{Re } \nu < \text{Re } \mu\}$ while the function $(\nu, \mu) \mapsto$
 1747 $\log\left(i^{\frac{\text{sgn}(b) - \text{sgn}(a)}{2}}(\kappa_a(\nu) + \kappa_b(\mu))\right)$ is analytic in the domain $\{(\nu, \mu) \in \mathbb{D} \times \mathbb{D}, \text{Re } \nu > \text{Re } \mu\}$.

1748 D.2 Integral of $\kappa_a(u + \nu)^{-1} \kappa_b(u + \mu)^{-1}$

1749 Let $a, b \in \mathbb{Z} + 1/2$. We consider the integral $\int_{-\Lambda}^{\nu} du \kappa_a(u + \nu)^{-1} \kappa_b(u + \mu)^{-1}$ with a path
 1750 of integration such that $(u + \nu, u + \mu)$ stays in \mathbb{D}_2 and $|\Lambda| \rightarrow \infty$, $\text{Re } \Lambda > 0$. The identity

$$\frac{1}{\kappa_a(u + \nu) \kappa_b(u + \mu)} = -\partial_u \log(e^{i\theta}(\kappa_a(u + \nu) + \kappa_b(u + \mu))) \quad (191)$$

1751 allows to compute the integral explicitly by choosing θ appropriately so that $\log(e^{i\theta}(\kappa_a(u +$
 1752 $\nu) + \kappa_b(u + \mu)))$ is analytic everywhere on the path of integration, with \mathbb{R}^- the branch cut
 1753 of the logarithm. According to appendix D.1, one can take $\theta = \theta_{a,b}(\mu - \nu)$ with

$$\theta_{a,b}(z) = \pi \text{sgn}(\text{Re } z) \frac{\text{sgn}(a) - \text{sgn}(b)}{4}. \quad (192)$$

1754 Subtracting the leading term $\log \sqrt{\Lambda}$ in the limit $\Lambda \rightarrow \infty$, $\text{Re } \Lambda > 0$, the regularized
 1755 integral is finally equal to

$$\int_{-\infty}^{\nu} \frac{du}{\kappa_a(u + \nu) \kappa_b(u + \mu)} = i\theta_{a,b}(\mu - \nu) - \log\left(e^{i\theta_{a,b}(\mu - \nu)} \frac{\kappa_a(\nu + \nu) + \kappa_b(\nu + \mu)}{\sqrt{8}}\right). \quad (193)$$

1756 This expression simplifies further when $\nu \rightarrow 2i\pi a - \nu$ since then $\kappa_a(\nu + \nu) \rightarrow 0$, and we
 1757 obtain

$$\int_{-\infty}^{2i\pi a - \nu} \frac{du}{\kappa_a(u + \nu) \kappa_b(u + \mu)} = -\log\left(\frac{\kappa_b(\mu - \nu + 2i\pi a)}{\sqrt{8}}\right). \quad (194)$$

1758

1759 D.3 Integral of $\kappa_b(u + \mu)/\kappa_a(u + \nu)$

1760 Let $a, b \in \mathbb{Z} + 1/2$. We consider the integral $\int_{-\Lambda}^{\nu} du \kappa_b(u + \mu)/\kappa_a(u + \nu)$ with a path of
 1761 integration such that $(u + \nu, u + \mu)$ stays in \mathbb{D}_2 and $|\Lambda| \rightarrow \infty$, $\text{Re } \Lambda > 0$. The identity

$$\begin{aligned} \frac{\kappa_b(u + \mu)}{\kappa_a(u + \nu)} &= -\partial_u \left(\frac{\kappa_a(u + \nu) \kappa_b(u + \mu)}{2} \right. \\ &\quad \left. + ((\nu - 2i\pi a) - (\mu - 2i\pi b)) \log(e^{i\theta}(\kappa_a(u + \nu) + \kappa_b(u + \mu))) \right) \end{aligned} \quad (195)$$

1762 allows to compute the integral explicitly by choosing $\theta = \theta_{a,b}(\mu - \nu)$ defined in (192) so
 1763 that $\log(e^{i\theta}(\kappa_a(u + \nu) + \kappa_b(u + \mu)))$ is analytic everywhere on the path of integration. The
 1764 contribution of the lower limit of the integral $-\Lambda$ is equal to

$$\Lambda + ((\nu - 2i\pi a) - (\mu - 2i\pi b)) \log(\sqrt{8\Lambda} e^{i\theta_{a,b}(\mu - \nu)}) - \frac{\nu + \mu - 2i\pi(a + b)}{2} \quad (196)$$

1765 when $\Lambda \rightarrow \infty$. Defining the regularized integral by subtracting the divergent term $\Lambda +$
 1766 $\frac{(\nu - 2i\pi a) - (\mu - 2i\pi b)}{2} \log \Lambda$ finally leads to

$$\int_{-\infty}^{\nu} du \frac{\kappa_b(u + \mu)}{\kappa_a(u + \nu)} = -\frac{\nu + \mu - 2i\pi(a + b)}{2} - \frac{\kappa_a(\nu + \nu)\kappa_b(\nu + \mu)}{2} \quad (197)$$

$$+ ((\nu - 2i\pi a) - (\mu - 2i\pi b)) \left(i\theta_{a,b}(\mu - \nu) - \log \left(e^{i\theta_{a,b}(\mu - \nu)} \frac{\kappa_a(\nu + \nu) + \kappa_b(\nu + \mu)}{\sqrt{8}} \right) \right).$$

1767

1768 D.4 Integral of $\chi_{\emptyset}''(u + \mu)/\kappa_a(u + \nu)$

1769 Let $a \in \mathbb{Z} + 1/2$. We consider the integral $\int_{-\infty}^{\nu} du \chi_{\emptyset}''(u + \mu)/\kappa_a(u + \nu)$ with a path of
 1770 integration such that $(u + \nu, u + \mu)$ stays in \mathbb{D}_2 . Let M be a positive integer, that will be
 1771 taken to infinity in the end. Using (61), $\partial_u \zeta(s, u) = -s\zeta(s + 1, u)$ and (51), one has

$$\int_{-\infty}^{\nu} du \frac{\chi_{\emptyset}''(u + \mu)}{\kappa_a(u + \nu)} = - \sum_{b=-M+1/2}^{M-1/2} \int_{-\infty}^{\nu} \frac{du}{\kappa_a(u + \nu)\kappa_b(u + \mu)} \quad (198)$$

$$- \frac{1}{2\sqrt{\pi}} \int_{-\infty}^{\nu} du \frac{e^{i\pi/4} \zeta\left(\frac{1}{2}, M + \frac{1}{2} + \frac{u + \mu}{2i\pi}\right) + e^{-i\pi/4} \zeta\left(\frac{1}{2}, M + \frac{1}{2} - \frac{u + \mu}{2i\pi}\right)}{\kappa_a(u + \nu)}.$$

1772 The large M asymptotics of the integral in the second line is dominated by the contribu-
 1773 tions $u \sim M$, for which (59) gives

$$- \frac{1}{2\sqrt{\pi}} \left(e^{i\pi/4} \zeta\left(\frac{1}{2}, M + \frac{1}{2} + \frac{u + \mu}{2i\pi}\right) + e^{-i\pi/4} \zeta\left(\frac{1}{2}, M + \frac{1}{2} - \frac{u + \mu}{2i\pi}\right) \right)$$

$$= \frac{\kappa_M(u + \mu) - \kappa_{-M}(u + \mu)}{2i\pi} + \mathcal{O}(M^{-3/2}). \quad (199)$$

1774 The integrals can then be computed using (193) and (197). After some simplifications,
 1775 one finds

$$\int_{-\infty}^{\nu} du \frac{\chi_{\emptyset}''(u + \mu)}{\kappa_a(u + \nu)} = \lim_{M \rightarrow \infty} \left(-M \log M + M \left(1 - \log \frac{\pi}{2} \right) - \frac{\sqrt{2M}}{\sqrt{\pi}} \kappa_a(\nu + \nu) \quad (200)$$

$$- \frac{\nu - \mu - 2i\pi a}{4} - \sum_{b=-M+1/2}^{M-1/2} \left(i\theta_{a,b}(\mu - \nu) - \log \left(e^{i\theta_{a,b}(\mu - \nu)} \frac{\kappa_a(\nu + \nu) + \kappa_b(\nu + \mu)}{\sqrt{8}} \right) \right) \right).$$

1776 with $\theta_{a,b}$ defined in (192). This expression can be simplified further when $\nu \rightarrow 2i\pi a - \nu$
 1777 since $\kappa_a(\nu + \nu) \rightarrow 0$. Using (71), we obtain

$$\int_{-\infty}^{2i\pi a - \nu} du \frac{\chi_{\emptyset}''(u + \mu)}{\kappa_a(u + \nu)} = -2I_0(\mu - \nu + 2i\pi a). \quad (201)$$

1778

1779 E Identities for the coefficients W_P, W_P^{Δ}

1780 In this appendix, we give some identities for the coefficients W_P and W_P^{Δ} defined in (77)
 1781 and (94).

1782 E.1 Differences of W_P

1783 We observe that for any $P \subset \mathbb{Z} + 1/2$, the last two terms in the definition (77) are
 1784 unchanged if the set P is replaced by $P - n$, $n \in \mathbb{Z}$. After some manipulations using
 1785 $|P|_+ + |P|_- = |P|$, $|P|_+ - |P|_- = \sum_{a \in P} \text{sgn}(a)$ and $\text{sgn}(a - n) = \sigma_a(B_n) \text{sgn}(a)$, one has

$$W_P - W_{P-n} = -i\pi n |P| + \text{sgn}(n) 2i\pi |P| |P \cap B_n|, \quad (202)$$

1786 with $\text{sgn}(0) = 0$. Using this identity together with $|P \ominus B_n| = |P| + |n| - 2|P \cap B_n|$ and
 1787 $|(P \ominus B_n) \cap B_n| = |n| - |P \cap B_n|$, we obtain

$$(W_{P \ominus B_n} - W_{P-n}) - (W_{P \ominus B_n - n} - W_P) = \text{sgn}(n) i\pi (|n| - 2|P \cap B_n|)^2, \quad (203)$$

1788 which can be rewritten as

$$\begin{aligned} & (W_{P \ominus B_n} - W_{P-n}) - (W_{(P \ominus B_n) - n} - W_P) \\ &= i\pi n + 2i\pi \text{sgn}(n) \left(\frac{|n|(|n| - 1)}{2} - 2|n| |P \cap B_n| + 2|P \cap B_n|^2 \right). \end{aligned} \quad (204)$$

1789 In particular, one has

$$(W_{P \ominus B_n} - W_{P-n}) - (W_{P \ominus B_n - n} - W_P) \in i\pi n + 2i\pi \mathbb{Z}. \quad (205)$$

1790

1791 E.2 Ratios of e^{W_P}

1792 We consider now the quantity e^{W_P} . Using again $|P|_+^2 - |P|_-^2 = |P| \sum_{a \in P} \text{sgn}(a)$, one has
 1793 in terms of the Vandermonde determinant V_P defined in (5) the identity

$$e^{W_P} = (-1)^{\frac{|P|(|P|-1)}{2}} e^{-i\pi \sum_{a \in P} a} \frac{(-1)^{|P|} V_P^2}{2^{2|P|}}. \quad (206)$$

1794 Considering ratios, one has in particular

$$e^{W_{P-n} - W_P} = (-1)^{n|P|}, \quad (207)$$

1795 which follows also directly from (202).

1796 We are also interested in the quantity $e^{W_{P \ominus B_n} - W_P}$, which can be computed from (206)
 1797 using the summation identity

$$\sum_{a \in P \ominus Q} f(a) - \sum_{a \in P} f(a) = \sum_{a \in Q} \sigma_a(P) f(a), \quad (208)$$

1798 where σ_a is defined in (29). The summation identity (208) is proved easily from the
 1799 Venn diagram for the sets P and Q . Applied to $Q = B_n$, $f(a) = a$, it gives after some
 1800 simplifications for $P \subset \mathbb{Z} + 1/2$

$$e^{-i\pi \sum_{a \in P \ominus B_n} a} = e^{-i\pi \sum_{a \in P} a} \times (-1)^{n(n+1)/2} i^{\sum_{a \in B_n} \sigma_a(P)}. \quad (209)$$

1801 Similarly, the summation identity (208) implies $|P \ominus B_n| = |P| + \sum_{a \in B_n} \sigma_a(P)$, which
 1802 leads to

$$(-1)^{\frac{|P \ominus B_n|(|P \ominus B_n| - 1)}{2}} = (-1)^{\frac{|P|(|P| - 1)}{2}} \times i^{-n} (-1)^{n|P|} (-1)^{n(n+1)/2} (-i)^{\sum_{a \in B_n} \sigma_a(P)}. \quad (210)$$

1803 Putting together the two identities above with (206), we finally obtain

$$e^{W_{P \ominus B_n} - W_P} = i^{-n} (-1)^{n|P|} \times \frac{(-1)^{|P \ominus B_n|} V_{P \ominus B_n}^2}{2^{2|P \ominus B_n|}} \Big/ \frac{(-1)^{|P|} V_P^2}{2^{2|P|}}. \quad (211)$$

1804

1805 **E.3 Ratios of $e^{2W_P^\Delta}$**

1806 We consider the quantity $e^{2W_P^\Delta}$ with W_P^Δ defined in (94). Similar simplifications as in the
1807 previous section give

$$e^{2W_{(P+n)\ominus(B_n\setminus(\Delta+n))}^{\Delta+n}-2W_P^\Delta} = \frac{X_{(P+n)\ominus(B_n\setminus(\Delta+n))}^{\Delta+n}}{X_P^\Delta} \quad (212)$$

1808 and

$$e^{2W_{P\ominus(B_n\setminus\Delta)}^{\Delta}-2W_{P-n}^{\Delta-n}} = e^{2W_{P\ominus(B_n\setminus\Delta)-n}^{\Delta-n}-2W_P^\Delta} = \frac{X_{P\ominus(B_n\setminus\Delta)}^\Delta}{X_P^\Delta} \quad (213)$$

1809 with

$$X_P^\Delta = (i/4)^{2|P\setminus\Delta|+|\Delta|} \prod_{a\in P\setminus\Delta} \prod_{\substack{b\in P\cup\Delta \\ b\neq a}} \left(\frac{2i\pi a}{4} - \frac{2i\pi b}{4} \right)^2. \quad (214)$$

1810

1811 **References**

- 1812 [1] T. Halpin-Healy and Y.-C. Zhang, *Kinetic roughening phenomena, stochastic growth,*
1813 *directed polymers and all that. Aspects of multidisciplinary statistical mechanics,*
1814 *Phys. Rep.* **254**, 215 (1995), doi:10.1016/0370-1573(94)00087-J.
- 1815 [2] T. Kriecherbauer and J. Krug, *A pedestrian's view on interacting particle systems,*
1816 *KPZ universality and random matrices,* *J. Phys. A: Math. Theor.* **43**, 403001 (2010),
1817 doi:10.1088/1751-8113/43/40/403001.
- 1818 [3] I. Corwin, *The Kardar-Parisi-Zhang equation and universality class,* *Random Ma-*
1819 *trices: Theory and Applications* **1**, 1130001 (2011), doi:10.1142/S2010326311300014.
- 1820 [4] A. Borodin and V. Gorin, *Lectures on integrable probability* (2012), [https://arxiv.](https://arxiv.org/abs/1212.3351)
1821 [org/abs/1212.3351](https://arxiv.org/abs/1212.3351).
- 1822 [5] J. Quastel and H. Spohn, *The one-dimensional KPZ equation and its universality*
1823 *class,* *J. Stat. Phys.* **160**, 965 (2015), doi:10.1007/s10955-015-1250-9.
- 1824 [6] T. Halpin-Healy and K. Takeuchi, *A KPZ cocktail-shaken, not stirred...,* *J. Stat.*
1825 *Phys.* **160**, 794 (2015), doi:10.1007/s10955-015-1282-1.
- 1826 [7] H. Spohn, *The Kardar-Parisi-Zhang equation - a statistical physics perspective* (2016),
1827 <https://arxiv.org/abs/1601.00499>.
- 1828 [8] K. Takeuchi, *An appetizer to modern developments on the Kardar-Parisi-Zhang uni-*
1829 *versality class,* *Physica A* **504**, 77 (2018), doi:10.1016/j.physa.2018.03.009.
- 1830 [9] A. Saenz, *The KPZ universality class and related topics* (2019), [https://arxiv.](https://arxiv.org/abs/1904.03319)
1831 [org/abs/1904.03319](https://arxiv.org/abs/1904.03319).
- 1832 [10] K. Takeuchi, M. Sano, T. Sasamoto and H. Spohn, *Growing interfaces uncover univer-*
1833 *sal fluctuations behind scale invariance,* *Sci. Rep.* **1**, 34 (2011), doi:10.1038/srep00034.
- 1834 [11] A. Somoza, M. Ortuño and J. Prior, *Universal distribution functions in*
1835 *two-dimensional localized systems,* *Phys. Rev. Lett.* **99**, 116602 (2007),
1836 doi:10.1103/PhysRevLett.99.116602.

- 1837 [12] H. van Beijeren, *Exact results for anomalous transport in one-*
1838 *dimensional Hamiltonian systems*, Phys. Rev. Lett. **108**, 180601 (2012),
1839 doi:10.1103/PhysRevLett.108.180601.
- 1840 [13] H. Spohn, *Nonlinear fluctuating hydrodynamics for anharmonic chains*, J. Stat. Phys.
1841 **154**, 1191 (2014), doi:10.1007/s10955-014-0933-y.
- 1842 [14] V. Popkov, A. Schadschneider, J. Schmidt and G. Schütz, *Fibonacci family of*
1843 *dynamical universality classes*, Proc. Natl. Acad. Sci. USA **112**, 12645 (2015),
1844 doi:10.1073/pnas.1512261112.
- 1845 [15] M. Kulkarni, D. Huse and H. Spohn, *Fluctuating hydrodynamics for a discrete Gross-*
1846 *Pitaevskii equation: Mapping onto the Kardar-Parisi-Zhang universality class*, Phys.
1847 Rev. A **92**, 043612 (2015), doi:10.1103/PhysRevA.92.043612.
- 1848 [16] A. Nahum, J. Ruhman, S. Vijay and J. Haah, *Quantum entanglement*
1849 *growth under random unitary dynamics*, Phys. Rev. X **7**, 031016 (2017),
1850 doi:10.1103/PhysRevX.7.031016.
- 1851 [17] M. Ljubotina, M. Žnidarič and T. Prosen, *Kardar-Parisi-Zhang physics*
1852 *in the quantum Heisenberg magnet*, Phys. Rev. Lett. **122**, 210602 (2019),
1853 doi:10.1103/PhysRevLett.122.210602.
- 1854 [18] J. de Gier, A. Schadschneider, J. Schmidt and G. Schütz, *Kardar-Parisi-Zhang*
1855 *universality of the Nagel-Schreckenberg model*, Phys. Rev. E **100**, 052111 (2019),
1856 doi:10.1103/PhysRevE.100.052111.
- 1857 [19] M. Kardar, G. Parisi and Y.-C. Zhang, *Dynamic scaling of growing interfaces*, Phys.
1858 Rev. Lett. **56**, 889 (1986), doi:10.1103/PhysRevLett.56.889.
- 1859 [20] M. Hairer, *Solving the KPZ equation*, Ann. Math. **178**, 559 (2013),
1860 doi:10.4007/annals.2013.178.2.4.
- 1861 [21] A. Kupiainen, *Renormalization group and stochastic PDEs*, Annales Henri Poincaré
1862 **17**, 497 (2016), doi:10.1007/s00023-015-0408-y.
- 1863 [22] M. Gubinelli and N. Perkowski, *KPZ reloaded*, Commun. Math. Phys. **349**, 165
1864 (2017), doi:10.1007/s00220-016-2788-3.
- 1865 [23] K. Johansson, *Shape fluctuations and random matrices*, Commun. Math. Phys. **209**,
1866 437 (2000), doi:10.1007/s002200050027.
- 1867 [24] J. Baik and E. Rains, *Limiting distributions for a polynuclear growth model with*
1868 *external sources*, J. Stat. Phys. **100**, 523 (2000), doi:10.1023/A:1018615306992.
- 1869 [25] M. Prähofer and H. Spohn, *Scale invariance of the PNG droplet and the Airy process*,
1870 J. Stat. Phys. **108**, 1071 (2002), doi:10.1023/A:1019791415147.
- 1871 [26] T. Sasamoto, *Spatial correlations of the 1D KPZ surface on a flat substrate*, J. Phys.
1872 A: Math. Gen. **38**, L549 (2005), doi:10.1088/0305-4470/38/33/L01.
- 1873 [27] P. Ferrari and H. Spohn, *Scaling limit for the space-time covariance of the stationary*
1874 *totally asymmetric simple exclusion process*, Commun. Math. Phys. **265**, 1 (2006),
1875 doi:10.1007/s00220-006-1549-0.

- 1876 [28] A. Borodin, P. Ferrari, M. Prähofer and T. Sasamoto, *Fluctuation properties of*
1877 *the TASEP with periodic initial configuration*, J. Stat. Phys. **129**, 1055 (2007),
1878 doi:10.1007/s10955-007-9383-0.
- 1879 [29] C. Tracy and H. Widom, *Total current fluctuations in the asymmetric simple exclu-*
1880 *sion process*, J. Math. Phys. **50**, 095204 (2009), doi:10.1063/1.3136630.
- 1881 [30] J. Baik, P. Ferrari and S. Péché, *Limit process of stationary TASEP near the char-*
1882 *acteristic line*, Comm. Pure Appl. Math. **63**, 1017 (2010), doi:10.1002/cpa.20316.
- 1883 [31] A. Borodin, I. Corwin and V. Gorin, *Stochastic six-vertex model*, Duke Math. J. **165**,
1884 563 (2016), doi:10.1215/00127094-3166843.
- 1885 [32] K. Matetski, J. Quastel and D. Remenik, *The KPZ fixed point* (2017), <https://arxiv.org/abs/1701.00018>.
1886
- 1887 [33] K. Johansson and M. Rahman, *Multi-time distribution in discrete polynuclear growth*
1888 (2019), <https://arxiv.org/abs/1906.01053>.
- 1889 [34] Z. Liu, *Multi-time distribution of TASEP* (2019), [https://arxiv.org/abs/1907.](https://arxiv.org/abs/1907.09876)
1890 [09876](https://arxiv.org/abs/1907.09876).
- 1891 [35] C. Tracy and H. Widom, *Level-spacing distributions and the Airy kernel*, Commun.
1892 Math. Phys. **159**, 151 (1994), doi:10.1007/BF02100489.
- 1893 [36] B. Derrida and J. Lebowitz, *Exact large deviation function in the asymmetric exclu-*
1894 *sion process*, Phys. Rev. Lett. **80**, 209 (1998), doi:10.1103/PhysRevLett.80.209.
- 1895 [37] E. Brunet and B. Derrida, *Probability distribution of the free energy of*
1896 *a directed polymer in a random medium*, Phys. Rev. E **61**, 6789 (2000),
1897 doi:10.1103/PhysRevE.61.6789.
- 1898 [38] K. Mallick and S. Prolhac, *Brownian bridges for late time asymptotics of KPZ fluctua-*
1899 *tions in finite volume*, J. Stat. Phys. **173**, 322 (2018), doi:10.1007/s10955-018-2136-4.
- 1900 [39] S. Prolhac, *Finite-time fluctuations for the totally asymmetric exclusion process*,
1901 Phys. Rev. Lett. **116**, 090601 (2016), doi:10.1103/PhysRevLett.116.090601.
- 1902 [40] J. Baik and Z. Liu, *Fluctuations of TASEP on a ring in relaxation time scale*, Comm.
1903 Pure Appl. Math. **71**, 0747 (2018), doi:10.1002/cpa.21702.
- 1904 [41] Z. Liu, *Height fluctuations of stationary TASEP on a ring in relaxation time scale*,
1905 Ann. Inst. H. Poincaré Probab. Statist. **54**, 1031 (2018), doi:10.1214/17-AIHP831.
- 1906 [42] J. Baik and Z. Liu, *Multi-point distribution of periodic TASEP*, J. Amer. Math. Soc.
1907 **32**, 609-674 (2019), doi:10.1090/jams/915.
- 1908 [43] M. Gorissen, A. Lazarescu, K. Mallick and C. Vanderzande, *Exact current statistics*
1909 *of the asymmetric simple exclusion process with open boundaries*, Phys. Rev. Lett.
1910 **109**, 170601 (2012), doi:10.1103/PhysRevLett.109.170601.
- 1911 [44] L.-H. Gwa and H. Spohn, *Six-vertex model, roughened surfaces, and an asymmetric*
1912 *spin Hamiltonian*, Phys. Rev. Lett. **68**, 725 (1992), doi:10.1103/PhysRevLett.68.725.
- 1913 [45] S. Prolhac, *Spectrum of the totally asymmetric simple exclusion process on a pe-*
1914 *riodic lattice - first excited states*, J. Phys. A: Math. Theor. **47**, 375001 (2014).
1915 doi:10.1088/1751-8113/47/37/375001.

- 1916 [46] R. Blythe and M. Evans, *Nonequilibrium steady states of matrix-product form:*
1917 *a solver's guide*, J. Phys. A: Math. Theor. **40**, R333 (2007), doi:10.1088/1751-
1918 8113/40/46/R01.
- 1919 [47] A. Lazarescu and K. Mallick, *An exact formula for the statistics of the current in*
1920 *the TASEP with open boundaries*, J. Phys. A: Math. Theor. **44**, 315001 (2011),
1921 doi:10.1088/1751-8113/44/31/315001.
- 1922 [48] T. Gautié, P. Le Doussal, S. Majumdar and G. Schehr, *Non-crossing Brownian*
1923 *paths and Dyson Brownian motion under a moving boundary*, J. Stat. Phys. (2019),
1924 doi:10.1007/s10955-019-02388-z.
- 1925 [49] C. Bender and T. Wu, *Anharmonic oscillator*, Phys. Rev. **184**, 1231 (1969),
1926 doi:10.1103/PhysRev.184.1231.
- 1927 [50] T. Klassen and E. Melzer, *The thermodynamics of purely elastic scattering theories*
1928 *and conformal perturbation theory*, Nucl. Phys. B **350**, 635 (1991), doi:10.1016/0550-
1929 3213(91)90159-U.
- 1930 [51] P. Dorey and R. Tateo, *Excited states by analytic continuation of TBA equations*,
1931 Nucl. Phys. B **482**, 639 (1996), doi:10.1016/S0550-3213(96)00516-0.
- 1932 [52] A. Voros, *The return of the quartic oscillator. The complex WKB method*, Annales de
1933 l'I.H.P. Physique théorique **39**, 211 (1983). [http://www.numdam.org/item/AIHPA_](http://www.numdam.org/item/AIHPA_1983__39_3_211_0/)
1934 [1983__39_3_211_0/](http://www.numdam.org/item/AIHPA_1983__39_3_211_0/).
- 1935 [53] S. Prohac, *Current fluctuations and large deviations for periodic TASEP on*
1936 *the relaxation scale*, J. Stat. Mech. **2015**, P11028 (2015), doi:10.1088/1742-
1937 5468/2015/11/P11028.
- 1938 [54] K. Motegi, K. Sakai and J. Sato, *Long time asymptotics of the totally asymmetric sim-*
1939 *ple exclusion process*, J. Phys. A: Math. Theor. **45**, 465004 (2012), doi:10.1088/1751-
1940 8113/45/46/465004.
- 1941 [55] E. Belokolos, A. Bobenko, V. Enolski, A. Its and V. Matveev, *Algebro-geometric Ap-*
1942 *proach in the Theory of Integrable Equations*, Springer Series in Nonlinear Dynamics.
1943 Springer, Berlin, doi:10.1007/s00220-007-0235-1 (1994).
- 1944 [56] O. Babelon, D. Bernard and M. Talon, *Introduction to Classical Integrable Systems*,
1945 Cambridge University Press, doi:10.1017/CBO9780511535024 (2003).
- 1946 [57] A. Zabrodin, *Lectures on nonlinear integrable equations and their solutions* (2018),
1947 <https://arxiv.org/abs/1812.11830>.
- 1948 [58] H. Fogedby, *Nonequilibrium dynamics of a growing interface*, J. Phys.: Condens.
1949 Matter **14**, 1557 (2002), doi:10.1088/0953-8984/14/7/313.
- 1950 [59] M. Janas, A. Kamenev and B. Meerson, *Dynamical phase transition in large-deviation*
1951 *statistics of the Kardar-Parisi-Zhang equation*, Phys. Rev. E **94**, 032133 (2016),
1952 doi:10.1103/PhysRevE.94.032133.
- 1953 [60] J. Baik and Z. Liu, *TASEP on a ring in sub-relaxation time scale*, J. Stat. Phys.
1954 **165**, 1051 (2016), doi:10.1007/s10955-016-1665-y.
- 1955 [61] N. Joshi, *The second Painlevé hierarchy and the stationary KdV hierarchy*, Publ.
1956 Res. Inst. Math. Sci. **40**, 1039 (2004), doi:10.2977/prims/1145475502.

- 1957 [62] A. Zabrodin, *Canonical and grand canonical partition functions of Dyson gases as tau-*
1958 *functions of integrable hierarchies and their fermionic realization*, Complex Analysis
1959 and Operator Theory **4**, 497 (2010), doi:10.1007/s11785-010-0063-8.
- 1960 [63] J. Quastel and D. Remenik, *KP governs random growth off a one dimensional sub-*
1961 *strate* (2019), <https://arxiv.org/abs/1908.10353>.
- 1962 [64] J. Feldman, H. Knörrer and E. Trubowitz, *Riemann Surfaces of Infinite*
1963 *Genus*, CRM Monograph Series 20. American Mathematical Society, Providence,
1964 doi:10.1090/crmm/020 (2003).
- 1965 [65] A. Krajenbrink, P. Le Doussal and S. Prolhac, *Systematic time expansion for the*
1966 *Kardar-Parisi-Zhang equation, linear statistics of the GUE at the edge and trapped*
1967 *fermions*, Nucl. Phys. B **936**, 239 (2018), doi:10.1016/j.nuclphysb.2018.09.019.
- 1968 [66] P. Le Doussal, S. Majumdar, A. Rosso and G. Schehr, *Exact short-time*
1969 *height distribution in the one-dimensional Kardar-Parisi-Zhang equation and*
1970 *edge fermions at high temperature*, Phys. Rev. Lett. **117**, 070403 (2016),
1971 doi:10.1103/PhysRevLett.117.070403.
- 1972 [67] S. Prolhac, *Tree structures for the current fluctuations in the exclusion process*, J.
1973 Phys. A: Math. Theor. **43**, 105002 (2010), doi:10.1088/1751-8113/43/10/105002.
- 1974 [68] S. Prolhac, *Perturbative solution for the spectral gap of the weakly asymmetric ex-*
1975 *clusion process*, J. Phys. A: Math. Theor. **50**, 315001 (2017), doi:10.1088/1751-
1976 8121/aa77de.
- 1977 [69] S. Prolhac, *Extrapolation methods and Bethe ansatz for the asymmetric exclu-*
1978 *sion process*, J. Phys. A: Math. Theor. **49**, 454002 (2016), doi:10.1088/1751-
1979 8113/49/45/454002.
- 1980 [70] Z. Liu, A. Saenz and D. Wang, *Integral formulas of ASEP and q-TAZRP on a ring*
1981 (2019), <https://arxiv.org/abs/1905.02987>.
- 1982 [71] R. Kenyon and D. Wilson, *Critical resonance in the non-intersecting lattice path*
1983 *model*, Probab. Theor. Rel. Fields **130**, 289 (2004), doi:10.1007/s00440-003-0293-z.
- 1984 [72] M. Poplavskiy, R. Tribe and O. Zaboronski, *On the distribution of the largest real*
1985 *eigenvalue for the real Ginibre ensemble*, Ann. Appl. Probab. **27**, 1395 (2017),
1986 doi:10.1214/16-AAP1233.
- 1987 [73] J. Baik and T. Bothner, *The largest real eigenvalue in the real Ginibre ensemble and*
1988 *its relation to the Zakharov-Shabat system* (2018), [https://arxiv.org/abs/1808.](https://arxiv.org/abs/1808.02419)
1989 **02419**.
- 1990 [74] B. Derrida and A. Gerschenfeld, *Current fluctuations of the one dimensional symmet-*
1991 *ric simple exclusion process with step initial condition*, J. Stat. Phys. **136**, 1 (2009),
1992 doi:10.1007/s10955-009-9772-7.
- 1993 [75] J.-M. Stéphan, *Return probability after a quench from a domain wall initial state*
1994 *in the spin-1/2 XXZ chain*, J. Stat. Mech. **2017**, 103108 (2017), doi:10.1088/1742-
1995 5468/aa8c19.
- 1996 [76] E. Brattain, N. Do and A. Saenz, *The completeness of the Bethe ansatz for the*
1997 *periodic ASEP* (2015), <https://arxiv.org/abs/1511.03762>.

- 1998 [77] R. Langlands and Y. Saint-Aubin, *Algebro-geometric aspects of the Bethe equations*,
1999 In *Strings and Symmetries*, vol. 447 of *Lecture Notes in Physics*, pp. 40–53. Berlin:
2000 Springer, doi:10.1007/3-540-59163-X_254 (1995).
- 2001 [78] R. Langlands and Y. Saint-Aubin, *Aspects combinatoires des équations de Bethe*, In
2002 *Advances in Mathematical Sciences: CRM's 25 Years*, vol. 11 of *CRM Proceedings*
2003 *and Lecture Notes*, pp. 231–302. Amer. Math. Soc., doi:10.1090/crpm/011 (1997).
- 2004 [79] K. Motegi and K. Sakai, *Vertex models, TASEP and Grothendieck polynomials*, J.
2005 Phys. A: Math. Theor. **46**, 355201 (2013), doi:10.1088/1751-8113/46/35/355201.
- 2006 [80] K. Motegi and K. Sakai, *K-theoretic boson-fermion correspondence and melt-*
2007 *ing crystals*, J. Phys. A: Math. Theor. **47**, 445202 (2014), doi:10.1088/1751-
2008 8113/47/44/445202.
- 2009 [81] A. Bobenko, *Introduction to Compact Riemann Surfaces*, vol. 2013 of *Lecture Notes in*
2010 *Mathematics*, Springer, Berlin, Heidelberg, doi:10.1007/978-3-642-17413-1_1 (2013).
- 2011 [82] R. Cavalieri and E. Miles, *Riemann Surfaces and Algebraic Curves: A First Course*
2012 *in Hurwitz Theory*, Cambridge University Press, doi:10.1017/CBO9781316569252
2013 (2016).
- 2014 [83] B. Eynard, *Lectures notes on compact Riemann surfaces* (2018), [https://arxiv.](https://arxiv.org/abs/1805.06405)
2015 [org/abs/1805.06405](https://arxiv.org/abs/1805.06405).
- 2016 [84] L. Beineke and F. Harary, *The genus of the n-cube*, Canadian Journal of Mathematics
2017 **17**, 494 (1965), doi:10.4153/CJM-1965-048-6.
- 2018 [85] G. Springer, *Introduction to Riemann surfaces*, Addison-Wesley (1957).
- 2019 [86] O. Costin and S. Garoufalidis, *Resurgence of the fractional polylogarithms*, Math.
2020 Res. Lett. **16**, 817 (2009), doi:10.4310/MRL.2009.v16.n5.a5.
- 2021 [87] O. Golinelli and K. Mallick, *Spectral gap of the totally asymmetric exclusion process*
2022 *at arbitrary filling*, J. Phys. A: Math. Gen. **38**, 1419 (2005), doi:10.1088/0305-
2023 4470/38/7/001.
- 2024 [88] N. Bogoliubov, *Determinantal representation of the time-dependent stationary cor-*
2025 *relation function for the totally asymmetric simple exclusion model*, SIGMA **5**, 052
2026 (2009), doi:10.3842/SIGMA.2009.052.
- 2027 [89] K. Motegi, K. Sakai and J. Sato, *Exact relaxation dynamics in the to-*
2028 *tally asymmetric simple exclusion process*, Phys. Rev. E **85**, 042105 (2012),
2029 doi:10.1103/PhysRevE.85.042105.
- 2030 [90] S. Prolhac, *Asymptotics for the norm of Bethe eigenstates in the periodic totally*
2031 *asymmetric exclusion process*, J. Stat. Phys. **160**, 926 (2015), doi:10.1007/s10955-
2032 015-1230-0.
- 2033 [91] V. Priezzhev, *Exact nonstationary probabilities in the asymmetric exclusion process*
2034 *on a ring*, Phys. Rev. Lett **91**, 050601 (2003), doi:10.1103/PhysRevLett.91.050601.
- 2035 [92] C. Tracy and H. Widom, *Integral formulas for the asymmetric simple exclusion*
2036 *process*, Commun. Math. Phys. **279**, 815 (2008), doi:10.1007/s00220-008-0443-3.